NTNU

Norwegian University of
Science and Technology

Depositional Environment and the Diagenetic Influence on the Pressure Solution Seam Behavior and Distribution in Carbonate Sediments

A sedimentological study of the Falk and Ørn Formation, Eastern Finnmark Platform, Northern Norway.

Cathrine Røkkum Winje

Geology
Submission date: May 2016
Supervisor: Mai Britt E. Mørk, IGB

Norwegian University of Science and Technology
Department of Geology and Mineral Resources Engineering

Abstract

Pressure solution seams and porosity have been investigated in carbonate sediments of the Falk and Ørn Formation in core 7030/03-U-01 offshore northern Norway on the eastern part of the Finnmark Platform. A detailed sedimentological log of the core was made based on core and thin sections, which included 10 sedimentary facies, hence 7 carbonate facies. Based on their vertical arrangement, 8 different facies sections were defined and were interpreted to represent different placements on a distal to proximal cross section of a carbonate ramp.

The recorded pressure solution seams were divided into two groups based on their mean amplitude value, where 1) dissolution seams include mean amplitude values lower than 1 mm, and 2) stylolites are defined when amplitudes are higher than 1 mm. The pressure solution seams within both classes were categorized by low or high amplitude, nodule-bounding and if several occur together in swarms. Additionally the stylolite's mean amplitude value and style have been registered. Due to the depositional environment and facies composition, the muddy facies (mudstone and wackestone) is shown to favor dissolution seams, and the *Palaeoaplysina*/phylloid algae boundstone stylolites. The formation of dissolution seams require a significant amount of clay present and has taken place under several circumstances, and is therefore common in the core, whereas stylolites require minor clay and seems to rely on the presence of early calcite cementation for developing. Formation of both types of seams is generally inhibited by a host rock comprising dolomite, though if they form, dissolution seams are most common. Despite different appearance of the dissolution seams and stylolites, the amount of clay and the host rock composition, including obstacles and restrictions, are the main controlling factors. Diagenetic processes associated with the seams development include both cementation and dolomitization.

A porosity classification was done for each facies, and intercrystalline porosity is the most widespread. It has developed in relation to dolomitization of *Palaeoaplysina*/phylloid algae boundstone and mudstone. These lithologies have porosity values that make good candidates for reservoirs, with highest values obtained in the dolomitized mudstone. The dolomitization is interpreted to have formed already in the depositional environment in shallow subtidal and intertidal environment. Dolomitization and intercrystalline porosity seem to be spatially related to the seams, with very local appearance. Beyond this, much of the core shows tight porosity. Within the *Palaeoaplysina*/phylloid algae boundstone tight porosity is associated

with abundant stylolites and associated cement. Tight porosity in the mudstone, in part reflect early calcite cementation and mechanical compaction. Porosity types such as interparticle, moldic and microporosity are also proven in the core, though their presence have only minor effects on the total properties.

Sammendrag

Trykkoppløsningssømmer og porøsitet har blitt undersøkt i karbonatsedimentene i Falk og Ørn formasjonene i kjerne 7030/03-U-01 på den nordnorske kontinentalsokkelen den østlige delen av Finnmark Plattformen. Det ble laget en detaljert sedimentologisk logg av kjernen basert på kjernen og tynnslip som inkluderte 10 sediment-facies, hvor 7 var karbonat-facies. Basert på deres vertikale arrangering, 8 ulike facies-seksjoner ble definert og tolket til å representere ulike plasseringer på et distalt til proksimalt tverrsnitt på en karbonatrampe.

De registrerte trykkoppløsningssømmene ble delt i to grupper basert på deres gjennomsnittlige amplitudeverdi hvor 1) oppløsningssømmer hadde gjennomsnittlig amplitudeverdi lavere enn 1 mm, og 2) stylolitter ble definert når amplitudene var høyere enn 1 mm. Trykkoppløsningssømmene i begge gruppene ble kategorisert med lav eller høy amplitude, nodul bindende og om flere opptrådde sammen i svermer. I tillegg ble stylolittenes gjennomsnittsverdi og stil registrert. På grunn av avsetningsmiljøet og facies sammensetning, favoriserte ”muddy” karbonat-facies (mudstone og wackestone) oppløsningssømmer og *Palaeoaplysina/*phylloid alge boundstone stylolitter. Dannelse av oppløsningssømmer trenger en signifikant mengde leire og har funnet sted under flere omstendigheter og er derfor vanlig i kjernen mens stylolittene trenger mindre leire og ser ut til å være avhengig av tilstedeværelse av tidlig kalsittsement for å utvikle seg. Dannelsen av begge typer sømmer er generelt begrenset av en vertsbergart som inneholder dolomitt men om de dannes er oppløsningssømmer mest vanlig. På tross av ulikt forekomst av oppløsningssømmene og stylolittene er leiremengede og vertsbergarts sammensetning inkludert hinder og restriksjoner de meste kontrollerende faktorene. Diagenese prosesser assosiert med sømmenes utvikling inkluderer både sementering og dolomittisering.

En porøsitetsklassifisering ble gjort for hver facies og interkrystallin porøsitet er mest utbredt. Den har utviklet seg i relasjon til dolomittisering av *Palaeoaplysina*/phylloid alge boundstone og mudstone. Disse litologiene har porøsitetsverdier som utgjør gode reservoarkandidater med høyest verdi oppnådd i dolomittisert mudstone. Dolomittiseringen er tolket til å ha bli dannet tidlig i avsetningsmiljøet i grunn subtidal og intertidalt miljø. Dolomittisering og interkrystallin porøsitet er relatert til sømmene, med en veldig lokal opptreden. Utenom dette har kjernen en tett porøsitet. I *Palaeoaplysina*/phylloid alge boundstone er tett porøsitet assosiert med stylolitter og assosiert sement. Tett porøsitet in mudstone, reflekterer tidlig

sementering og mekanisk kompaksjon. Porøsitetstyper som interpartikkel, moldic og mikroporøsitet er observert i kjernen men deres tilstedeværelse har en mindre påvirkning på den totale porøsitetsfordeling.

Acknowledgement

This thesis is a part of a master's degree in geology at the Department of Geology and Mineral Resources Engineering at the Norwegian University of Science (NTNU), Trondheim. Professor Mai Britt E. Mørk has been the main supervisor for this project and I would like to thank her for help and guidance throughout the writing of the thesis.

I also want to thank professor II at NTNU Atle Mørk for help and great advice during the logging process at Dora.

I would thank my fellow students for many great years in Trondheim. I would give a special thank to Anette U. Granseth for always taking time to help and discuss during the writing of this thesis.

And finally, I would thank my family and boyfriend for the great support and patience during the writing of this thesis.

Cathrine Røkkum Winje 16.05.16, Trondheim

Contents

Abstract.....i

Sammendrag.....iii

Acknowledgement.....v

1 Introduction **1**

1.1 Aim of study 1

1.2 Study area 1

1.3 Previous work 3

2 Regional geology **5**

2.2 Stratigraphy 10

3 Theory **15**

3.1 Terminology 15

3.2 Carbonates **15**

4 Database and methodology **25**

4.1 Data 25

4.2 Practical work and methodology 26

4.3 Sources of error **33**

5 Sedimentology **35**

5.1 Facies 35

5.2 Vertical Facies Arrangement 53

5.3 Porosity classification of the carbonate facies 61

6 Results **67**

6.1 Classification of stylolites and dissolution seams 67

6.2 Petrography of the carbonate sections 82

6.3 The pressure solution seams effect on the host rock 86

7 Discussion **93**

7.1 Depositional Model 93

7.2 The seams distribution 98

7.3 The seams effect on the host rock 104

7.4 Porosity distribution 105

8 Conclusion **109**

9 Further work 111

10 References 112

List of figures

Figure 1.1. Map of the studied area showing the main structural 2
Figure 2.1. Geological events, paleolatitude of Laurentia……. 6
Figure 2.2. Simplified stratigraphic log of the. 11
Figure 3.1. Schematic diagram showing relationship. 16
Figure 3.2. Figure from Choquette and James (1987). 18
Figure 3.3. Figure from Choquette and James (1987). 19
Figure 3.4. Fields of occurrences of common waters and. 22
Figure 4.1. A modified version of the Dunham (1962). 27
Figure 4.2. The classification system used for the different seams. 29
Figure 5.1. Core photos of (A) Dark claystone, facies 1.. 39
Figure 5.2. Core photos of facies 3, very fine sandstone. 40
Figure 5.3. Core photos of the mudstone, facies 4..... 42
Figure 5.4. Core photos of the wackestone, facies 5 (A) 43
Figure 5.5. The different occurrences of the Foraminiferic wackestone/packstone 45
Figure 5.6. Core photos of the Palaeoaplsyina/phylloid algae boundstone 47
Figure 5.7. Core photos of (A) the stromatolite bindstone facies 8. 49
Figure 5.8. Core photo of (A) Grainstone, facies 9 with densely packet foraminifera. 50
Figure 5.9. Core photos of the different anhydrite facies presented within the core.. 52
Figure 5.10. The identified fossil occurring at 141.5 – 141.0 m depth. 53
Figure 5.11. Legend for the sedimentary logs. 54
Figure 5.12. The sedimentological log drawn of the core including 174 – 118. 55
Figure 5.13. Continued sedimentological log of the core from 118 – 62 m depth. 57
Figure 5.14 Continued sedimentological log including 62 – 26 m. 59
Figure 5.15. Micrograph of the different facies and their. 62
Figure 5.16 Micrograph of the different facies and their porosity distribution. 63
Figure 5.17. (A) A summary of the different porosity classes. 66
Figure 6.1. (A) The number of dissolution seams per meter, versus depth and lithology 69
Figure 6.2. Figure showing the type of styles of stylolites and their distribution 71

Figure 6.3. The distribution of the nodule-bonding seams in the core. 73
Figure 6.4(A) The mean amplitude value for the individual registered stylolite..... 75
Figure 6.5. The two lower boundstones in section 2 blown up 76
Figure 6.6. The style of the stylolites and their distributions with depth..... 77
Figure 6.7. Shows how the swarms of dissolution seams. 79
Figure 6.8. Includes Figure 5.17 representing the porosity……. 80
Figure 6.9. Micrograph showing the cement distribution composition of section 2.. 83
Figure 6.10. Micrograph of (A) Microdolomite texture present. 84
Figure 6.11. Scattered packet dolomitzed mudstone. 85
Figure 6.12. (A) Picture taken form the core where a pressure solution 87
Figure 6.13. (A) A formaminifera that is crosscut by a stylolite. 89
Figure 6.14. Micrograph taken in plane light showing thicker 90
Figure 6.15. (A) Two stylolites where one of them terminates into the other 91
Figure 7.1. Cross section of the interpreted carbonate ramp……... 94

List of tables

Table 1 Classification system introduced by Lønøy (2006). 24
Table 2. The Udden – Wentworth grain-size scale 27
Table 3. The classification of the pressure solution seams. 30
Table 4. Cement terminology after Ehrenberg et al. (1998b). 33
Table 5. Overview of the interpreted facies in the core. 35
Table 6. An overview of the porosity classifications. 61

1 Introduction

1.1 Aim of study

The aim of this study has been to provide knowledge about the controlling factors of the pressure solution seams distribution and behavior within core 7030/03-U-01, where the depositional environment has been interpreted for the core, the seams has been systematized after different characteristics and studied in thin sections. Additionally, the porosity types for the different lithologies have been classified in thin sections and evaluated. Investigation of the controlling factors of the porosity distribution has been done and the seams effect on the porosity has been noted.

1.2 Study area

The Barents Sea shelf is located on the north-western corner of the Eurasian plate, bordering the Arctic Ocean in the north, Novaya Zemlya in the east, the Norwegian and Russian coasts in the south and the Norwegian - Greenland Sea in the west (Worsley, 2008). The shelf is covering an area of approximately 1.3 million km^2, and together with its average water depth of 300 m, it constitutes one of the largest areas of continental shelf in the world (Doré, 1995). The Barents Sea is split by a north-south trending monoclinal that separates the sea in to one eastern- and one western geological province (Worsley, 2008, Smelror et al., 2009). The studied core (7030/03-U-01) was drilled at the Finnmark Platform, located in the western province (Figure 1.1). Here the current structural elements are a result of a complex tectonic development, represented by basins, structural highs and platforms (Figure 1.1) reflecting different tectonical events along the western and north-western margins of the Eurasian plate through time (Worsley, 2008).

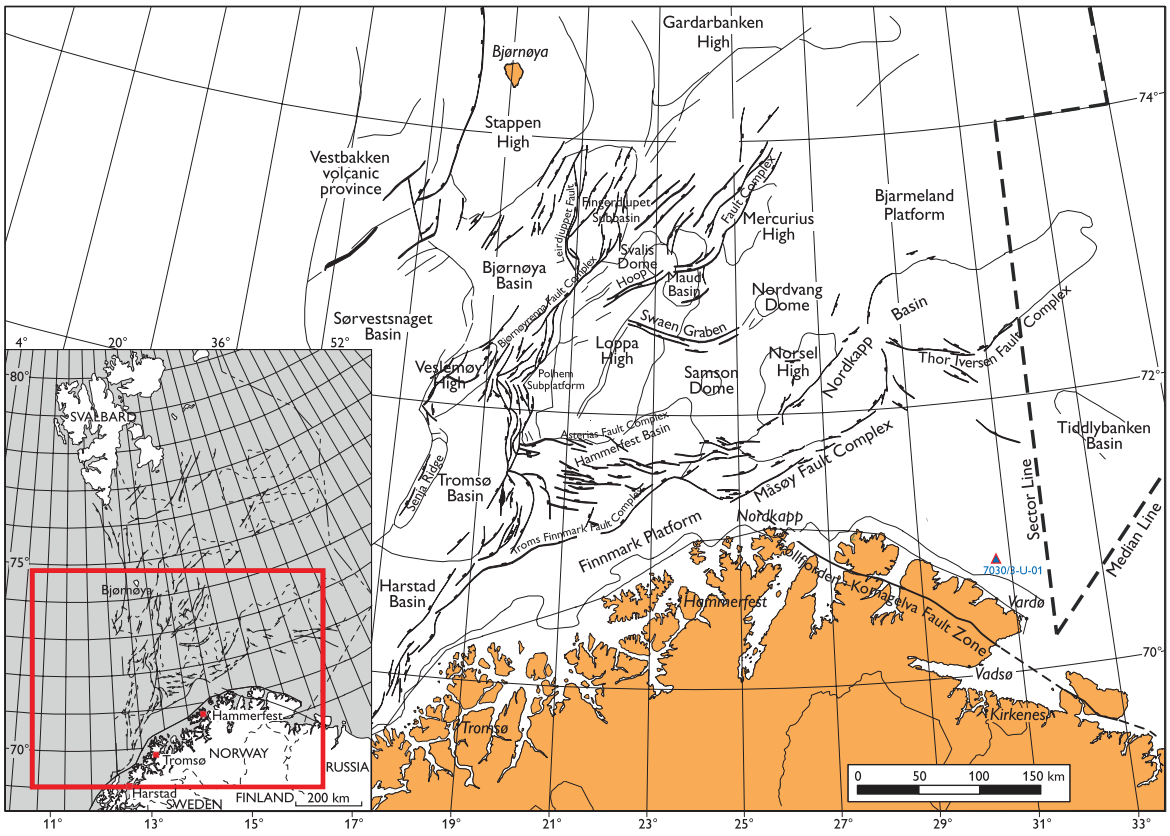

Figure 1.1. Map of the studied area showing the main structural elements, modified from Larssen et al. (2002). The triangle shows the location of the studied well.

The Finnmark Platform is defined after the nomenclature introduced by Gabrielsen et al. (1990), for more detailed information on earlier nomenclature it is referred to Gabrielsen et al. (1990).

The Finnmark Platform is oriented parallel to the coastline of the northern counties of Norway and is bounded in the south by the Norwegian mainland, in the west by the Ringvassøy-Loppa Complex and by the Hammerfest and Nordkapp basins in the north as shown in Figure 1.1 (Bugge et al., 1995, Larssen et al., 2002, Samuelsberg et al., 2003). The Platform can generally be divided into two different structural provinces, where the areas west of approximately 25°E shows relatively stable tectonic history whereas in the east, where the studied core is located (Figure 1.1) an underlying rift topography occurs (Larssen et al., 2002). However, in overall the Finnmark Platform has been a relatively stable segment of the western Barents Sea since the Late Paleozoic (Gabrielsen et al., 1990, Samuelsberg et al., 2003).

1.3 Previous work

Since petroleum exploration started in the western part of the Barents Sea in the 1980s, an accumulation of geological information about the Finnmark Platform and the upper Paleozoic succession has developed (Larssen et al., 2002, Smelror et al., 2009). As the research mostly has occurred due to hydrocarbon exploration, most of the information is based on these exploration programs. In addition, outcrops of the Upper Paleozoic sediments onshore Svalbard has shown to be good analogues to the geology of the Barents Sea and the introduction of 3D seismic has helped extending a far more detailed knowledge of the Upper Paleozoic carbonate build-ups at the Finnmark Platform (Smelror et al., 2009).

The Finnmark platform has been investigated in different scales. This includes Samuelsberg et al. (2003) who presented a larger scaled definition of the platforms evolution. Based on seismic data and information from four exploration wells and some shallow drillings from IKU program, a seismic facies analysis of the Upper Paleozoic succession on the Eastern Finnmark Platform was established. In total five seismic sequences were defined and further used to describe the evolution of the Finnmark Platform which also was compared with areas nearby.

Bugge et al. (1995) published one of the earlier studies of the Upper Paleozoic succession on the Finnmark Platform. Based on fourteen seismic units correlated with eight cores, including well 7030/03-U-01 which is the core studied here, four stratigraphic units were defined. These were further discussed with emphasis on stratigraphy based on seismic, sediments and biostratigraphical data.

A more detailed work of the Finnmark carbonate platform Upper Paleozoic sediments and their development has been done by Ehrenberg et al. (1998a). Based on well 7128/6-1 and 7128/4-1 it has been defined nine lithostratigraphic units with accompanied facies interpretation and cycles. These have further been used to define seven depositional sequences that together represent a one-dimensional model for the depositional evolution of the platform. As an extension of this paper Ehrenberg et al. (2000) published a paper on the sequence stratigraphy on the Upper Carboniferous-Permian succession of the inner Finnmark carbonate platform. Here a correlation between well 7128/6-1 and five shallow IKU cores, including the one studied here was done, motivated by hydrocarbon exploration. As a result a

two-dimensional model for deposits at the inner platform was made, where dip-oriented lateral variation in lithology and parameters for reservoir condition were described.

A more detailed study on the diagenesis and reservoir quality of the Finnmark carbonate Platform was published by Ehrenberg et al. (1998b) as a supplement to Ehrenberg et al. (1998a). Here the study material was the same, and the defined lithostratigraphic units and sections were used as a base. Mainly the study emphasizes different diagenetic features and how they can be related to the depositional environment and the existing porosity. In total, four distinct stages including different reservoir conditions were identified as correlative to the platforms evolution. Ehrenberg et al. (1998b) emphasized different types of cement and dolomite and their effect on the porosity within the defined four stages. Stylolites are also mentioned in their study and are investigated in greater detail in the present thesis.

2 Regional geology

In late Paleozoic, the Barents Sea region and the Finnmark Platform were part of the E-W oriented shelf constituting the northern part of Pangea (Stemmerik and Worsley, 2005, Worsley, 2008). During this time period, the area shifted paleolatitude from approximately 20º N to approximately 45º N with the rate of 2-3 mm per year (Stemmerik, 2000, Stemmerik and Worsley, 2005, Ramberg et al., 2007). Also, as a result of continental plate movement, second-order sea level fluctuations characterize the Late Paleozoic (Mid Carboniferous – Early Permian) together with third-order glacio-eustatic fluctuations in the sea level reflecting the different phases of the Gondwana glaciations (Stemmerik and Worsley, 1989, Ramberg et al., 2007, Worsley, 2008). The gradual shift in latitude carried the shelf through several climatic zones, and in combination with the other dominating factors occurring in the Late Paleozoic they naturally had a big influence on the depositional conditions, which resulted in a complex composition of the sediments succession in the Barents Sea (Stemmerik, 2000, Ramberg et al., 2007, Worsley, 2008). The geological events and the resulting lithostratigraphy are summarized in Figure 2.1.

2.1.1 Early Paleozoic

Generally two tectonic events and accompanied structural features have been important and controlling for the structural trend of Late Paleozoic structural products; the NW-SE trending structures formed by the Late Precambrian Baikalian orogeny and the NE-SW structural trend developed by the Caledonian orogeny (Siedlecka, 1975, Faleide et al., 1984, Gudlaugsson et al., 1998). In Early Devonian, the Barents Sea shelf was located close to equator at the northern side, which resulted in arid conditions (Faleide et al., 1984, Ramberg et al., 2007). The sedimentation in the northern and western part was controlled by the formation and erosion of the Early Devonian Caledonian orogeny, where continental siliciclastic sediments were deposited in the intra-cratonic and foreland basins that were defined by the Caledonian structures (Faleide et al., 1984, Smelror et al., 2009). These sediments are sparse in the western Barents Sea and at the Finnmark Platform as they only occur in a few grabens and sub-basins (Smelror et al., 2009). A climatic shift from the arid southern zone to the

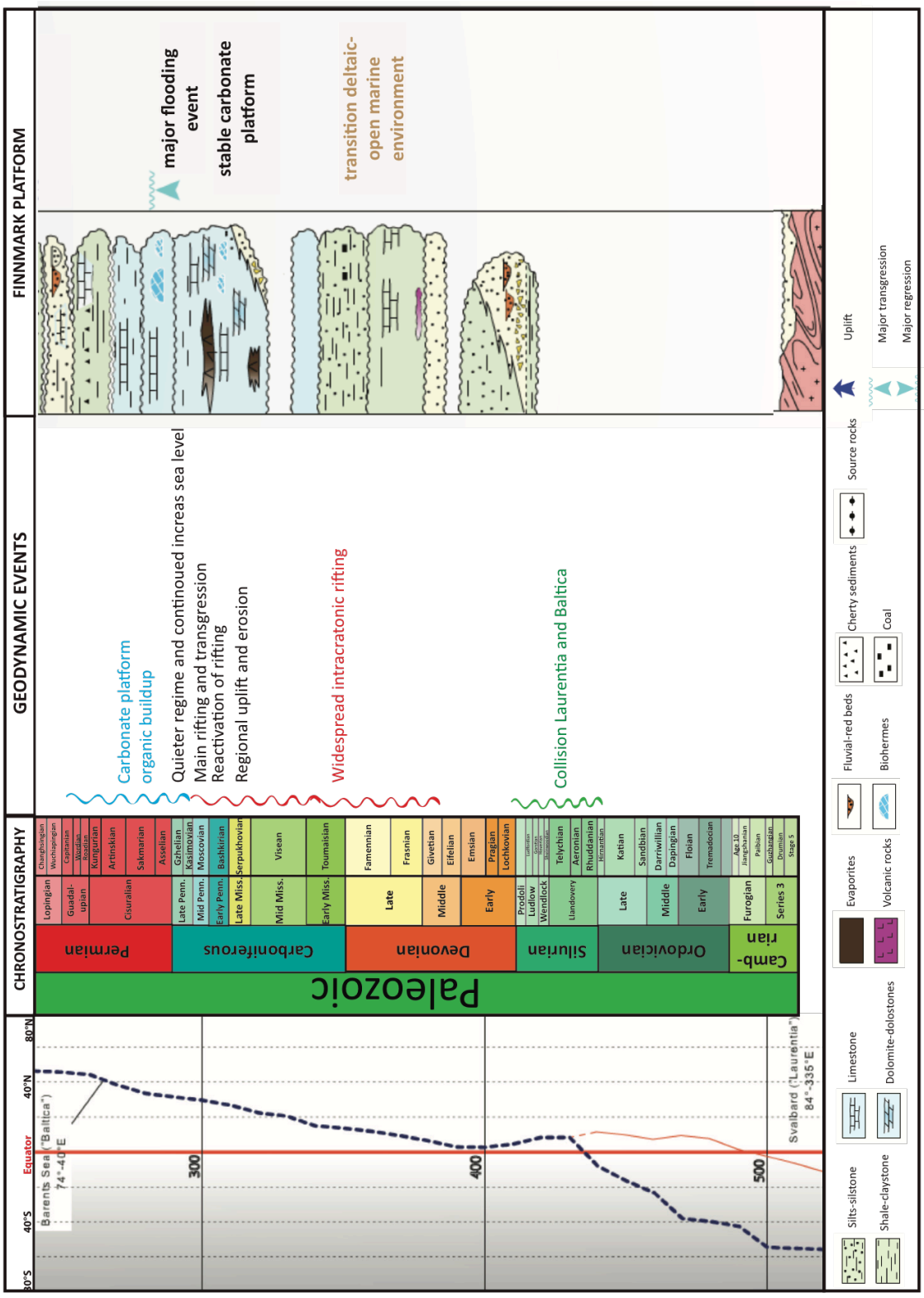

Figure 2.1. Geological events, paleolatitude of Laurentia and the Barents Sea and litostratigrahy of the Finnmark Platform. Figure modified after Smelror et al. (2009).

equatorial tropics occurred during the transition between Early and Middle Devonian, which was reflected in the sediments as they changed from red to grey siliciclastic sediments (Ramberg et al., 2007, Worsley, 2008).

2.1.2 Late Devonian - Early Carboniferous

The depositional conditions and the sediment patterns that dominated in the Early Devonian continued until the transitions between the Late Devonian – Early Carboniferous (Smelror et al., 2009). At this point a shift from the Caledonian compressional system to an extensional regime took place with half grabens of different sizes and rift basins as products (Faleide et al., 1984, Stemmerik and Worsley, 1989, Gudlaugsson et al., 1998, Ramberg et al., 2007). The rift basins were defined by both the Caledonian NE-SW trending structural framework and by newly establishing structures with dextral movements along WNW-NW-trending faults (Faleide et al., 1984, Stemmerik and Worsley, 1989, Ramberg et al., 2007, Smelror et al., 2009). These rifting movements also defined the beginning of the long-term Atlantic and Artic linked rift systems (Stemmerik et al., 1991, Stemmerik, 1997, Stemmerik and Worsley, 2005). The Finnmark Platform was generally experiencing the same formation of NE-SW trending extensional fault as the rest of the western Barents Sea, though with internal structural variations (Gudlaugsson et al., 1998, Samuelsberg et al., 2003). The northeastern part of the Finnmark Platform was dominated by a relatively quiet regime with uniform subsidence whereas in the southeastern part the formation of several rotated half-grabens following the NW-SE oriented Baikalian structures were formed (Samuelsberg et al., 2003). The Barents Sea shelf and the Finnmark Platform were located at a latitude of 20 °N (Figure 2.1) during this time, which represent a warm and humid terrestrial environment and fluvial and lacustrine sediments known as the Billefjorden Group were gradually taking over the deposition in the half-graben areas (Larssen et al., 2002, Stemmerik and Worsley, 2005, Ramberg et al., 2007, Worsley, 2008, Smelror et al., 2009). Although the Billefjorden Group was dominating at the Finnmark Platform, internal variations occurred where the western part was dominated by flood plain deposits whereas the eastern part consisted of both continental and marine deposits (Bugge et al., 1995, Samuelsberg et al., 2003).

In the Visean time the half-graben sedimentation in the Barents Sea changed from fluvial to alluvial fan sediments, and in the Late Visean fluvial deposits at the Finnmark Platform were

succeeded by shale and carbonates due to a transgression from the east (Bugge et al., 1995, Worsley, 2008, Smelror et al., 2009).

2.1.3 Middle- Carboniferous

During the Serpokohivan times a regional uplift resulted in an erosional unconformity, and together with the simultaneous change in climate from humid to semi-arid and arid they made a boundary separating the Early and Middle Carboniferous sediments in most of the areas of the Barents Shelf (Bugge et al., 1995, Stemmerik and Worsley, 2005, Worsley, 2008, Smelror et al., 2009). The same trend is seen in most of the areas at the Finnmark Platform, and a break in the deposition lasted until Late Moscovian (Figure 2.1) (Stemmerik, 2000, Stemmerik and Worsley, 2005, Ramberg et al., 2007). This unconformity was followed by a reactivation of rifting and subsidence during mid – late Bashkirian, following a similar structural evolutional trend as in the Early Carboniferous, though more intensely (Steel and Worsley, 1984, Stemmerik and Worsley, 1989, Stemmerik and Worsley, 2005, Ramberg et al., 2007). In addition to occur along old basin margins new N-S oriented local rift basins and new half-graben systems in the Barents Sea were formed (Steel and Worsley, 1984, Stemmerik et al., 1991, Ramberg et al., 2007). At the Finnmark Platform the product of this rifting were rotated fault blocks following the WSE-ENE Caledonian trend west of 28°E and ESE-WNW Baikalian trend east of 28°E (Dengo and Røssland, 1992). The main rifting occurred during the late Bashkirian and early Moscovian in the Barents Sea area at the same time as a regional transgression took place (Stemmerik, 2000, Smelror et al., 2009). This increased sea level combined with the climatic conditions had a major effect on the depositional environments in the Barents Sea where the siliciclastic deposits gradually became overlaid by warm-water carbonate sediments at the platform areas whereas evaporites occurred at the deep basin and peritidal areas (Stemmerik, 2000, Stemmerik and Worsley, 2005, Smelror et al., 2009). At the Finnmark Platform the syn-rift deposition occurred within the half-grabens and the ongoing transgression did not reach the platform area until the Late Moscovian, then the platform was incorporated into a E-W oriented marine shelf (Bugge et al., 1995, Samuelsberg et al., 2003). The change in depositional conditions and accompanied sediments were the same at the platform as in the rest of the Barents Sea and this transition also defines the change from unstable pre-platform state to the stable platform (Gabrielsen et al., 1990, Bugge et al., 1995, Samuelsberg et al., 2003).

2.1.4 Late Carboniferous – Early Permian

In the Upper Carboniferous a quieter tectonic regime was dominating, where a decrease in the local rifting and a more uniform subsidence where taking over the areas of the Barents Sea (Ramberg et al., 2007, Smelror et al., 2009). The continuing sea level rise from the mid-Carboniferous submerged the old structural highs and transformed the region into a big intracratonic basin (Stemmerik and Worsley, 1989). The climate was still warm and arid, and the depositions occurred in cyclic parasequences, reflecting the sea-level alternations caused by the Gondwanan glaciation (Larssen et al., 2002, Ramberg et al., 2007, Worsley, 2008). The sediments deposited, known as the Gipsdalen Group (see section 2.2.1) were dominated by shallow marine warm water carbonates in periods with high glacio-eustatic sea levels whereas in periods with low-stand, sabkha sediments and local siliciclastics were deposited (Stemmerik and Worsley, 1989, Larssen et al., 2002, Stemmerik and Worsley, 2005, Ramberg et al., 2007, Worsley, 2008). By the Early Gzelian the Finnmark Platform was a large warm-water carbonate shelf (Samuelsberg et al., 2003). A short-lived sea level fall occurred during the late Gzelian which led to an exposure and erosion simultaneous as the former epicontinental sea was transformed into sabkha areas (Stemmerik and Worsley, 1989, Ramberg et al., 2007). The removal of the Gondwanan ice cap is assumed to be the reason for the following sea level rise that occurred in the mid-Sakmarian as much of the areas were drowned and transformed into a carbonate platform (Stemmerik and Worsley, 1989, Worsley, 2008). This flooding event marked the end of the prominent high frequency fluctuations in the sea level at the same time as a change from shallow warm water to temperate conditions took place (Ramberg et al., 2007, Worsley, 2008). As a consequence of these new conditions, sediments consisting of cool water biota, also known as the Bjarmeland Group, replaced the former warm water biota in the Barents Sea and the Finnmark Platform was during the Sakmarian transformed into a temperate - cool water platform (Stemmerik and Worsley, 1989, Larssen et al., 2002, Samuelsberg et al., 2003, Stemmerik and Worsley, 2005, Worsley, 2008). The sediments deposited during this time were most common at the basinal margins and the depositions at the Finnmark Platform was limited to a narrow belt along the northern margin, whereas a sparser or absent sediment accumulation occurred at the inner platform areas and the structural heights (Samuelsberg et al., 2003, Stemmerik and Worsley, 2005, Worsley, 2008). An uplift of the southern Barents Sea and thereby the Finnmark platform

occurred during the Upper Sakmarian – Lower Artinskian that led to a fresh water alteration of the carbonates (Stemmerik and Worsley, 2005, Worsley, 2008).

2.1.5 Late Permian

The sediments deposited during the Kungurian – Wuchiapingian, known as the Tempelfjorden Group, are separated from the underlying succession by a short period of erosional unconformity in most areas in the Barents Sea, whereas at the platforms the boundary occur as a minor time of subaerial exposure surface (Stemmerik, 2000, Worsley, 2008). Shortly after the unconformity and the subaerial exposure took place, a flooding event occurred as a result of a rise in the relative sea-level (Stemmerik, 2000, Worsley, 2008). This sea level rise was mainly a consequence of the development of the intracratonic seaway at the western margin, connecting the Boreal Realm with the Zechenstein Basin in northern Europe, and in addition, an increase in tectonic subsidence and a rise in the eustatic sea level seems to have played an essential role (Stemmerik, 2000, Stemmerik and Worsley, 2005, Worsley, 2008). The flooding made the basins and basin margins deeper at the same time as the sediment deposition changed from cool-water carbonates to the Tempelfjorden Groups deep-water spiculites, shales and minor siliciclastics (Stemmerik and Worsley, 2005, Worsley, 2008, Larssen et al., 2002).

2.2 Stratigraphy

The Late Paleozoic succession in the south-western Barents Sea shelf can be separated into three different lithostratigraphic groups (Figure 2.2), where each reflects individual depositional environments (Worsley, 2008). Of these groups, two comprises carbonate sediments; the Gipsdalen Group with warm-water carbonates and the cold water carbonates within Bjarmeland Group (Larssen et al., 2002). However, within this study only the former one is relevant for the project and would be emphasized.

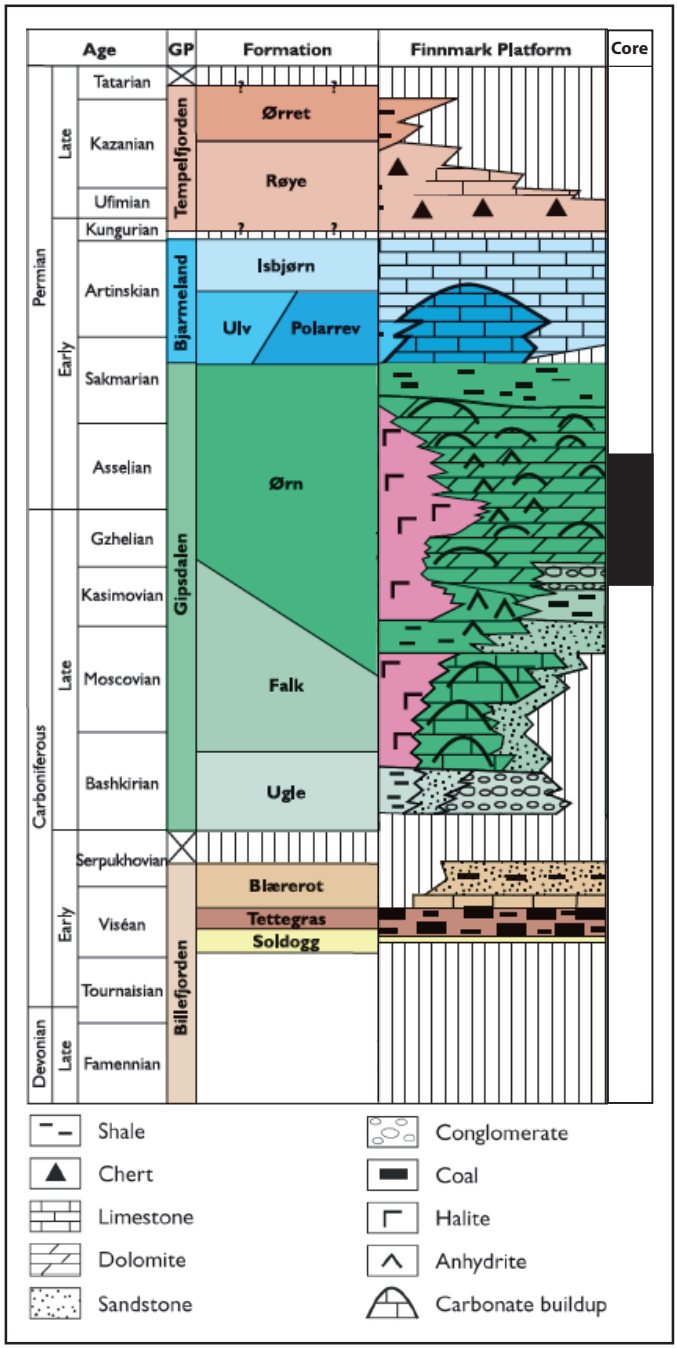

Figure 2.2. Simplified stratigraphic log of the Upper Paleozoic succession correlated with the geological time scale on the Finnmark Platform, figure modified from Larssen et al. (2002). The logged core of this study belongs to the Falk and Ørn Formation and is also marked in the figure (Bugge et al., 1995).

2.2.1 The Gipsdalen Group - Stratigraphy

The Gipsdalen Group represents the sediments deposited in the southern Norwegian Barents Sea in the period Mid Carboniferous to Early Permian (Upper Serpukhovian – Sakmarian/Lower Artinskian) (Larssen et al., 2002). The climate during the groups deposition was warm and arid at the same time as the sediment pattern was reflecting the changing phases of the Gondwana glaciations by high frequency and high fluctuations in the sea level (Stemmerik, 2000, Worsley, 2008). The group is divided into three formations, where each represents diachronous stages of depositional environments (Larssen et al., 2002, Worsley, 2008). The basal Ugle Formation consists of terrestrial red-bed sandstones, siltstones and conglomerates, which were deposited in an arid to semi-arid environment in a period of active rifting in the Late Serpukhovian to Bashkirian (see section 2.1.3), the following Falk and Ørn Formation will be described underneath. At the Finnmark Platform this group was deposited in a northwards dipping low-angle ramp (Larssen et al., 2002).

2.2.2 The Falk Formation

The Falk Formation was deposited during Late Carboniferous at the Finnmark Platform (Figure 2.2) (Larssen et al., 2002). In general, the deposition of the formation occurred in a shallow shelf environment during an overall transgression. The sediments characterizing the formation are mainly a mixture of sandstones and carbonates of shallow-marine origin, and marine siltstone (Larssen et al., 2002). Based on the sediments occurrence in formation, the formation could roughly be divided into a lower and upper part. The lower part represents the sediments deposited during the ongoing transgression and comprises cyclic units of facies from shoreface sandstone and offshore silt that mainly includes coarse-grained sandstone and varying amount of shale and dolomite. The upper part on the other hand reflects that most of the platform was flooded and a deposition in offshore to lower shoreface environments prevailed. Here, fine-grained siliciclastic sediments and subtidal carbonates as mudstone to boundstone facies with fossils as brachiopods, crinoids, foraminifers, corals and some *Palaeoaplysina* plates and phylloid algae were dominating (Larssen et al., 2002). A varying thickness of the Falk Formation occur within the wells summarized by Larssen et al. (2002), ranging from 58 – 201.7 m. Equivalent deposits to the Falk Formation can also be correlated

with sediments at Bjørnøya and Spitsbergen. For more detailed information regarding this correlation and the Falk Formation see Larssen et al. (2002).

2.2.3 The Ørn Formation

The overlying Ørn Formation is of Late Carboniferous to Early Permian age (Figure 2.2)(Larssen et al., 2002). This formation is characterized by warm-water carbonate biota that occur in cycles and includes foraminifera, fusulinids, calcareous algae and fragments of *Palaeoaplysina*, together with minor crinoids, bryozoans, brachiopods and corals (Larssen et al., 2002). The lower succession of the formation occurring at the platform areas is generally recognized as comprising three different compositions, where the lower part occur in cycles and consist of mixed layers of dolomitic mudstone and bryozoan wackstone with thin shales. These are followed by *Palaeoaplysina* build-ups interbedded with fusulinid wackestone and at the end topped by a dolomitic mudstone with sufficient nodules of anhydrite. The upper succession in the same areas is characterized by foraminifera- and algal-rich packstones and grainstones overlain by cyclic successions of shales and silty crinoids wackestones which gradually pass into a foraminifer-dominated packstone and grainstone (Larssen et al., 2002). At the Finnmark Platform the lower part of the formation consist of large local up-dip sabkha deposits together with units of dolomitic mudstone with anhydrite nodules. As a result of stacking of smaller build-ups, huge carbonate mounds occur in the more distal areas of the platforms. Concurrent at the deepest parts of the platform, interbedded subtidal, highstand carbonates and lowstand anhydrite occur whereas in the basin center halite appears as a consequence of a lowstand, and the basin was isolated from the sea (Larssen et al., 2002). The formation shows a big thickness variance in the wells summarized by Larssen et al. (2002), ranging from 79 m up to over 1000 m and correlative sediments are found at Bjørnøya and Spitsbergen (Larssen et al., 2002).

3 Theory

3.1 Terminology

Build-ups: A common feature within the core is accumulations of the fossil *Palaeoaplysina.* Several terms have been used to describe this reef building organism however, within this study the structures would be termed build-ups with the definition "A body of locally formed (laterally restricted) carbonate sediment which processes topographic relief" (Wilson, 1975, p.20).

Pressure solution seams: The seams in this study is divided into two categorizes including dissolution seams and stylolites, however when referring to both of the seams, the term pressure solution seams would be used for simplicity.

3.2 Carbonates

Carbonate sediments are made as skeletals marine organisms or as direct precipitation from sea water, and therefore, the majority of carbonates are made close to their deposition (Bosence and Wilson, 2003). According to Bosence and Wilson (2003) there are three types of carbonate factories including warm-water, cool-water and pelagic, however within this study, only the warm-water environment is relevant. The warm water carbonate factory occurs in shallow-marine tropical waters that often are supersaturated with calcium carbonate. In this environment, high productions of organisms depending on the photosynthesis to exist occur (Bosence and Wilson, 2003).

3.2.1 Formation and setting

After deposition the carbonate sediments are generally more exposed to diagenetic processes than the siliciclastic sediments (Boggs, 2011). Digenesis of carbonate sediments " includes the dissolution, neomorphism and replacement of unstable minerals, the compaction of grains and lithification by precipitation the precipitation of void-filling cements" (Scoffin, 1987, p. 89). In the deep burial-diagenetic regime (Figure 3.1), also known as the analogue

mesogenetic zone by Choquette and Pray (1970), the diagenetic features are controlled by both intrinsic and extrinsic factors according to Choquette and James (1987). The most important intrinsic ones are mineralogy, amount and origin of organic matter, presence of liquid hydrocarbons and pore water chemistry (Choquette and James, 1987, Moore and Wade, 2013). Occurrence of Mg-calcite and aragonite in the carbonate sediments during burial would make the sediments more exposed to dissolution and cementation, whereas the existent of clay minerals or other unstable minerals would make the deposits more exposed to physical and chemical compaction. If liquid hydrocarbons are present during burial, prevention of chemical compaction in the sediments would occur (Choquette and James, 1987). Also, the pore water chemistry is important within the burial diagenetic regime, though, mostly in coherence with chemical compaction. For instance, chemical compaction would be prevented by the presence of Mg-rich pore water and further, the pore water naturally would be recipient of ions when dissolution or absorption by cementation and replacement occur (Choquette and James, 1987, Flügel, 2010).

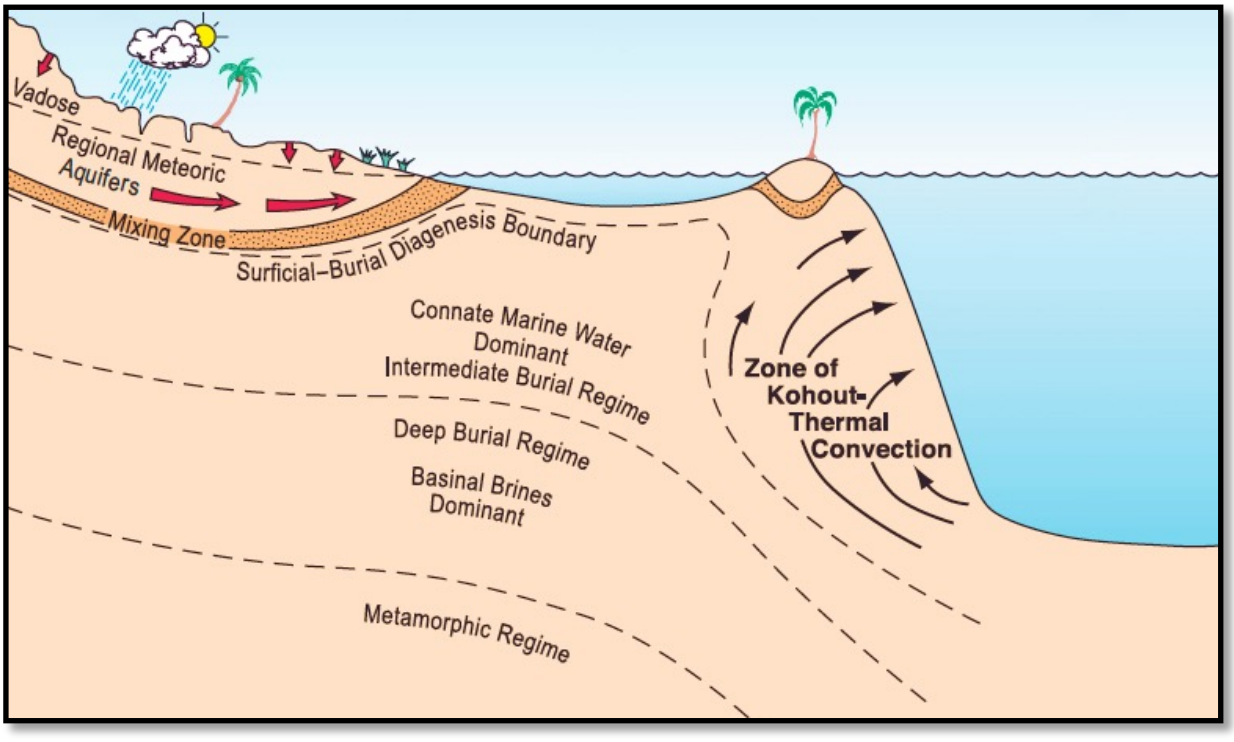

Figure 3.1. Schematic diagram showing relationship of the different burial diagenetic regimes. Figure taken from Moore (1989).

Among the extrinsic factors, temperature and pressure are the most important (Choquette and James, 1987, Moore and Wade, 2013). The temperatures rely on the sediments thickness and

geothermal gradient. An increased temperature would result in decreased solubility of calcite which would favor calcite cementation (Choquette and James, 1987). Furthermore, a combination of increased temperature and pressure would promote chemical reactions among minerals, releasing water and ions that could promote diagenetic processes (Choquette and James, 1987, Moore and Wade, 2013). Higher temperature over time results in maturation of the organic matter to hydrocarbons and other organic compounds through catagenesis (Barnes et al., 1984). The other important extrinsic factor within the burial diagenetic regime is the pressure. Though, only the lithostatic, hydrostatic and the direct pressure are considered to be prominent within this regime (Choquette and James, 1987, Moore and Wade, 2013). In general the effective stress is small, however in some situations the pore pressure will be higher than the lithostatic causing a overpressure where pore fluid is supporting the overburden load. Several processes could favor this condition and the result could be inhibiting of physical compaction, pressure solution and cementation (Choquette and James, 1987). Concurrently, if the effective stress becomes too low, the mechanical and chemical compaction would be slow and could stop (Moore and Wade, 2013).

3.2.2 Processes and products

Within the burial diagenetic regime several processes occur, though mechanical and chemical compaction are considered to be most important in affecting the marine carbonate sediments (Choquette and James, 1987, Flügel, 2010).

Mechanical compaction

Mechanical compaction of marine sediments can mainly be divided into three stages with some overlap (Choquette and James, 1987, Flügel, 2010). Firstly, within the first meters after burial the most important process of mechanical compaction among muddy sediment would occur (Choquette and James, 1987, Flügel, 2010). This would include dewatering as a result of particle setting and repacking, and the porosity loss of mud would be 20-25% (Choquette and James, 1987, Flügel, 2010). Secondly, in the following stage, also occurring in the first meter after burial, a reorientation of the grains appears and the muddy sediments continue to dewater until a stable framework is formed. Here, the porosity would be reduced to around 40%. And thirdly as the final stage of the mechanical compaction, the overburden pressure would affect the grain contacts, resulting in plastic deformation or brittle fractures or

breakages (Choquette and James, 1987, Flügel, 2010). The sedimentological products formed during mechanical compaction of carbonate sediments has a broad diversity due to the varying compositions of the original components as shown in Figure 3.2 (Choquette and James, 1987).

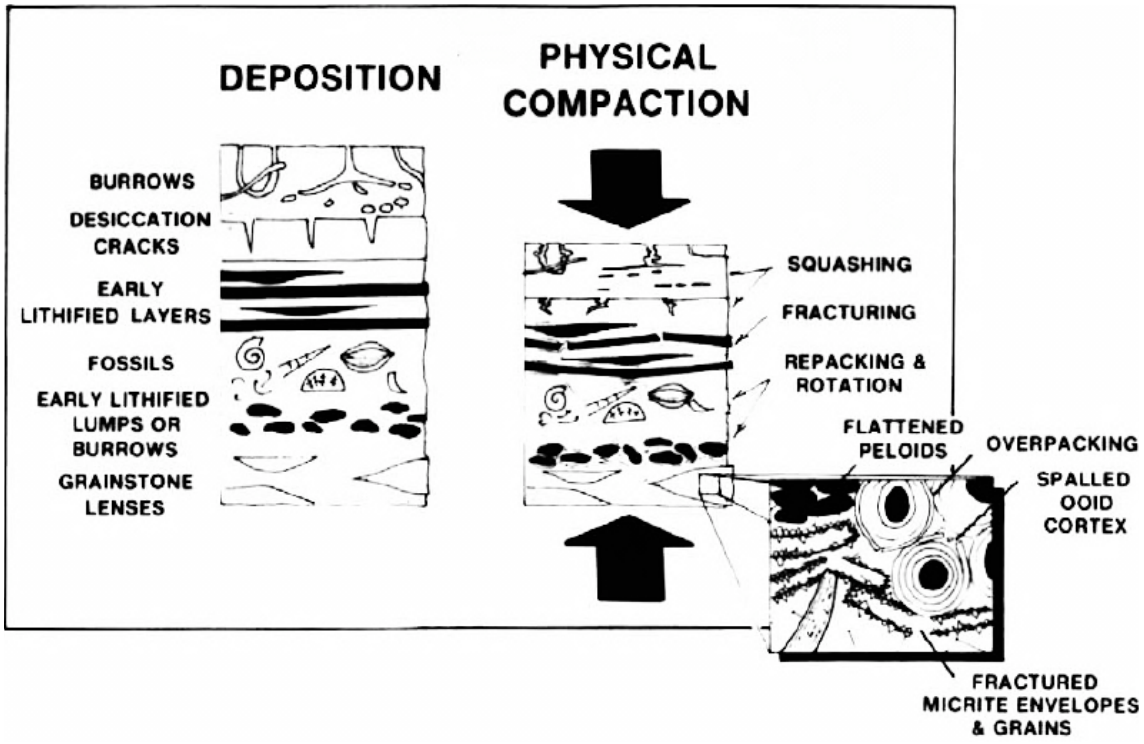

Figure 3.2. Figure from Choquette and James (1987) showing the sedimentological products formed by mechanical compaction.

Chemical compaction

Following the mechanical compaction when a stable framework has formed within the carbonates, a continued applied overburden pressure would result into chemical compaction also called pressure solution (Choquette and James, 1987, Flügel, 2010, Moore and Wade, 2013). The pressure solution process takes place by a concentration of the applied pressure at contact points at the surface between grains, crystals or limestone beds, and tends to develop along seams at right angle to the maximum stress, that normally is parallel to the bedding (Choquette and James, 1987, Scoffin, 1987). Within the contact point, an increased solubility of the stressed mineral would occur because of the enlarged elastic strain, and dissolution releasing ions would occur (Choquette and James, 1987). Since the stress is reduced away from the contact point the ions would move into these areas either by diffusion, fluid flow or

both and could precipitated as cement in the nearby areas where the pressure is lower, or it could be transfer more distally (Choquette and James, 1987, Scoffin, 1987).

According to Wanless (1979), when studying carbonate sediments behavior when they are exposed to stress, it could be helpful to think of them as a package of crystals that have different resistance and response to change, at the same time as the amount of impurities would affect the behavior. Due to these impurities, the products formed by chemical compaction are various (Figure 3.3), though the most common ones are stylolites and dissolution seams that internally could occur in various occurrences, styles, amplitudes and scales (Wanless, 1979, Choquette and James, 1987, Moore and Wade, 2013). The stylolites

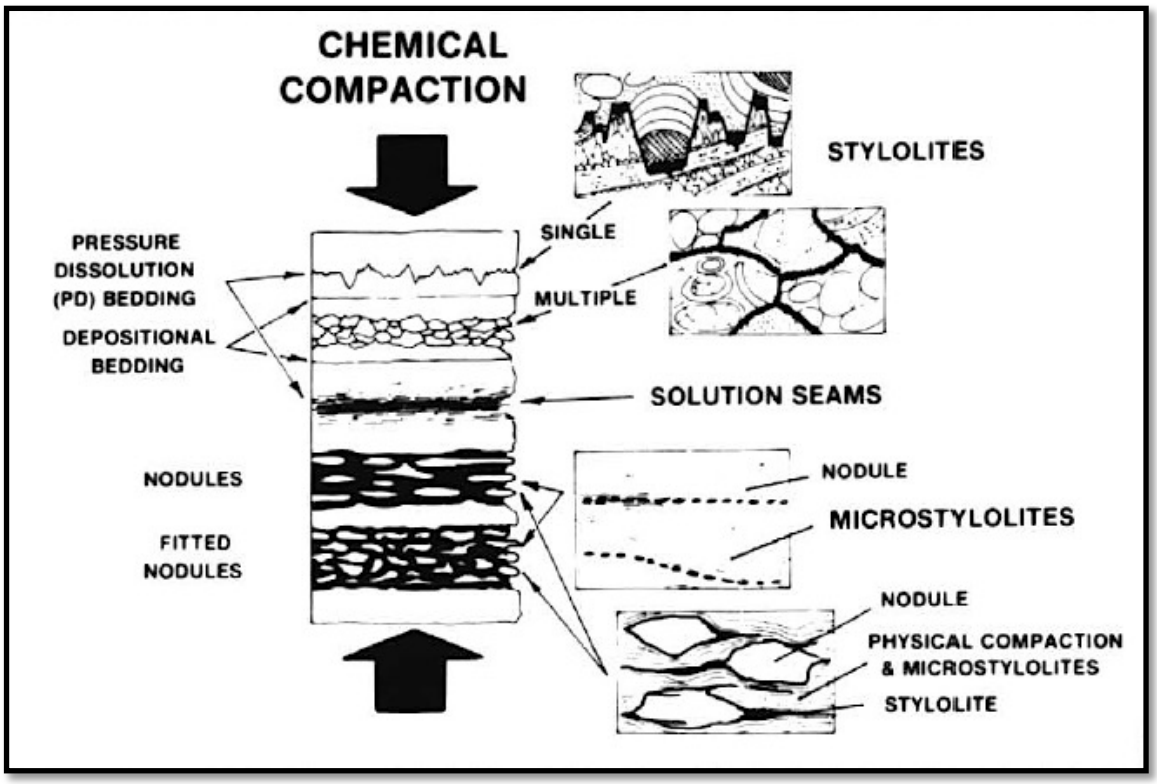

Figure 3.3. Figure from Choquette and James (1987) showing the products formed by chemical compaction.

are normally recognized as irregular sutures that have a tooth-like, columnar style on one side that fits into the counterpart at the other side, and often, insoluble materials are concentrated at the stylolites surface (Figure 3.3). The dissolution seams on the other hand, are thin seams of insoluble material that can show similar styles as the stylolites, although in a minor scale at the same time as they normally are more flat and occur as both individuals and as swarms

(Figure 3.3) (Flügel, 2010). The formation of stylolites involves reduction of the bulk volume and therefore also transformations in the original sedimentary fabric including reduction in the porosity (Flügel, 2010, Moore and Wade, 2013). The factors determining the type of seam to form rely on the resistance to stress together with the amount of insoluble material in the host rock. Where the host rock is missing or is low in insoluble material (<5-10%) and the limestone boundaries have structural resistance, stylolites would form (Wanless, 1979, Tucker et al., 1990). However, where higher amounts (>10%) of insoluble material as clay or organic material are present in the host rock, dissolution seams would form (Wanless, 1979, Choquette and James, 1987). As the seams are so various, several attempts of establishing a classification system for the seams has developed, e.g. Park and Schot (1968) with focus on the geometry of the stylolite seam in combination with its relation to the bedding plane of the host rock, Logan and Semeniuk (1976) with focus on the morphology and Railsback (1993b) who quantified the morphology of the pressure solutions surfaces. However, due to the complexity of the seams it is debated how to classify the pressure solution seams (Koehn et al., 2007).

Within carbonate sediments, the chemical compaction could take place already from a couple of hundred meters burial ranging up to 1500 m depth (Boggs, 2011). However, the timing of when it would take place would rely on several interacting factors e.g. the overburden pressure, temperature, early cementation and dolomitization, chemistry and flow rates of the water, pore-fluid pressure, occurrence of liquid hydrocarbons, $CaCO_3$ mineralogy, content of clay mineral and organic matter, and host rock porosity and permeability (Choquette and James, 1987).

Dolomitization

Dolomite is limestone comprising more than 50 % of the mineral dolomite, also known as calcium magnesium carbonate [CaMg(CO3)2] which often is a diagenetic product of limestone (Tucker et al., 1990, Boggs, 2011). This diagenetic process occur by dolomite replacing calcium carbonate by the reaction:

$$2CaCo_3 + Mg^{2+} = CaMg(CO_3)_2 + Ca^{2+}$$

The formation of dolomite mainly rely on the relationship between the Mg/Ca ratio and salinity e.g. if a high salinity is present a higher Mg/Ca ratio is needed in order for dolomite to form (Figure 3.4) (Folk and Land, 1975). Also, elevated temperatures seems to favor the dolomitization process (Boggs, 2011, Nichols, 2009). According to Hanken et al. (2010) the presence of sulphate ions (SO^{2-}_4) would inhibit dolomitization, and as the sea water inside reefs are reducing and thereby low on sulphate, dolomitization is favored here. Numerous models have been suggested to explain the dolomitization process, though some features among the models recur: the primary rock must be limestone, the reacting water must be sea water concurrent as the supply of sea water must occur during a longer period in order for extensive dolomitization to take place (Nichols, 2009). In general the different models could be divided into five categories including evaporitic, seepage-reflux, meteoric-marine mixing, burial and seawater models where some overlap occur, nevertheless each comprises different type of dolomitization fluid, flow and geological setting (Tucker et al., 1990). However, in this study only the evaporitic and see-page reflux would be relevant. The evaporitic model occurs in muddy carbonates or at supratidal flats and according to Hanken et al. (2010) its presence can be recognized by several conditions including chickenwire anhydrite structure (Flügel, 2010). This model includes evaporation of capillarity brines where upward flow from the saturated groundwater zone replaces the water lost by capillary evaporation (Tucker et al., 1990, Boggs, 2011). The see-page reflux model on the other hand rely on the density difference between brines and normal seawater. Due to surface evaporation of water, brines could be concentrated in brays or surface ponds, and as the brines have a higher density than normal sweater, they would sink downward. This results in large volumes of Mg-rich brine that flushed downward trough calcium carbonate sediments forming dolomitization (Boggs, 2011).

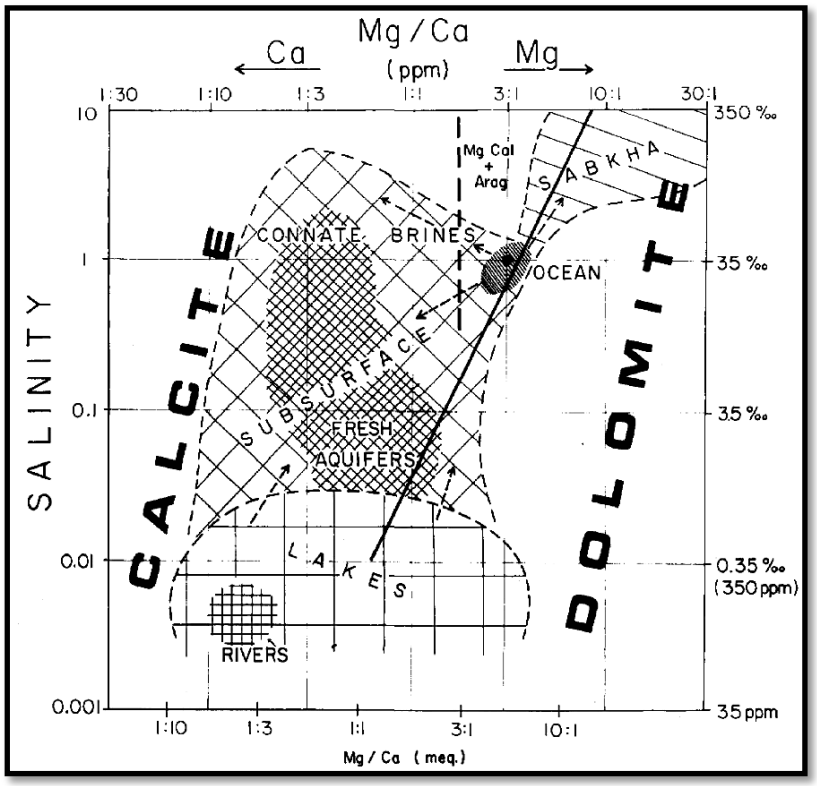

Figure 3.4. Fields of occurrences of common waters and dolomite based on the salinity versus Mg/Ca ratio from Folk and Land (1975).

Often it is difficult to separate calcite and dolomite in optical microscope due to their similar optical properties. However, dolomite usually occurs as rhombe-shaped crystals that replace the original calcite fabric. Furthermore, staining the thin sections of Alizarin Red-S would help separate the two as calcite would react by becoming pink whereas dolomite would not be affected (Nichols, 2009). During total dolomitization, rhombic crystals would replace the primary fabric of the limestone where the original composition is unrecognizable. Generally an alteration from calcite to dolomite would decrease the mineral volume concurrent as the porosity would increase (Nichols, 2009). When dolomites develop they form a crystal framework, which have increased resistance to chemical compaction, therefore the presence of early (pre-burial or very shallow burial) dolomitization could prevent the pressure solution process and thereby the formation of stylolites (Choquette and James, 1987).

Cement

Another important factor affecting the timing of chemical compaction, is cementation (Choquette and James, 1987). This process includes chemical precipitation from solution into the pores, inside grains or holes formed by earlier dissolution, and in order for this process to

occur, the pore fluid must be supersaturated with the cement mineral (Flügel, 2010). Generally, carbonate cementation is favored by higher temperatures and higher pH (Flügel, 2010). Several factors are controlling the precipitation of cement and dissolution of carbonate sediments e.g. pore fluid composition, flow rate of water through the pores, primary porosity and permeability etc. (Flügel, 2010). By studying cement stratigraphy i.e. crystal shape and order of deposition, the diagenetic history can be determined for the rock (James and Choquette, 1984, Flügel, 2010, Ahr, 2011). When evaluating and differentiate cement types, morphology and arrangement of cement crystals are used (Flügel, 2010). According to Flügel (2010) there are numerous types of cement that could form within the different environment that occur. However, in this study the cement classification would be at a basic level with emphasis on early and late calcite cement after Ehrenberg et al. (1998b).

3.2.3 Porosity in carbonates

The porosity is an important factor in hydrocarbon exploration as it is the measurement of the total pore space to the total volume of the rock, often given in percentage (Tucker et al., 1990, Lucia, 2007). Due to the biological origin and chemical reactivity in the carbonate sediments the porosity here is way more complex than within the siliciclastic ones (Lucia, 2007, Moore and Wade, 2013). The biological origin and primary porosity rely on skeletal framework of the organisms, reef framework and fossil related shelter porosity, whereas the chemical reactivity may cause secondary porosity by diagenetic processes as dissolution, reprecipitation and dolomitization (Moore and Wade, 2013). The initial porosity in carbonate sediments could range between 40-70%, while the ultimate porosity commonly is 5-15% within the reservoir facies (Moore and Wade, 2013). Several classification systems for porosity have developed through time, though with different emphasis, this include Archie (1952) with the first attempt to combine engineering and geological information, or Choquette and Pray (1970) which linked sedimentological fabric and thereby in some extent the depositional setting and diagenetic evolution, and Lucia (1995) who defined the rock-fabric and incorporated the diagenetic overprints with petrophysical characters. However, in the present thesis, the classification system after Lønøy (2006) that is presented in Table 1 would be used. This classification system includes 20 different classes based on pore size, pore distribution and pore types where combined with the sedimentological and diagenetic features with flow related properties.

Table 1 Classification system introduced by Lønøy (2006).

Pore Type	Pore Size	Pore Distribution	Pore Fabric
Interparticle	Micropores (10–50 μm)	Uniform	Interparticle, uniform micropores
		Patchy	Interparticle, patchy micropores
	Mesopores (50–100 μm)	Uniform	Interparticle, uniform mesopores
		Patchy	Interparticle, patchy mesopores
	Macropores (>100 μm)	Uniform	Interparticle, uniform macropores
		Patchy	Interparticle, patchy macropores
Intercrystalline	Micropores (10–20 μm)	Uniform	Intercrystalline, uniform micropores
		Patchy	Intercrystalline, patchy micropores
	Mesopores (20–60 μm)	Uniform	Intercrystalline, uniform mesopores
		Patchy	Intercrystalline, patchy mesopores
	Macropores (>60 μm)	Uniform	Intercrystalline, uniform macropores
		Patchy	Intercrystalline, patchy macropores
Intraparticle			Intraparticle
Moldic	Micropores (<10–20 μm)		Moldic micropores
	Macropores (>20–30 μm)		Moldic macropores
Vuggy			Vuggy
Mudstone microporosity	Micropores (<10 μm)		Tertiary chalk
			Cretaceous chalk
		Uniform	Chalky micropores, uniform
		Patchy	Chalky micropores, patchy

4 Database and methodology

4.1 Data

This master thesis is based on core 7030/03-U-01 from the western Barents Sea (Figure 2.1). The core was drilled in 1987 as a part of the shallow drilling program of the Barents Sea that was initiated by IKU Petroleum Research (renamed SINTEF petroleum research in 1999). The entire program took place between 1982 and 1993 where the aim was to obtain more geological information about the Upper Paleozoic sediments (Bugge et al., 1995).

The core used in this study is located offshore Northern Norway on the eastern part of the Finnmark Platform, as marked in Figure 1.1. In total the core consists of 147.4 m of sediments, which was taken between 173.7 m and 26.3 m depth below the seabed. Available petrophysical information from the drilling are gamma and sonic measurements (Bugge et al., 1995). In addition, calcite/dolomite ratio and plug porosity for the core have been measured and presented by Ehrenberg et al. (2000). For more detailed and supplementary information regarding the drilling method see Bugge et al. (1995).

Core 7030/03-U-01 consists of sediment of Late Carboniferous to Early Permian age. Originally no former formation names were used and the sedimentary successions were only defined by age; late Kasimovian – Early Gzhelian to late Asselian (Bugge et al., 1995). However, as stated in Larssen et al. (2002), these sedimentary units have now been defined as the Falk Formation and Ørn Formation, and therefore based on this nomenclature, the sediments within the core constitute mainly the upper Falk Formation and the lower – middle Ørn Formation which are the terms used within this study (Larssen et al., 2002).

4.2 Practical work and methodology

4.2.1 Sedimentological log

The data collected from the core has been presented in a detailed sedimentary log in Figures 5.12, 5.13 and 5.14. Originally the log was drawn in 1:20 scale, and thereafter Adobe Illustrator was used to digitize it by re-drawing the raw-log into a presentation log in a scale of 1:50, which gave a sufficient level of accuracy for the purpose of this study. In addition a simplified log was drawn in 1:600 scale for comparison with the different graphs in the study. In the logging-process, features such as lithology, grain size and amount and type of fossils have been emphasized and registered in the log. The different carbonates observed were described using a modified version of the Dunham (1962) classification system and some of the extensions of the boundstone introduced by Embry and Klovan (1971). The classification scheme is presented in Figure 4.1 and comprises the classes mudstone to boundstone, where boundstone also includes bindstone. The clastic sediments were defined by grain size observations and arranged by the Udden-Wentworth scale which includes clay to medium sand (Table 2) (Wentworth, 1922).

In the logging-process both the processed show cuts and original cuts of the core were used. To separate limestone and dolomite and to prove presence of calcite cement, dilute 10% hydrochloric acid (HCl) was used. The grain sizes and the individual fossils were defined by using a loupe and a stereo microscope and the classification of fossils was done by visual comparison with Adams and MacKenzie (1998) and with guidance of professor II at NTNU Atle Mørk. A standard digital camera was used to take the different photos. In addition, a needle was used to define the hardness of the sediments, separating anhydrite, calcite and chert.

Most of the logging was done in teamwork with fellow master student Robert Bjørklund who also did his master thesis on this core.

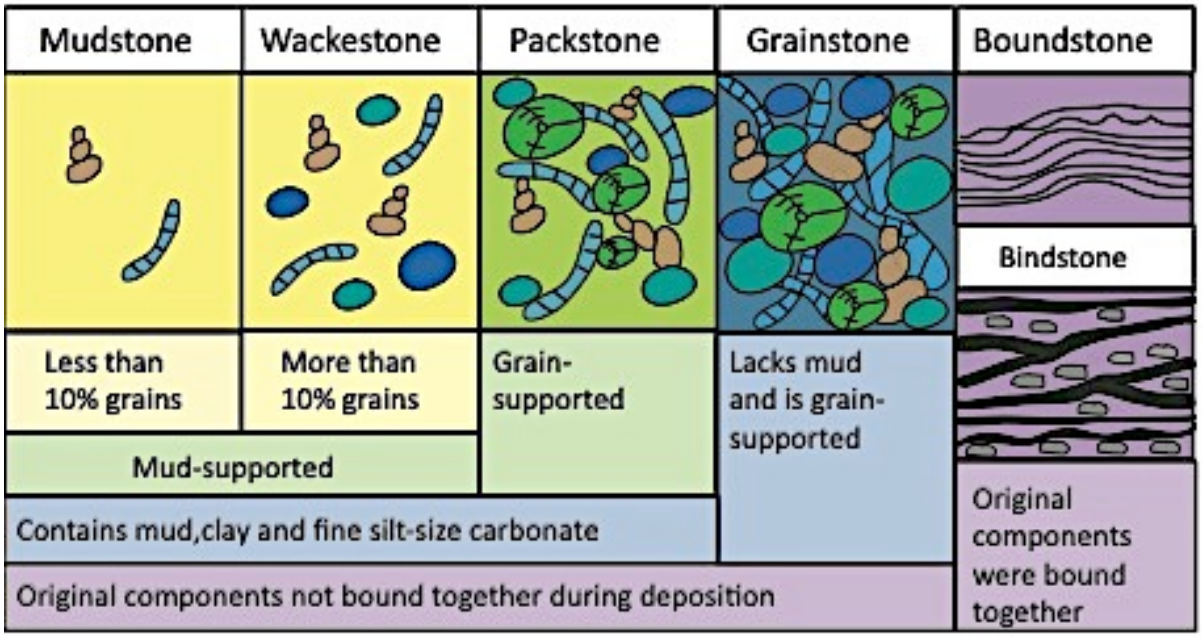

Figure 4.1. A modified version of the Dunham (1962) classification system and the extensions of boundstone including bindstone introduced by Embry and Klovan (1971). The classification scheme was used during the description of the observed carbonate sediments in the logging process.

Table 2. The Udden – Wentworth grain-size scale, modified from Wentworth (1922). This grain-size scale has been used when arranging the clastic sediments observed in the logging process.

Diametre (mm)	Size class
0.50 - 0.25	Medium Sand
0.25 - 0.0125	Fine sand
0.0125 - 0.063	Very fine sand
0.063 - 0.004	Silt
< 0.004	Clay

Assumptions done while making the sedimentary log

Individual pores including moldic porosity, cemented and non-cemented vuggy porosity are observed in several areas throughout the core. However, in some situations, these features occur together and intermixed with visible fossils, at the same time as a visible systematic

shape, similar to the fossils can be seen. In these situations the porosity types are assumed to be dissolved fossils and therefore, the final facies classifications of these areas were done based on the amount of these visible porosity types even though the origin of the porosity is impossible to determine.

Based on the reaction when testing with 10% HCl it has been defined three different carbonate lithologies. The term limestone is used when a clear reaction occurs, dolomitic limestone when a small but clearly visible reaction takes place, whereas dolomite is used when no reaction can be seen.

A classification as dolomitic mudstone is used for totally dolomitized intervals where original structures and presence of fossils are impossible to identify.

In the Falk formation several intervals have abundant amounts of fossils, and since these intervals are lacking thin sections an interpretation has been done by visual interpretation from the core where the facies has been set to a wackstone with higher amounts of silt.

4.2.2 Logging of pressure solution seams

Among the carbonate facies in the core, 295 bedding parallel pressure solution seams were observed and registered. Since the individual pressure solution seam can show a big variation in the amplitude height, a calculation of the mean amplitude value was done as a base to categorize the seams into main groups. The calculation was done based on five random amplitudes, which were chosen as a sufficient number to exclude the effect of dominant values in the calculations (Figure 4.2D). Based on the calculated mean amplitude value, the different pressure solution seams were separated into two main groups. In the situations where the mean amplitude was exceeding 1 mm, the term stylolites were used, whereas when the mean amplitude was less than 1 mm high, dissolution seams were used (Table 3). Each of the individual pressure solution seams has been categorized by morphology and recorded by depth. The morphology of the registered seams are characterized by a classification system (Figure 4.2) based on a combination of the sutured seams after Wanless (1979) modified by Choquette and James (1987) and the classification after Logan and Semeniuk (1976), both presented within Flügel (2010, p.319). Both of the seams were classified by either high or low

amplitude (Figure 4.2A). The stylolites were also classified by a) irregular, b) hummocky, and c) smooth (Figure 4.2C), based on the two-dimensional morphology perpendicular to the stylolite surface. In addition the stylolites were quantified by the mean amplitude size (Figure 4.2D). As mentioned, most of the seams show big internal variation, therefore the qualitative classification of the amplitudes of both groups are based on the overall trend. Multiple, intersecting surfaces were counted twice, and categorized as swarms (Figure 4.2B). Several of the pressure solutions seams are bounding different grains, which have been registered as nodule-bounding (Figure 4.2B).

The seams registered in the logging processes are just based on the seams seen in show cuts and original cuts. The individual measurements were done by a meter stick direct at the core. Each pressure solution seam was plotted against the depth in an Excel spread sheet to map the seams distribution in amount, amplitudes magnitude, style, nodule-bonding, and swarms. Thereafter the Excel spread sheet was incorporated into Adobe Illustrator to correlate with the 1:600 sedimentary log.

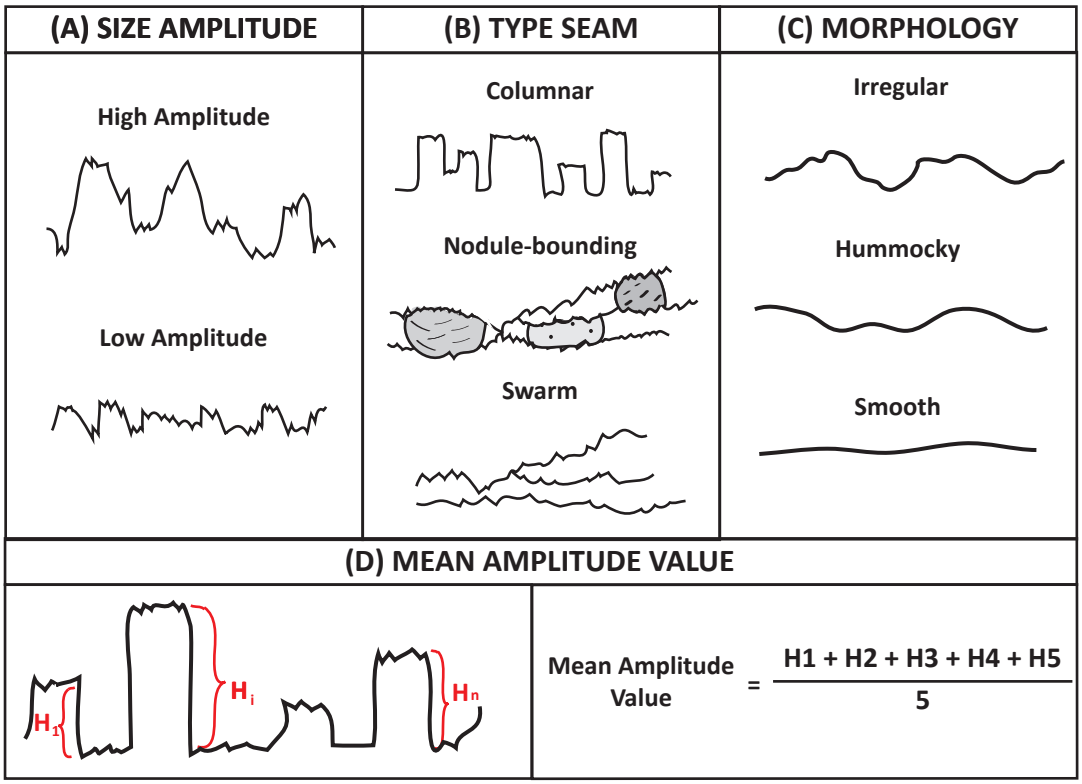

Figure 4.2. The classification system used for the different seams, based on Wanless (1979) modified by Choquette and James (1987) and the classification after Logan and Semeniuk (1976), both presented in Flügel (2010 p.319). (A) Include the size of the amplitude, (B) the type of seams, (C) morphology of the seams and (D) the calculation of the mean amplitude value.

Table 3. The classification of the pressure solution seams. The scale has been used to categorize the individual seams during the logging process.

Size amplitude (mm)	Type of pressure solution seam
< 1.0	Dissolution seam
> 1.0	Stylolite

4.2.3 Facies description and facies association

The different observations collected in the logging process and in the thin sections were systematized and further interpreted by using the concept of facies. Facies is defined by Reading (1978) as a rock with distinct characters as composition, color, fossils and sedimentary textures that reflect a particular process or environment. The characteristics that have been emphasized in this study are as mentioned, the lithology, the amount and type of fossils in addition to the grain size (see section 4.2.1). Dolomite is a common feature within the core and is interpreted to originate from a secondary process because it often has preserved the structures of the original rock, concurrent as it occurs adjacent to non-dolomitized areas with similar or equal texture (Boggs, 2011). Although facies are based on characteristics originating from the rocks primary deposition, a choice has been made to incorporate a description of the dolomitized areas of the individual facies where it occur, since this aspect is relevant for the study. In total 10 different main facies are interpreted for the core and can be seen summarized in Table 5. However, since isolated facies rarely have an interpretation value, the individual facies has to be seen in correlation with the nearby facies. Therefore, groups of facies associations have been made in situations where adjacent individual facies are considered to have a genetically or environmental relationship that gives a distinct association (Reading, 1978).

4.2.4 Optical microscopy

The core is represented by 115 petrographic thin sections, which were made during the IKU stratigraphic drilling project. Each thin section was studied in detail with different aims as described below. Thin sections epoxy were colored with blue or green to show porosity. For this purpose a standard petrographic microscope with plain polarized light and crossed polarized light was used, in addition, a camera mounted on the microscope was used to take images of the thin sections.

Facies determination

The thin sections were used as a supplement and help to determine the different classifications of both the siliciclastics and carbonate sediments that were observed during the logging process. By studying the thin sections a more accurate grain size and classification of grain type could be done, along with the determination of type and amount of microfossils present. Naturally the same classification systems as presented and described in chapter 4.2.1 were used and the classification of the microfossils were done by visual comparison with Adams and MacKenzie (1998), in addition Flügel (2010) was used as a supplement for facies determinations. In some of the thin sections, Alizarin-red-S was added as a help for separating the dolomite and the calcite, since limestone becomes pink-red whereas dolomite will be unstained in this reaction.

Porosity classification

The classification of porosity types in the core was also done by studying the available thin sections. However, this classification was limited to the carbonate facies in the core, as these sediments are relevant for the study. Although the thin sections were originally made for another project, a classification of the porosity could be done for all the carbonate facies. Naturally, some facies were more represented than others, which gave some facies a more reliably and exact classification compared to those just represented by one thin section. The thin sections impregnated with colored epoxy were chosen as the study material for this purpose, since the porosity is clearly visible within these compared to those not impregnated. The different pore types were classified by the classifications system by Lønøy (2006) which emphasizes pore type, pore size and pore distribution (Table 1). It must be stated that the thin sections are just representing a 30 μm thick cross-sectional cut of the rock and thereby just

represent a small fraction of the rocks; therefore the classification is just an indication of the general pore types occurring in the individual facies.

Stylolite occurrence

The thin sections were also used to investigate the stylolites that were registered in the logging process. Naturally, due to the thin sections original aim, only a limited amount of stylolites were possible to study in microscopic scale. By studying the stylolites in this scale, their influence and possible diagenetic influence on the host rock could closer be observed, and in addition to their behavior in general. The thin sections were not marked with any direction; therefore a misleading concerning which features are occurring on which side of the stylolites, could have been made.

Cement and dolomite

The thin sections were also used to study the present cements and dolomite in the core. However, due to supplementary usage and limitation of time, the cement has just been classified and interpreted by a simplified version of the different types of cement and dolomite used in study of diagenesis at the Finnmark Platform by Ehrenberg et al. (1998b). This with emphasis on cement type and crystal size where the terminology after (Ehrenberg et al., 1998b), presented in Table 4 have been used. It must be stated that the cement study within this thesis is limited to standard petrographic microscope study, in contrast to Ehrenberg et al. (1998b) which also has used cathodoluminiescence and blue-light fluorescence.

Table 4. Cement terminology after Ehrenberg et al. (1998b).

Cement type	Crystal size (mm)
Calcite:	
Micrite	<0.004
Microspar	0.004 - 0.02
Fine spar	0.02 – 0.1
Coarse spar	0.1-1
Dolomite:	
Microdolomite	<0.02
Fine rhombic	0.02 - 0.1
Coarse rhombic	0.1 - 1

4.3 Sources of error

The interpretation of depositional environment is based on observation done in the logging process In areas lacking thin sections, the only source was the core. Here, the interpretation of grain size was done by visual estimations and therefore some errors concerning the sizes of the grains, especially separation of silt and clay are possible. Another problem attached to the lacking thin sections are to distinguish siliciclastic and dolomitized areas as in some parts of the core, both of these two features are common and therefore difficult to separate just by the untrained human eye.

In relation to optical microscopy there are many possible errors, especially when some of the thin sections have poor quality. Several of the thin section were not stained with Alizarin-Red-S. Therefore some misinterpretation could have been done in the thin sections where the chance of both, dolomite and calcite could be present.

5 Sedimentology

5.1 Facies

In total 10 different facies have been defined based on the log from core 7030/03-U-01, and two of the facies include several sub-facies. The individual facies are described and a depositional environment is interpreted for all of the main facies. In Table 5 a summary of all the interpreted facies are presented.

Table 5. Overview of the interpreted facies in the core. U = undolomitized, DL = dolomitic limestone and partly dolomitized, D = dolomitized.

Facies	Description	Sub facies	Dolomitized	Interpretation
1	Clay	-----	U	Basin - Deep ramp
2	Siltstone	Homogenous siltstone Mud rich siltstone Calcite rich siltstone	U, DL	Deep ramp
3	Very fine sandstone	-----	U,DL	Deep ramp
4	Mudstone	-----	U,DL	Intertidal - lagoon/tidal flat
5	Wackestone	-----	U, DL, D	Lagoon
6	Foraminiferic wackestone /packstone	-----	U, DL, D	Lagoon with occasionally good circulation
7	*Palaeoaplysina* /phylloid algae boundstone	-----	U, DL, D	Shallow ramp - shallow subtidal,
8	Stromatolite bindstone		U	Intertidal to supratidal
9	Grainstone	-----	U	Sand shoal in a lagoon
10	Anhydrite	Massive anhydrite Chickenwire anhydrite Nodule anhydrite	U	Supratidal, mud flats

Siliciclastics

5.1.1 Facies 1: Clay

Description: Facies 1 is characterized as a brown or grey to black homogenous unit, consisting of clay sized grains (Figure 5.1A). Generally the shale occurs in beds with thickness around a few cm, although several beds up to 2 m occur. Sedimentary structures are not preserved within this facies, however parallel laminated partings are common in the thickest beds. The facies occur mainly in the lower part of the core, below 122.55 m depth. Fossils are generally sparse in the facies although some rare, small skeletal fragments of trilobite and crinoids appear. Calcite cement is generally common within this clay facies, but is lacking in the upper part of the core.

Interpretation: The deposition of clay implies a quiet-water environment that allows suspended clay particles to settle. This condition could represent several environments and therefore the clay has been seen in correlation with the other facies it occur with (Boggs, 2011). The clay is commonly associated with the siltstone (F2) as the silt normally grade into the clay and in correlation with the other present facies in the core, deep environment in the basin is indicated. This interpretation is also supported by the common horizontal lamination occurring in thicker layers, which according to Boggs (2011) is natural for this environment. The changing color from grey to black reflects an increasing amount of carbon and implies a restricted basin where abundant organic matter are preserved at the same time as dominating reducing conditions prevailed (Boggs, 2009). Furthermore, the presence of calcite cement in the clay indicates presence of biogenetic carbonates (Walderhaug and Bjørkum, 1998). Though, as the depositional environment of the clay is interpreted to be the basin were conditions for formation of biogenetic carbonates are un-favored, the biogenetic carbonates have most likely been transported from the carbonate factory at shallower depths. However, the source of the biogenetic carbonates is impossible to determine as their original composition is dissolved and most likely followed by reorganization of the clay grains where the former space occupied by biogenetic carbonates were replaced (Stephens et al., 1973).

5.1.2 Facies 2A: Homogeneous siltstone

Description: Facies 2A is a homogeneous siltstone that appears as a massive unit with lack of sedimentary structures (Figure 5.1B). Alternating colors from grey to brownish and varying degrees of brighter brown areas are characteristic for this facies. Fossils are not present, but some local bioturbation occur. Occasionally, scattered elongated vugs in less than 1 mm scale are present. The homogenous siltstone appears mostly in intervals with a thickness around a few decimeters, although at 136.60 m depth, a 4 m thick continuous layer occurs where chert-filled vugs and pyrite are present.

In thin section, this facies is observed to be partly dolomitized within two intervals between 133.40 and 120.30 m depth. This alteration is not clearly visible in the core, but could be represented by slightly browner areas in some places. Vugs in few mm scale are common in both of the altered intervals. Chert and calcite nodules are abundant features in the lowermost interval in addition to some bioturbation, whereas nodules of anhydrites are prevailing in the uppermost one.

5.1.3 Facies 2B: Clay-rich siltstone

Description: This facies is comprised by siltstone with a larger portion of clay than normally expected in a clean siltstone, however the amount of clay is varying (Figure 5.1C). The color appears mostly as brown-grey to grey with some alternating brighter areas. Generally the facies is devoid of structures and appear as massive, whereas unsystematic bioturbation are more common and can be seen as sub-angular to sub-round areas with finer-grained matrix. Local features within the clay-rich siltstone are nodules of chert and calcite. The clay-rich siltstone is not a common facies in the core, but occurs in the interval between 126.20 – 120.30 m depth.

5.1.4 Facies 2C: Clay-rich siltstone with calcite cement

Description: Facies 2C is closely related to clay rich siltstone (2B) in composition whereas facies 2C is dominated by calcite cement and occur exclusively within the Falk Formation (Figure 5.1D). The mud rich siltstone with calcite cement appears with a greyish to brown

color with some alternating brighter spots. In some areas the silt appears as a massive and structureless unit, however, in general the facies includes a varying degree of bioturbation, which has differentiated much of the original structures. The facies has a diversity of fossils in the clay-rich areas such as foraminifera, crinoids, brachiopods, bryozoans, corals and occasionally gastropods, whereas the fossil fauna is more limited in other parts. Mostly the fossils occur as skeletal fragments, but some preserved ones are also observed. Nodules of anhydrite and chert in addition to small spots with green material occur several places. Calcite cement can be seen as infill within fractures, but is generally difficult to spot in the core as it is mixed with silt and mud, however, it has been identified in thin section and by diluted HCl in the core.

Interpretation: These three defined facies reflect a similar energy level as in the claystone (F1) although, based on the larger grains, some higher energy must have been present. The presence of bioturbation within these siltstone facies implies an area of relatively low energy level, below wave base. Seen in combination with the adjacent facies very fine sandstone (F3) and clay (F1) the main environment for these facies is interpreted as deep ramp below mean fairweather base. The higher bioturbation and clay content within facies 2B and 2C than in facies 2A suggest a somewhat higher energy level for facies 2A (Boggs, 2011). Based on this, the homogeneous silt may have been deposited closer to the shallow ramp at slightly higher level of energy than the clay deposition, although low enough for some bioturbation to occur. Further, the two other facies are interpreted to lie deeper and closer to clay (F1) environment where fine particle can settle and burrowing organism can prevail (Boggs, 2011). The diversity and high amounts of fossils together with the abundant calcite cement within facies 2C, indicates a deposition that favor carbonate formation and therefore a limited clastic supply (Nichols, 2009). The fossil assemblage indicates normal salinities and shallow marine to shelf setting. However, since the majority of fossils are skeletal fragments an allochthonous origin is interpreted, where bioclasts have been transported from shallower areas with higher energy levels out to the deep ramp (Scholle and Ulmer-Scholle, 2003, Hanken et al., 2010).

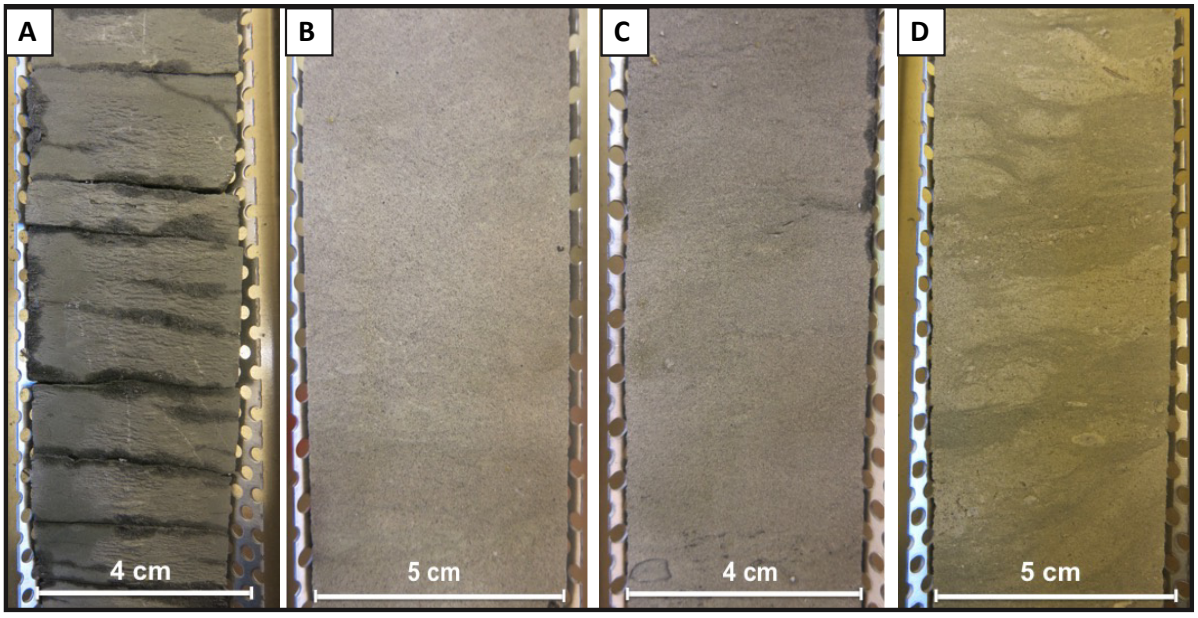

Figure 5.1. Core photos of (A) Dark claystone, facies 1. (B) Homogeneous siltstone, facies 2A. (C) Clay-rich siltstone, facies 2B. (D) Clay-rich siltstone with calcite cement, facies 2C, note the white areas of calcite cement.

5.1.5 Facies 3: Very fine sandstone

Description: The very fine sandstone is common from 156.90 to 131.90 m depth and is massive with a grey to brownish color (Figure 5.2A). The facies generally occurs structureless, however locally, varying burrows can be seen. Some burrows can be seen as less than a mm to a few mm thick planar and occasionally wavy laminated dark structures whereas others are horizontally and greyish with a thickness of a cm. The densities of the burrows are varying. In some places, the facies also contains chert and small amounts of pyrite. Abundant calcite cement is present in the lowermost parts in the core, and lacking in the uppermost part.

A partly dolomitization occurs within the interval 135.50 - 132 m depth. Here, mm-scaled vugs are present, which frequently have been partly or completely cemented (Figure 5.2B). Local mm to one cm-scaled nodules having calcite enclosed by a chertified rim occurs. In addition chert occur sporadic in the partly dolomitized very fine sandstone.

Interpretation: The grain size in this facies reflects a higher energy level than in the clay (F1) and silt (F2A, F2B, F2C), though since these three facies mostly are seen in combination

with each other a somehow similar environment must prevail. Therefore an indication of deep ramp is given though closer to the shore than clay and silt. The local presence of burrows in the facies could be explained by occasionally higher clay-content as a result of a small change in the depositional environment, somewhat closer to the basin (Boggs, 2011).

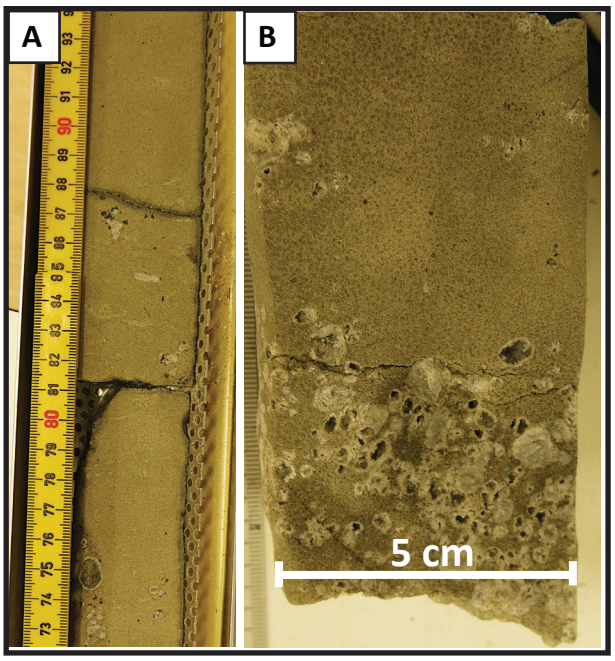

Figure 5.2. Core photos of facies 3, very fine sandstone. (A) The very fine sandstone as massive grey and structureless. (B) Dolomitized very fine sandstone with vugs that are partly and completely cemented.

Carbonates

5.1.6 Facies 4: Mudstone

Description: The mudstone facies is characterized by being dominated by mud-sized particles and that millimeter-sized bioclasts makes up less than 10% of the total rock volume (Figure 4.1) (Dunham, 1962). The facies is the dominant in the Ørn Formation and shows an alternating brown to greyish color (Figure 5.3A). This facies is characterized by mm thick, dark and lighter lamina and cm thick horizontal lamina, but is commonly also structureless and homogeneous. The intervals 98.50 - 97.20 and 44.90 - 34 m depth show an increased content of siliciclastic grains. Cm scale rugose corals and mm scale fragments of trilobites, foraminifera, brachiopods, gastropods and crinoids are common fossils in some intervals of the mudstones, whereas peloids occur occasionally. The amount of bioturbation is varying, as

some intervals appear totally bioturbated, and others are partially or non. In the mudstone facies, chert can bee seen as both nodules and as 12 to 18 cm thick bands.

Several of the mudstone intervals have been affected by dolomitization, some areas are only partly dolomitized while in others the original structure has been totally overprinted by dolomitization. The dolomitized parts can be seen as alternating undulating greyish- beige to yellowish fine-grained intervals (Figure 5.3C) and in some intervals the primary structures has been overprinted by an undulating darker structure with visible porosity. A few fossils of foraminifera and trilobites occur within the dolomitized areas in addition to some sparse bioturbation. A general trend in these altered areas is the presence of anhydrite-filled vugs, and locally appearance of nodules and bands of anhydrite or chert in addition to glauconite.

Interpretation: The deposition of mudstone reflects an environment with a low energy level, favoring conditions for the fine particles to settle (Tucker et al., 1990, Boggs, 2011). The formation of carbonate mud could be a result from inorganic precipitation such as transformation of aragonite to calcite and organic processes from breakdown of calcareous algae (Boggs, 2011). Based on the facies association, a lagoonal environment is interpreted though with varying conditions. In areas with homogenous mudstone, which lacks fossils or occur with peloids and occasionally are dolomitized with bands and nodules of anhydrite, a shallow marine environment and non-agitated water with varying hypersaline conditions are indicated to have been present in the lagoon and sometimes tidal flats is interpreted (Scholle and Ulmer-Scholle, 2003, Flügel, 2010, Moore and Wade, 2013). However, intervals with sparse amounts of fossils the fauna is indicating normal salinity and in combination with the common bioturbation and the nearby facies, better water circulations is indicated in the lagoon (Tucker et al., 1990, Scholle and Ulmer-Scholle, 2003).

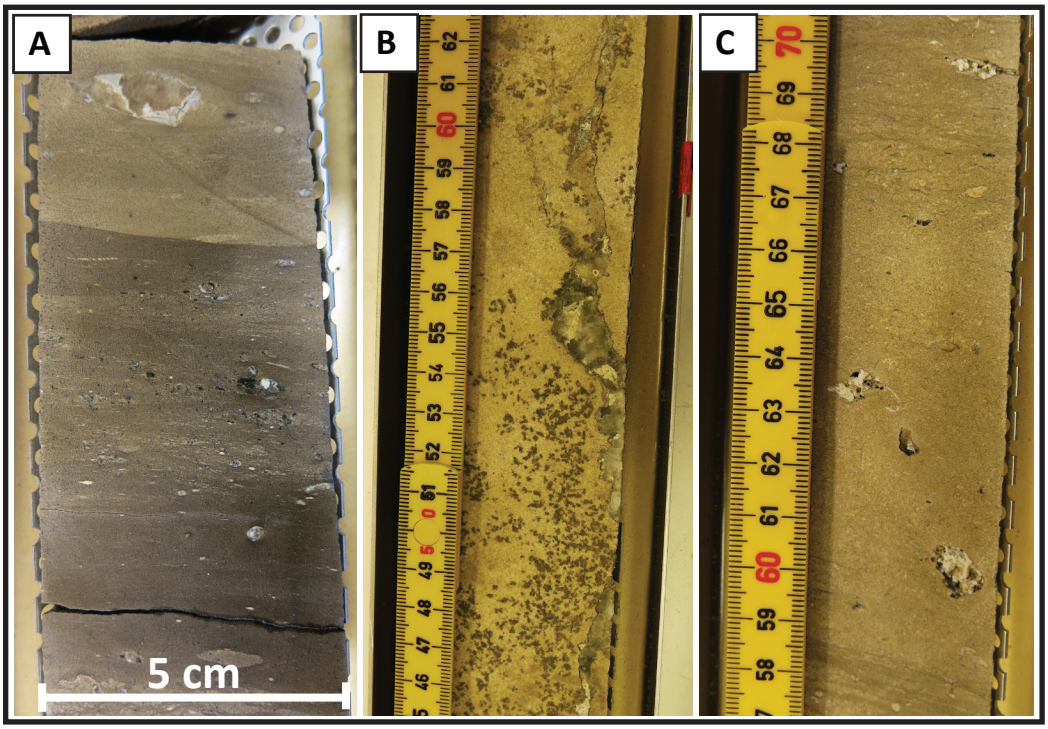

Figure 5.3. Core photos of the mudstone, facies 4. (A) Undolomitized mudstone (B) Mudstone with dark spheroidal scattered peloids (C) Dolomitized mudstone.

5.1.7 Facies 5: Wackestone

Description: The wackestone facies is composed of calcite mud interdispersed with intact fossils or skeletal fragments that constitute more than 10% of the total rock volume (Figure 4.1) (Dunham, 1962). In the Falk Formation the facies occurs only occasionally as mm bright fragments of crinoids and foraminifera in a fine-grained grey matrix that is intermixed with siliciclastic clay and silt (Figure 5.4A). In the overlying Ørn Formation the facies is common, consisting of mm to cm sized fossils, either clustered or scattered in brownish carbonate mud (Figure 5.4B). In the Ørn Formation the fossil fauna occurs both as homogenous, consisting of foraminifera, and as heterogeneous with an assemblage of crinoids, foraminifera, bryozoan, corals and occasionally brachiopods. The fossils within this facies are generally well preserved but some local fragments occur. Occasionally within the Ørn Formation, siliciclastic clay and silt appears intermixed with the fossil fauna, and locally chert nodules occur.

In the Ørn Formation, the wackestone is affected partly or totally by dolomitization several places, seen as brown-yellow color. Some fossils are preserved, although frequently they have

been dissolved to moldic porosity or vugs. Vuggy porosity is a common feature in the dolomitized areas and occasionally the vugs are filled with calcite or anhydrite. Anhydrite and chert also commonly occur as bands and nodules in the dolomitized intervals. Local glauconite also occur.

Interpretation: The conditions favoring deposition of wackestone are closely related to the deposition of mudstone (F4) requiring a quiet environment, also supported by the appearance of well preserved fossils within this facies (Tucker et al., 1990, Flügel, 2010). Furthermore, the assemblage of fossils suggest environments lying within shallow marine waters with normal salinities (Scholle and Ulmer-Scholle, 2003, Hanken et al., 2010). Based on these observations, the deposition of wackestone facies is interpreted to be in a lagoon with good circulations and below wave base (Tucker et al., 1990, Flügel, 2010).

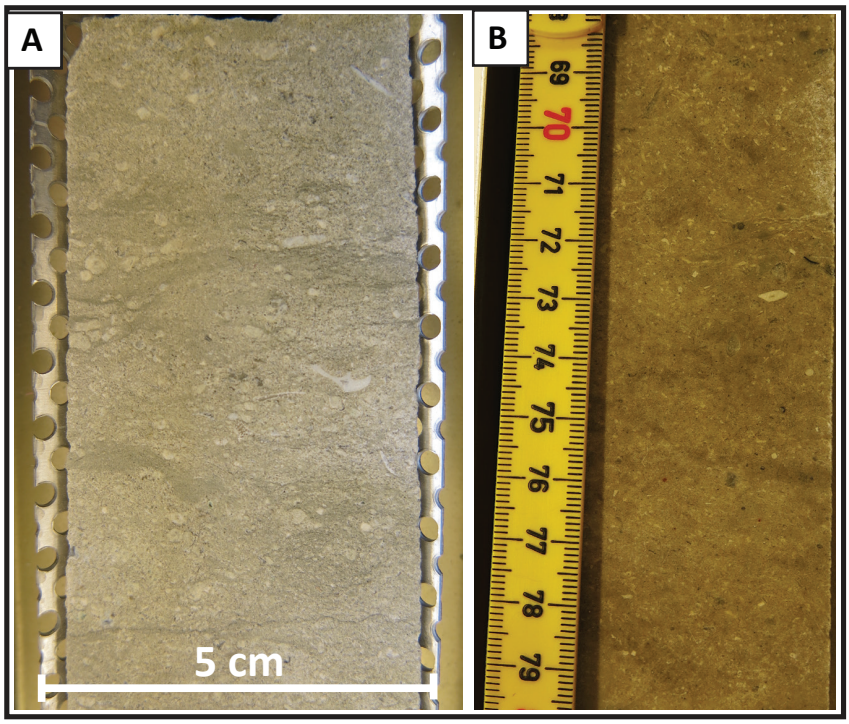

Figure 5.4. Core photos of the wackestone, facies 5 (A) The wackestone in the Falk Formation occur with fine-grained grey matrix that is intermixed with siliciclastic clay and silt together with fossil fragments. (B) Undolomitized wackestone in the Ørn Formation with brownish carbonate mud intermixed with fossil fragments.

5.1.8 Facies 6: Foraminiferic wackestone/packstone

Description: Facies 6 is characterized by mm sized yellowish foraminifera often fusulinids, occurring within darker carbonate mud (Figure 5.5). The foraminiferic tests are often well preserved and in several places the occurrence of hollow chambers can be recognized (Figure 5.5B), whereas original internal structure are lost several places due to chemical alteration. Foraminifera exclusively dominate the fossils within this facies however crinoids, trilobites and bryozoes occasionally occur. The composition of the wackestone/packstone varies through the core as some intervals are densely packed with only small amounts of matrix (Figure 5.5C), while in other parts the foraminifera are scattered with abundant amounts of matrix. Often the bioclasts are preferentially oriented parallel to the bedding and in several intervals affected by compaction (Figure 5.5A). Usually the facies forms beds in cm or dm thickness of densely packed sediments of a homogeneous fauna, consisting of yellow to whitish colored foraminifera enclosed in a dark muddy matrix (Figure 5.5A). In the interval between 96.10 and 96.0 m depth, the foraminifera are well preserved, and with a trend of gradually increasing size upwards, getting up to almost 3 mm. In some local areas an increase in clastic clay fraction is observed.

The facies is locally partly or totally dolomitized. In the dolomitized areas, many of the fossils are preserved, and several have been partly or totally dissolved, so that only moldic porosity or vugs remains. The different porosity types occur as both unfilled, and pores cemented by anhydrite.

Interpretation: The foraminiferic wackestone/packstone was deposited in an environment with low to moderate energy level, with conditions for carbonate mud to settle that prevented transportation of the fossils (Flügel, 2010). The overall abundant amounts of fossils and the increasing size of the foraminiferic tests in the interval between 96.10 and 96.0 m depth, indicates an oxygen rich environment that favored growth of the foraminifera specimen (Flügel, 2010, James and Wood, 2010). Further, the good preservation of the tests implies that the foraminifera lived at or near the location where they were deposited, at the same time as a relative low energy level prevailed and prevented the test from abrasion and damage (Flügel, 2010). The intact foraminifera, where the chambers can be observed, are classified as multicoluar and the good preservation also indicates a more stable composition with a low content of Mg calcite that is deposited in a warm environment (Scholle and Ulmer-Scholle,

2003, Hanken et al., 2010). A marginal hypersaline or subsaline environment is associated with homogenous fossil fauna, whereas a higher fossil diversity suggest that normal conditions prevailed (Scholle and Ulmer-Scholle, 2003). In the intervals where the compacted foraminifera occur, a former wackestone that has been compacted and transformed into a packstone could explain the lower content of mud and densely packed fossils (Shinn and Robbin, 1983). In combination with the other nearby present facies this facies is interpreted to be from a lagoonal environment that occasionally had water circulation (Flügel, 2010).

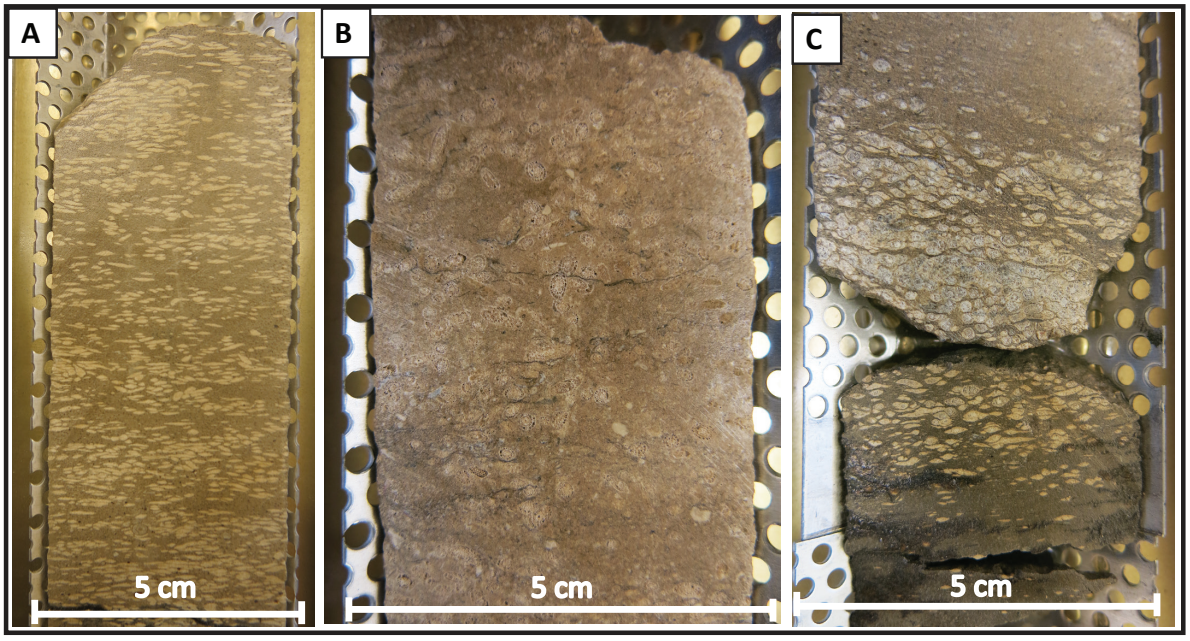

Figure 5.5. The different occurrences of the Foraminiferic wackestone/packstone in the core. (A) Yellow foraminifera oriented parallel to the bedding. (B) Well preserved foraminifera where much of the original structure can be seen as hollow chambers. (C) Densely packed foraminifera with minor amount of interbedded matrix.

5.1.9 Facies 7: *Palaeoaplysina*/phylloid algae boundstone

Description: Facies 7 is characterized by build-ups dominated by the platy organisms *Palaeoaplysina* and phylloidal algae that are interbedded with different amounts of carbonate mud (Figure 5.6). The facies has an alternating color from darker brown-grey to lighter beige. The individual build-ups occur with a thickness from 0.40 m up to almost 4 m in the interval between 155.35 - 30.40 m depth and where a trend of decreasing thickness occur upwards in the core. The individual plates of *Palaeoaplysina* are 2 – 3 mm thick, some of the plates show curvature, but generally the plates lie almost horizontal on top of each other. Some of the

Palaeoaplysina plates have preserved the primary internal structure of cellular skeleton (Figure 5.6C), however in the majority it has been dissolved and destroyed. In the lower part of the core, beds or single plates of phylloid algae are often mixed with the *Palaeoaplysina*, though this trend occurs just occasionally in the upper part. In some of the 1-2 mm thick plates of phylloid algae the characteristic tubules are still preserved, though mainly these have a poor preservation (Figure 5.6A). In addition to the dominating platy organism, the content of fossil fauna is varying from numerous to sparse with crinoids, gastropods, foraminifera, brachiopods, bryozoan and corals as the most common fossils. According to Gregory P. Wahlman, micropaleontologist (e-mail communication, 19.06.15) the green algae Donezella (Figure 5.6D) is possible present in the boundstone, though a closer study is needed in order to prove it. Within the individual build-ups, separating the plates, and in between the singel build-ups varying amounts from mm to cm thick beds of carbonate mud is present. Several places in the build-ups abundant vuggy porosity occur, either as calcite-cemented vugs or as un-cemented, in addition to some sparse nodules of anhydrite and chert. In the interval between 153.75 – 153.0 m depth and at 76.50 m depth, a structure associated with breccia formed by mechanical damage can be seen where the platy fossils occur in a chaotic order (Figure 5.6B).

Where the facies occurs in the interval between 151.75 and 101.60 m depth it is dominantly dolomitized and shows a varying color from light grey to light yellow-beige. In several places the build-ups are totally overprinted by dolomitization and therefore the original structure and hence the separation between the phylloid algae and *Palaeoaplysina* are difficult to determine. Occasionally, intact *Palaeoaplysina* plates, phylloid algae and crinoids occur. Cementation is generally widespread in these altered areas, whereas the intensity within the different build-ups is varying. Anhydrite (F10A) is closely associated with these dolomitized areas as several 10 – 12 cm thick individual anhydrite layers are interbedded in the build-ups. In addition, intercalated anhydrite nodules and anhydrite coexisting with dolomite in some intervals occurs. In the interval from 117.92 - 109.24 m a alternating vuggy porosity occur and between 103.60 – 103.20 m depth an alteration between dolomite and calcite layers are registered. Locally calcite nodules are also present.

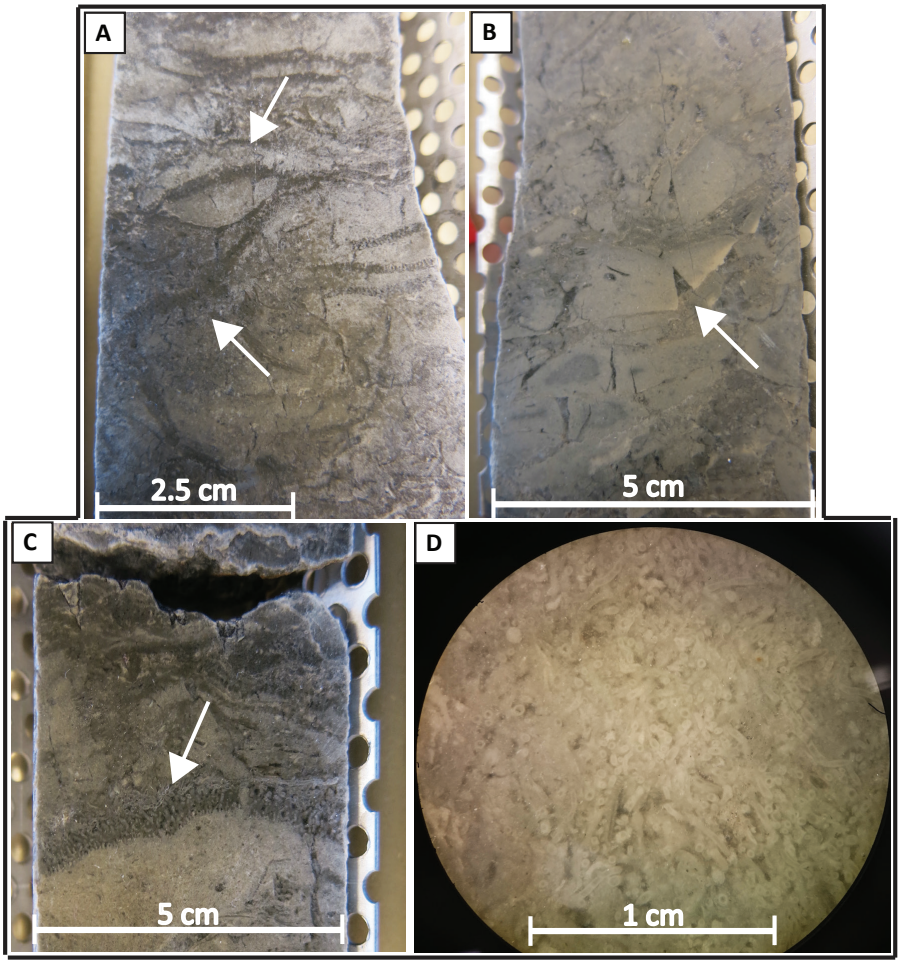

Figure 5.6. Core photos of the Palaeoaplsyina/phylloid algae boundstone, facies 7. (A) Phylloid algae (marked with the arrow) occurring in the boundstone facies. (B) Structure associated with breccia formed by mechanical damage of a platy organism. (C) Intact internal structure of the *Palaeoaplysina* plate (D) The possible green algae Donezella.

Interpretation: The dominating distinct fossils within the *Palaeoaplysina*/phylloid algae boundstone facies are characterized by an in-situ organic growth that formed build-ups as reefs at the shelf edge or as small isolated dome-shaped structures, and where the thickness of these are dependent of the sea level fluctuations and the available accommodation space, which in this case is suggested to be up to 6 m (Skaug et al., 1982, Scholle and Ulmer-Scholle, 2003, Flügel, 2010, Moore and Wade, 2013, Anderson and Beauchamp, 2014). Based on the adjacent facies, it is suggested a shallow subtidal environment at the shallow ramp for facies 7. According to studies done by Hanken and Nielsen (2013), the density of the *Palaeoaplysina* could show large internal variations and observations of matrix to *Palaeoaplysina* ratio may be as high as 20:1. This suggests that the interbuild-up mudstone (F4) that often is seen as thin layers separating individual build-ups could be a part of the build-up itself, and therefore the closely packed build-ups only separated by thin mudstone is

interpreted as one build-up. The intermixed fossils and carbonate mud implies that both of the reef-building organisms acted as sediment bafflers accumulating mud and organisms (Anderson and Beauchamp, 2014, Flügel, 2010). In the areas where the structure of breccia occur and where the fossils are in a chaotic order, an indication of deposition adjacent to the reef as back-reef or lagoonal setting is suggested (Flügel, 2010).

5.1.10 Facies 8: Stromatolite bindstone

Description: The stromatolite bindstone is a subcategory of the boundstone, and can be seen as stacked band with a thickness ranging between less than 1 mm to a few mm that generally are bright grey colored alternating with darker bands of mud (Figure 5.7). The bands have no sedimentary structures, however an approximately horizontal unsystematic wavy lamination pattern occurs in some intervals. In some places the individual bands occur as fractured (Figure 5.7B), however they mostly are intact. The total thickness of the stacked bands is generally around 10 cm and the facies occur exclusively within the Ørn Formation.

Interpretation: The stromatolite reflect a environment in water depths where enough light is available for the photosynthesis to occur (Hanken et al., 2010, Boggs, 2011). Due to the limited These organisms could appear in all the settings from supratidal to subtidal, although in association with the adjacent facies a supratidal to intertidal environment has been set (Flügel, 2010, Hanken et al., 2010, Boggs, 2011). The laminated stromatolites reflect an environment with quiet conditions where the settlements of fine-grained sediment are favored (Hanken et al., 2010, Boggs, 2011). Further, the stromatolite bindstone are mostly found in close association to the mudstone (F4) and therefore a intertidal environment is indicated (Hanken et al., 2010, Boggs, 2011). The individual fractured band within the stromatolite could indicate a limited period of arid conditions within the intertidal environment.

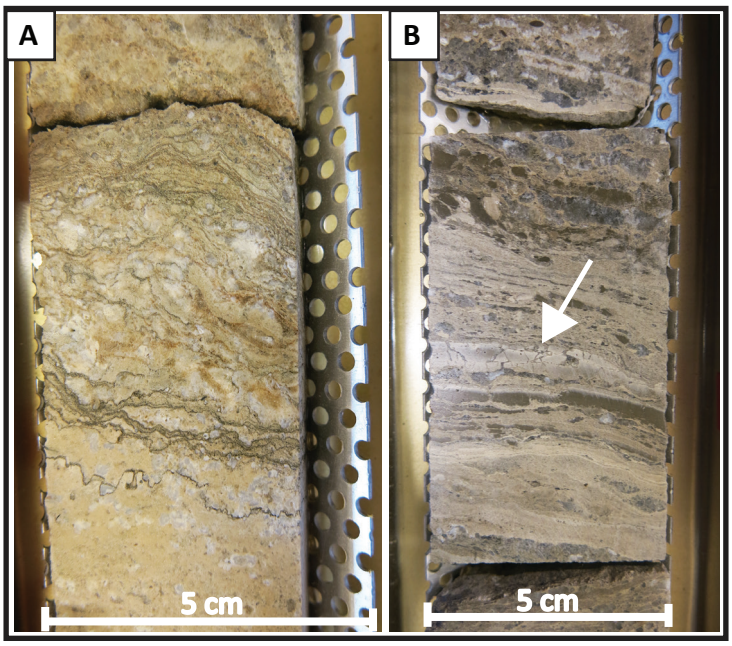

Figure 5.7. Core photos of (A) the stromatolite bindstone facies 8. (B) Stromatolite bindstone where some of the bands are fractured marked with arrow.

5.1.11 Facies 9: Grainstone

Description: Grainstone is not a common facies in the core but it occurs from 66 to 65.30 m depth. The facies is composed of densely packed skeletal material where the amount of carbonate mud is scarce (Figure 5.8). The most prominent fossils are foraminifera, crinoids and peloids (Figure 5.8A), which mostly occur as fragments with less than 1 mm size. The fossil fragments occur in a chaotic arrangement where no sedimentary structures appear. A yellowish color intermixed with alternating white areas is characteristic for the facies, and occasionally dark areas with clusters of peloids occur, scattered or as bands.

Interpretation: The facies reflect an environment with an energy level that favored the removal of the mud (Tucker et al., 1990). Further, a restricted environment with shallow marine hypersaline or subsaline conditions are indicated by the low diversity of fossils, though great amount of foraminifera (Scholle and Ulmer-Scholle, 2003). Based on these conditions a lagoon is indicated by the fauna and restrictions, although the energy level is too high. Since the facies occur only once in the core, a sudden and exceptional happening is indicated. Therefore, in the correlation with the other nearby facies as the muddy facies of

mudstone (F5) and packstone (F6), a sand shoal accumulated by a tidal current in the lagoon is interpreted for this grainstone (Flügel, 2010).

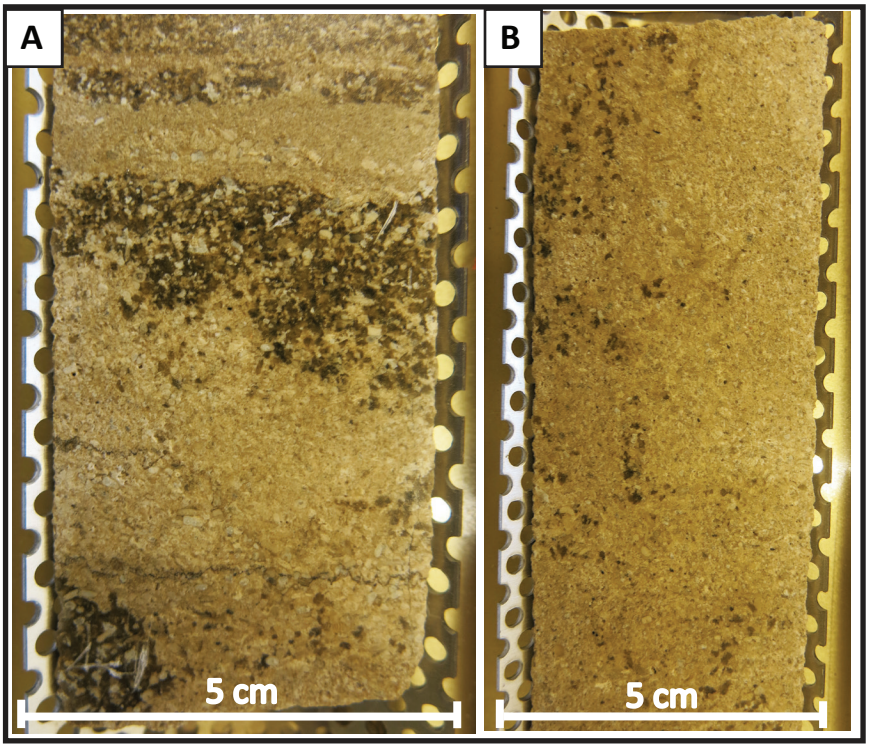

Figure 5.8. Core photo of (A) Grainstone, facies 9 with densely packet foraminifera, crinoids, though only the dark peloids are visible at the picture. (B) Same as in picture A, only with a smaller amount peloids.

5.1.12 Facies 10A: Structureless anhydrite

Description: The structureless anhydrite appears as a milky-white homogeneous unit in addition to as a mixed unit consisting of greyish mud with undulating white areas of anhydrite. The milky-white one appears mostly as 2 - 12 cm thick individual layers within the *Palaeoaplysina*/ phylloid algae boundstone (F7) and in the mudstone (F4), whereas the mixed unit is continuous in the interval 81.58 – 80.18 m depth. In the mixed unit the mud is dominantly intermixed with anhydrite with no systematic pattern. No apparent structures or fossils are present within this facies.

5.1.13 Facies 10B: Chickenwire / mosaic anhydrite

Description: Chickenwire or mosaic structure with a very varying color from milky-white, bluish white and gradually darker white to brownish is characterizing this facies (Figure 5.9A,B). The structure is formed by irregular round anhydrite nodules in mm to cm scale that are separated from each other by brownish, mm thick bands of clay. The nodules have no systematic structure, but are rather chaotic. The facies occurs as one continuous unit from 85 – 82.90 m depth.

5.1.14 Facies 10C: Nodular anhydrite

Description: The nodular anhydrite facies is comprised by round anhydrite nodules (Figure 5.9C), and appear in several settings in the core, both in the continuous anhydrite strata ranging from 87.55 – 79.10 m depth and as individual local nodules within dolomitized present facies. In general the nodules are in mm – cm scale and have a milky-white color with no sedimentary structures.

Interpretation: The presence of anhydrite reflects an environment within the capillary zone with a mean annual temperature above 20º C, in addition to seasonal temperatures above 35º C and a available source of highly saline brines (Kendal, 2010, Boggs, 2011). Since anhydrite is an evaporite mineral a sabkha environment is indicated or a shallow standing water (Boggs, 2011). Where the anhydrite occurs as interbands or internodules within other facies (F10C), a displacement, dilution and replacement of the host rock is indicated, where the sizes of these individual features reflect the available amount of brine during the formation (Kendal, 2010, Boggs, 2011). In the areas where the chickenwire structure is dominating, a growth in situ within a clay-dominated host rock is implied, here a flooding more than once a month is indicated in the sabkha area, where the clay bands are a result of growing anhydrite nodules that force the clay aside (Tucker et al., 1990, Boggs, 2011). Therefore a supratidal environment where periodical spring tide or wind occurred which formed mud flats are interpreted (Kendal, 2010).

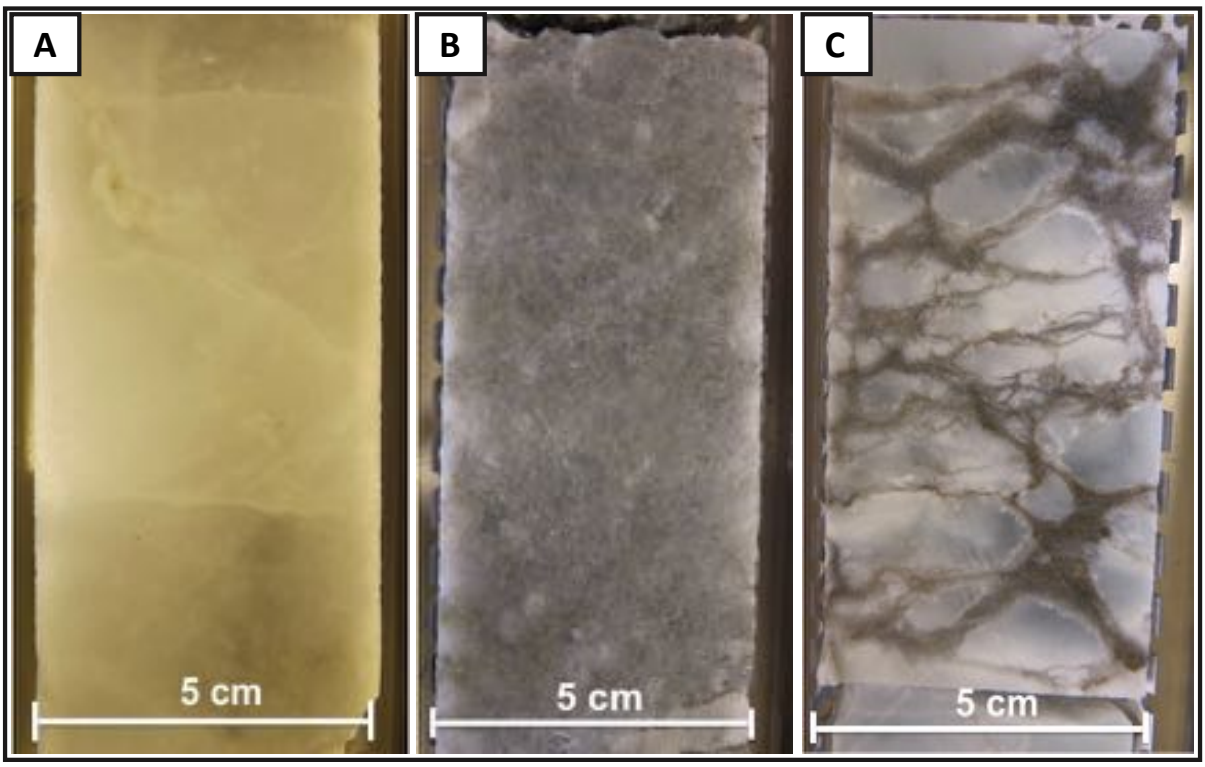

Figure 5.9. Core photos of the different anhydrite facies presented within the core. (A) The milky-white structureless anhydrite (F10A). (B) The mixed greyish and white anhydrite (F10A). (C) The chickenwire anhydrite (F10B).

5.1.15 Additional observations

Description: In the interval from 141.5 – 141 m depth in the core a fossil with numerous spherical to somehow elongate spheroidal tube occur (Figure 5.10). Mostly the individual tube has a relatively thick rim around a hollow darker core, although tight tubes lacking the hollow core also occur. The only internal structure within some of the tubes is a whitish circle around the hollow core that is following the same shape as the individual tube. The individual spheroidal tube is a few mm in size and has a grey to white color. The tubes have a random distribution and are intermixed with a small amount of light-brown fine-grained matrix that together appear in a 4 cm round cluster enclosed by a 2-5 mm thick darker fine grained rim.

Interpretation: The interpretation of this fossil required some investigation, as it has never been identified before within this core or in nearby cores of the same age. By looking up at articles and books at the internet a root mantle of Psaronius stem was suggested and further confirmed by C.Pott (e-mail communication, 29.04.15). The Psaronius was a tree fern with approximately height of 10 m and lived during the Pennsylvanian to Permian (Taylor et al.,

2009). According to DiMichele and Phillips (2002refered to), (Taylor et al., 2009) (p.418.) the tree fern could have lived in poorly drained areas that is seasonally dry. The presence of this fossil in the core could be interpreted to be some driftwood.

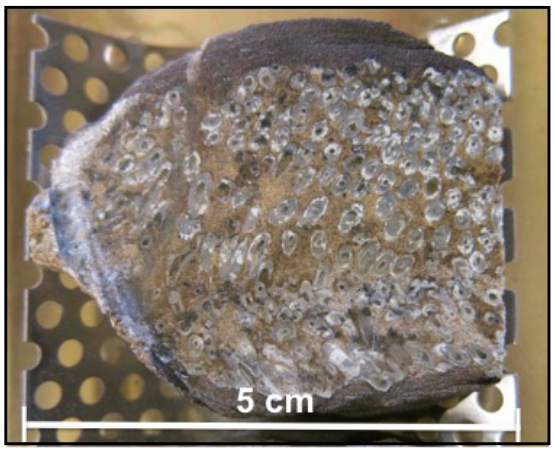

Figure 5.10. The identified fossil occurring at 141.5 – 141.0 m depth in the core. Interpreted as a root mantle of Psaronius stem, see text for details.

5.2 Vertical Facies Arrangement

The core log is presented in Figure 5.12, 5.13 and 5.14. Since the data within this study is limited to only one core and thereby just one-dimension, the interpretation of the depositional model must be based on the vertical arrangement of the different facies representing the core. In order to describe this vertical arrangement and the depositional interpretation, the log has been divided into 8 sections based on erosional surfaces or changes in the biological or chemical diversity, which reflect differences in the broadly similar succession (Reading, 1978). These 8 sections have been described and interpreted separately to understand the development of the whole system.

Section 1

Section 1 represents the upper and only part of the Falk Formation in the core and has a total thickness of 18.6 m (Figure 5.12). Siliciclastic sediments including clay to very fine sandstone (F1 – F3) with abundant amounts of calcite cement, mainly defines the section. In addition, some layers of silt-rich wackestone occur. Up to the erosional unconformity at 161.15 m depth, up-fining sequences including siltstone (F2C) with high amounts of fossil fragments is dominating with several m thick units, only interbedded by some silt-rich

wackestone, and terminated by 0.2 – 0.5 m thick clay layers. Above the unconformity, a 0.6 m thick up-fining sequence consisting of very fine sandstone and clay rich wackestone occurs. A relatively thick coarsening upward unit at 160.45 m depth follows these sediments, which last throughout the section and comprise calcareous clay to very fine sandstone (F1 – F3) with an approximately homogeneous thickness ratio and absence of fossils.

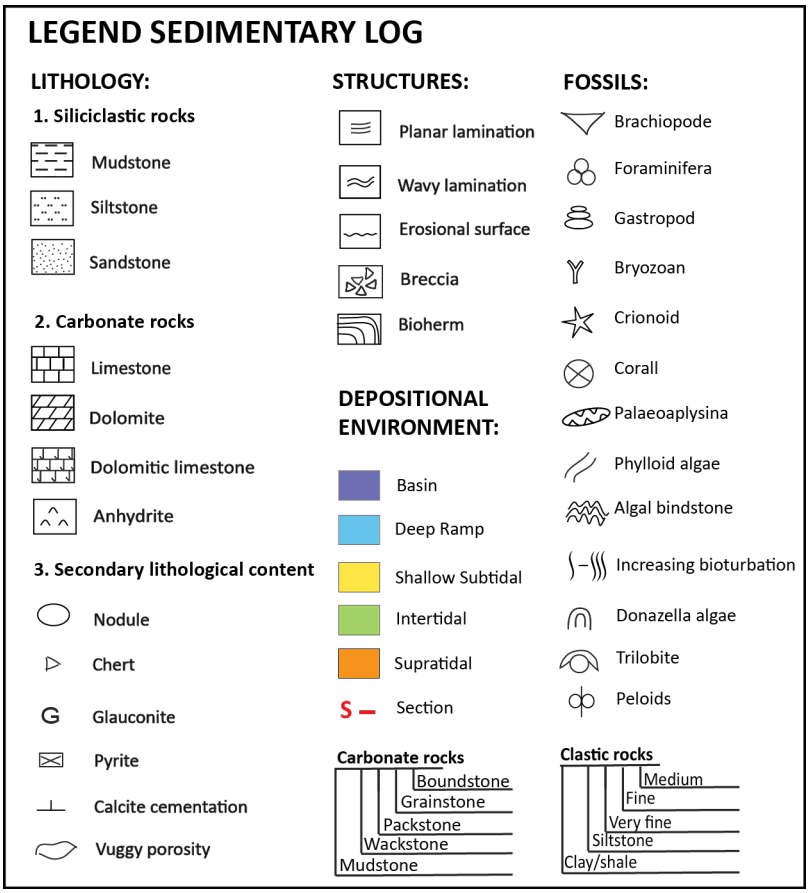

Figure 5.11. Legend for the sedimentary logs.

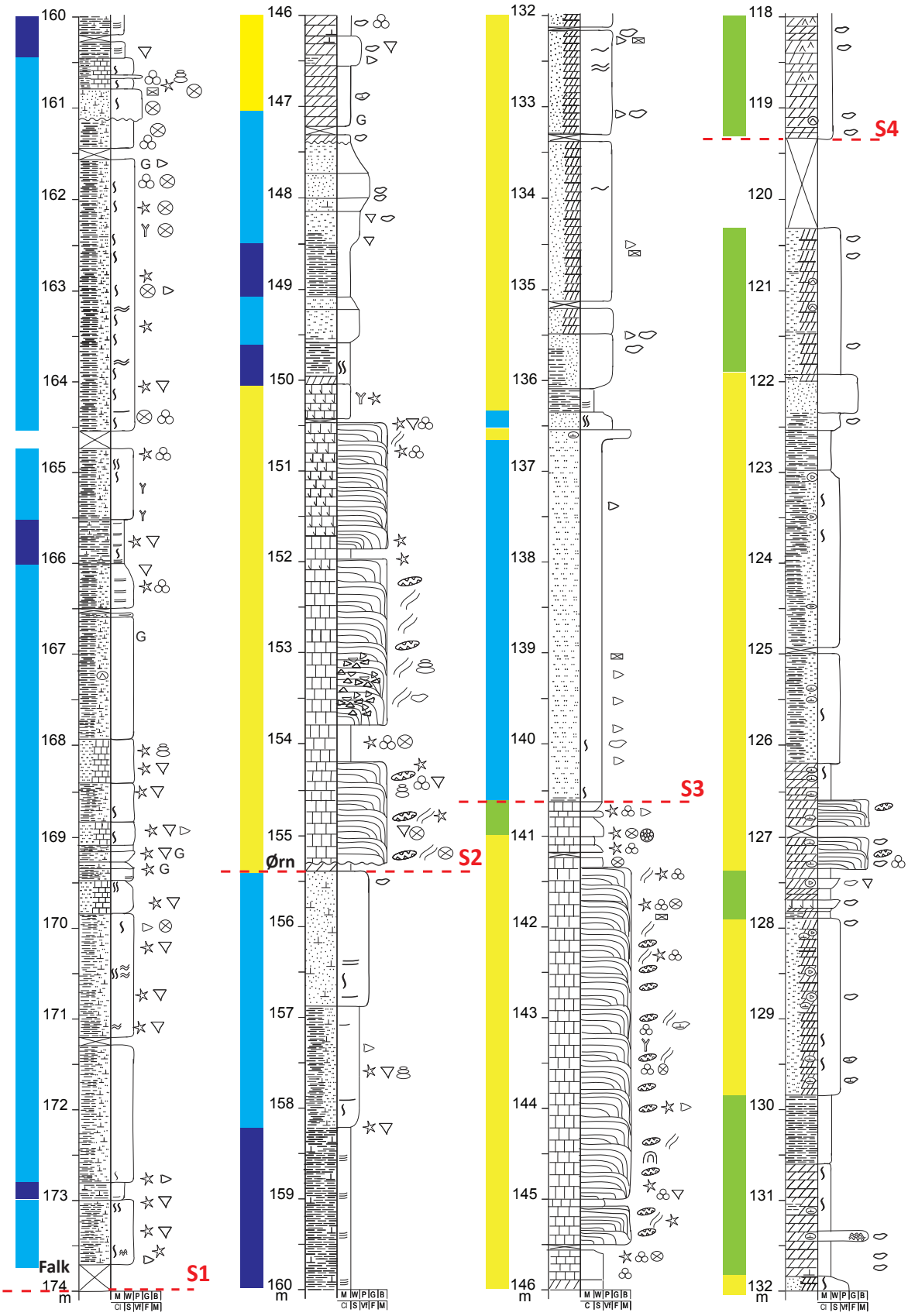

Figure 5.12. The sedimentological log drawn of the core including 174 – 118 m depth and thereby section 1, 2, 3 and partly 4 showing the vertical arrangement of the facies. The Falk Formation comprises section 1, whereas the Ørn Formation starts at section 2. Legend presented in **Figure 5.11**.

Section 2

The transition between section 1 and section 2 is the boundary between the Falk and Ørn Formation and is marked by a clear change in the deposited sediments, from being dominated by siliciclastic to also include carbonate sediments (Figure 5.12). The section is approximately 15 m thick and comprises two continuous individual carbonate units that are separated by one siliciclastic unit, reaching up to several m in thickness. Decimeter up to several meter thick individual *Palaeoaplysina*/phylloid algae boundstone (F7) with alternating amounts of inter-build-up layers are mainly representing the carbonate sediments, at the same time as a few dm thick intervals of mudstone (F4), wackestone (F5) and occasionally foraminiferic packstone (F6) are interbedded and enclosing these build-ups. Internal brecciation is observed in one of the lowest boundstones. From 149.90 – 147.40 m depth a siliciclastic unit occurs, which includes shale (F1), homogenous silt (F2A) and very fine sandstone (F3) that are alternating between coarsening- and fining upwards trends.

Section 3

Section 3 is 21.1 m thick and comprises mainly coarsening upward siliciclastic sediments, which includes laminated shale (F1), silt (F2A, F2B) and very fine sandstone (F3) (Figure 5.12). The relationship among these facies appears in different order of magnitude, from cm to m scale, however the total thickness of the individual units are commonly around 3 m. Commonly these siliciclastic deposits lack fossils, though some bioturbation occur. Two units of carbonate sediments with a thickness from a few dm up to approximately 2 m occur. These are presented by a few cm to dm thick layers of mudstone, wackestone and *Palaeoaplysina*/ phylloid algae boundstone. The individual layers representing section 3, both of siliciclastic and carbonate origin, has a varying degree of dolomitization, ranging from undolomitized to totally dolomitized.

Section 4

Starting from section 4 and continuing throughout the core, carbonate sediments dominate the depositions (Figure 5.12 and 5.13). Section 4 is 18.95 m thick and consists mainly of *Palaeoaplysina*/phylloid algae boundstone (F7) together with mud-dominated inter-build-up sediments including mudstone (F4) and wackestone (F5). The relationship between these facies is not fixed, although a trend comprising 0.25 – 1.20 m thick mudstone followed by 0.5

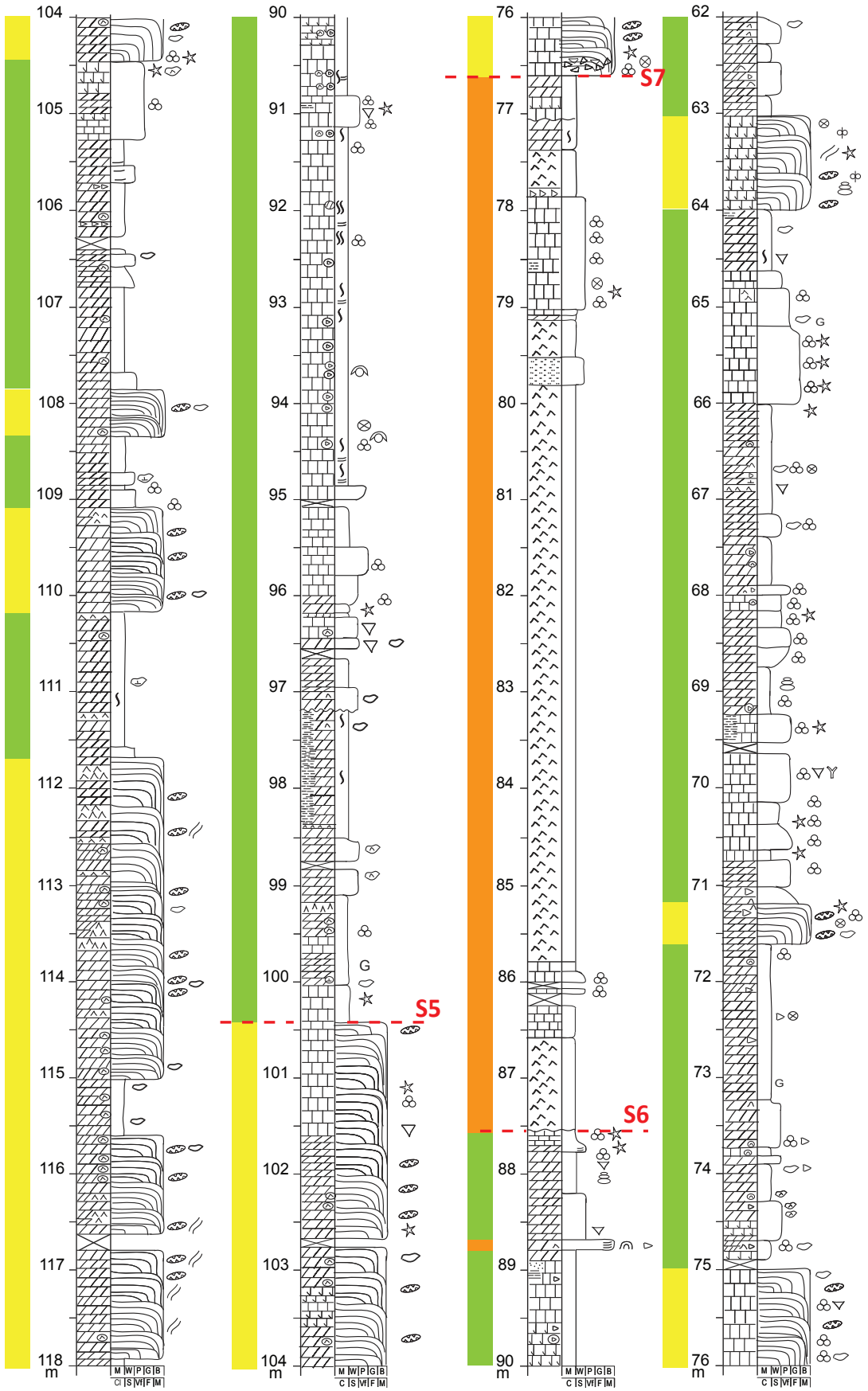

Figure 5.13. Continued sedimentological log of the core from 118 – 62 m depth, including section 4, 5, 6 and partly 7.

– 4 m boundstone enclosed by a few dm thick wackestone are occurring. Located between some of the individual build-ups, an association of dm scaled mudstone topped by cm thick wackestone occurs. Dolomitization is prominent throughout section 4, except in the uppermost part. Varying distribution of anhydrite beds and nodules are following the dolomitization, however a decrease in anhydrite beds and nodules appears in the upper part.

Section 5

This section has a total length of 12.9 m and is mainly characterized by the muddy facies, mudstone (F4) and wackestone (F5), however, some cm thick beds of foraminiferic wackestone/packstone (F6) are associated with the mudstone (Figure 5.13). The proportions between the individual facies are varying, where the relationship of size are relatively similar in some areas, whereas in others the mudstone have a clearly dominating thickness. The frequency of chert nodules seems to follow the thickness trend of the mudstone, as nodules are more abundant in the thicker intervals of mud. Several places, some siliciclastic clay is intermixed in the wackestone. The fossil content is higher in section 5 than in section 4 whereas the dolomitization is much less. Trilobites have only been recognized in section 5.

Section 6

Section 6 has a total thickness of 10.95 m including a 7 m thick layer of anhydrite (F10A, F10B and F10C) (Figure 5.13). Some cm-thick beds of mudstone and homogeneous siltstone accompanied with cm to dm-sized wackestone are the only facies intercalated within the anhydrite bed. The wackestones has a limited fossil fauna and a cm thick band of chert encrusts the uppermost wackestone. The whole section is terminated by an transition in facies from dolomitized mudstone to undolomitized boundstone.

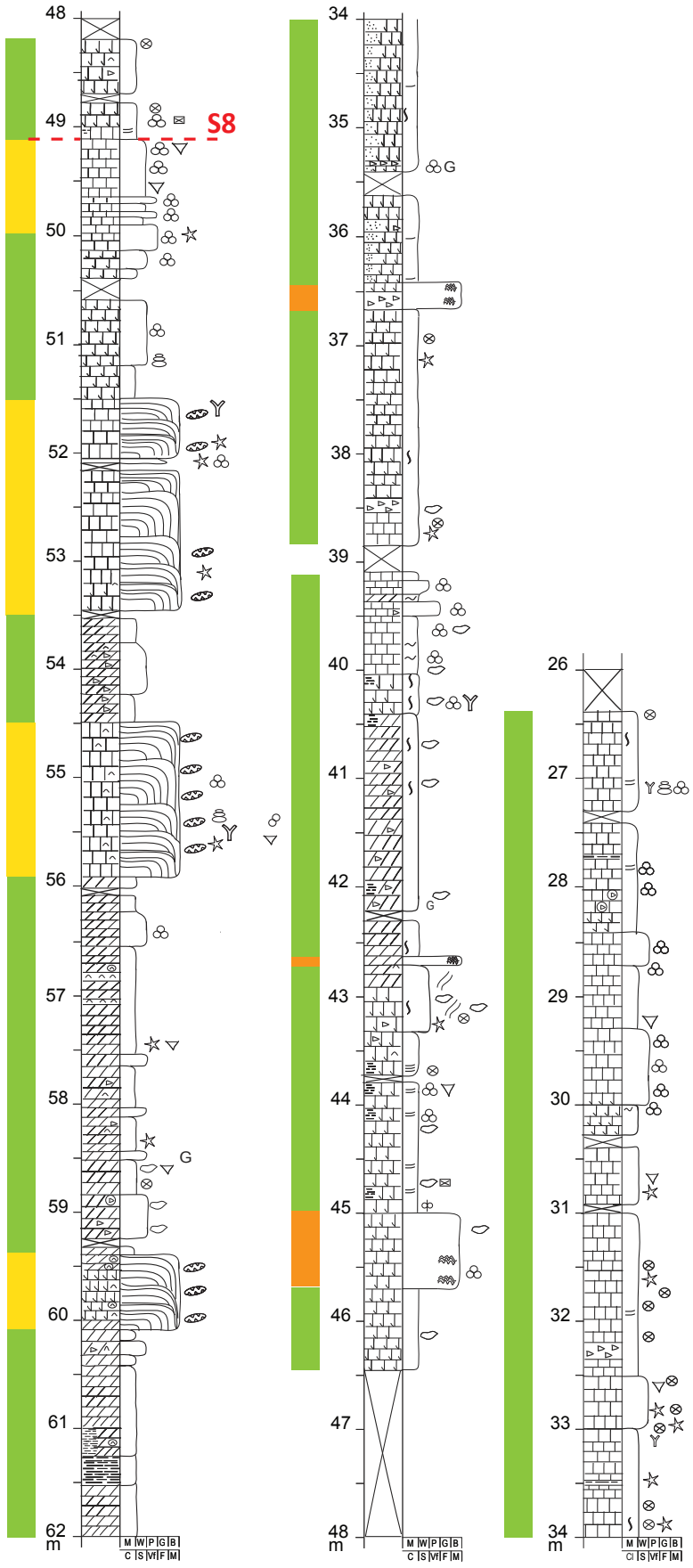

Figure 5.14 Continued sedimentological log including 62 – 26 m depth and partly section 7 and 8.

Section 7

Following the erosional surface separating section 6 and 7 (Figure 5.13), depositions of *Palaeoaplysina*/phylloid algae boundstone (F7) has resumed. The build-ups occur from a few dm in thickness up to a limit of 2 m and the lowermost one shows brecciating in the lower 20 cm. Closely associated with the boundstone in the lower part (below 62 m depth) are inter-build-up sediments as mudstone, wackestone and packstone, however towards the upper part of the section, only wackestone and mudstone are present as inter-build-up sediments. The sediments located between the build-ups are varying in order and thickness, with beds ranging from a few cm up to a couple of meters. The grainstone (F9) occurs exclusively within this section at 66 – 65.20 m depth, and as in the other facies in the section, foraminifera and crinoids dominate the fossil fauna. Mudstone and wackestone are dominated by dolomite, and occasionally the bpundstone has been affected by dolomite. In general, the dolomitized areas have a limited fossil content. The total thickness of the section is approximately 28 m.

Section 8

The uppermost 22.7 m thick section is mainly characterized by mudstone with some layers of wackestone and some thin beds of packstone, in addition as some layers of stromatolite bindstone (F8) are present (Figure 5.14). In general the mudstone layers are ranging from approximately 0.6 m up to a couple of m in thickness, whereas the wackestone range from a few cm up to 0.5 m. The thickness of the bindstone ranges from a dm up to almost 7 dm. In some of the mudstones an increase of clastic input as clay and silt occur. The fossil fauna within section 8 is rather sparse except foraminifera and an increase of rugose corals compared to the other sections occur. Up to 34 m depth the mudstone is dolomitized, the rest of the section is undolomitized. The section has an alternating amount of chert nodules and bands.

5.3 Porosity classification of the carbonate facies

The porosity types within the carbonate facies are classified by the classification system after Lønøy (2006), see Table 1, section 2.4.2. A summary of these is presented Table 6.

Table 6. An overview of the porosity classifications occurring within the different carbonate facies, where a detailed description is written in the text. The detailed definition of pore size is defined in Table 1. U = undolomitized, DL = dolomitic limestone and partly dolomitized, D = dolomitized.

Facies	Pore Type	Pore Size	Pore Distribution	U, DL, D
Mudstone (F4)	Tight			U, DL, D
	Interparticle	Micro- Macro	Patchy	U, DL,
	Intercrystalline	Micro - Macro	Patchy/Uniform	DL, D
	Moldic	Meso - Macro	Patchy/Uniform	DL, D
	Microporosity		Patchy/Uniform	U
Wackestone	Tight			U
(F5)	Interparticle	Meso-Macro	Patchy	DL
	Intercrystalline	Micro -Macro	Patchy/Uniform	D
	Moldic	Macro	Patchy	U, D
Foraminiferic	Tight			U
wackestone	Intercrystalline	Micro	Patchy	D
/packstone (F6)	Moldic	Meso - Macro	Patchy	D
***Palaeoaplysina*/p**	Tight			U, DL
hylloid algae	Interparticle	Micro-Macro	Patchy	U
boundstone (F7)	Intercrystalline	Micro-Macro	Patchy	DL, D
	Moldic	Macro	Patchy	D
Bindstone (F8)	Tight			DL
	Interparticle	Macro	Patchy	DL
	Intercrystalline	Macro	Patchy	DL
Grainstone (F9)	Moldic	Macro	Patchy	U
Anhydrite (F10)	Tight			

Mudstone (F4): Most of the mudstones in the core are partly or totally dolomitized where patchy intercrystalline micro - to macropores (Figure 5.15B) are dominating, though sometimes patchy moldic meso – macropores occur, either as dominant porosity type or mixed with the intercrystalline porosity. In a few partly and totally dolomitized mudstones, tight composition occurs. In addition, in some of the partly dolomitized mudstones interparticle micro- to macroporosity porosity occurs. Among the undolomitized mudstones tight porosity is common (Figure 5.15A). However, many thin sections representing the mudstone appear very muddy, which makes it difficult to separate the porosity, though in the areas where it is possible, patchy and uniform chalky microporosity, and occasionally patchy interparticle microporosity are present.

Wackestone (F5): In the dolomitized wackestone, the dominating porosity is patchy intercrystalline micro- to macropores, although some uniform distribution occurs. Patchy moldic macropores are also a present porosity type within the dolomitized wackstone facies, and a noteworthy example of this is at 127.57 m depth that is shown in Figure 5.15C where huge subrounded pores of moldic porosity are present. Often a mixture between moldic macropores and intercrystalline porosity with a patchy distribution occur in the dolomitized wackestone. When partly dolomitized, interparticle mesopores is occurring, and when undolomitized the facies appear as tight.

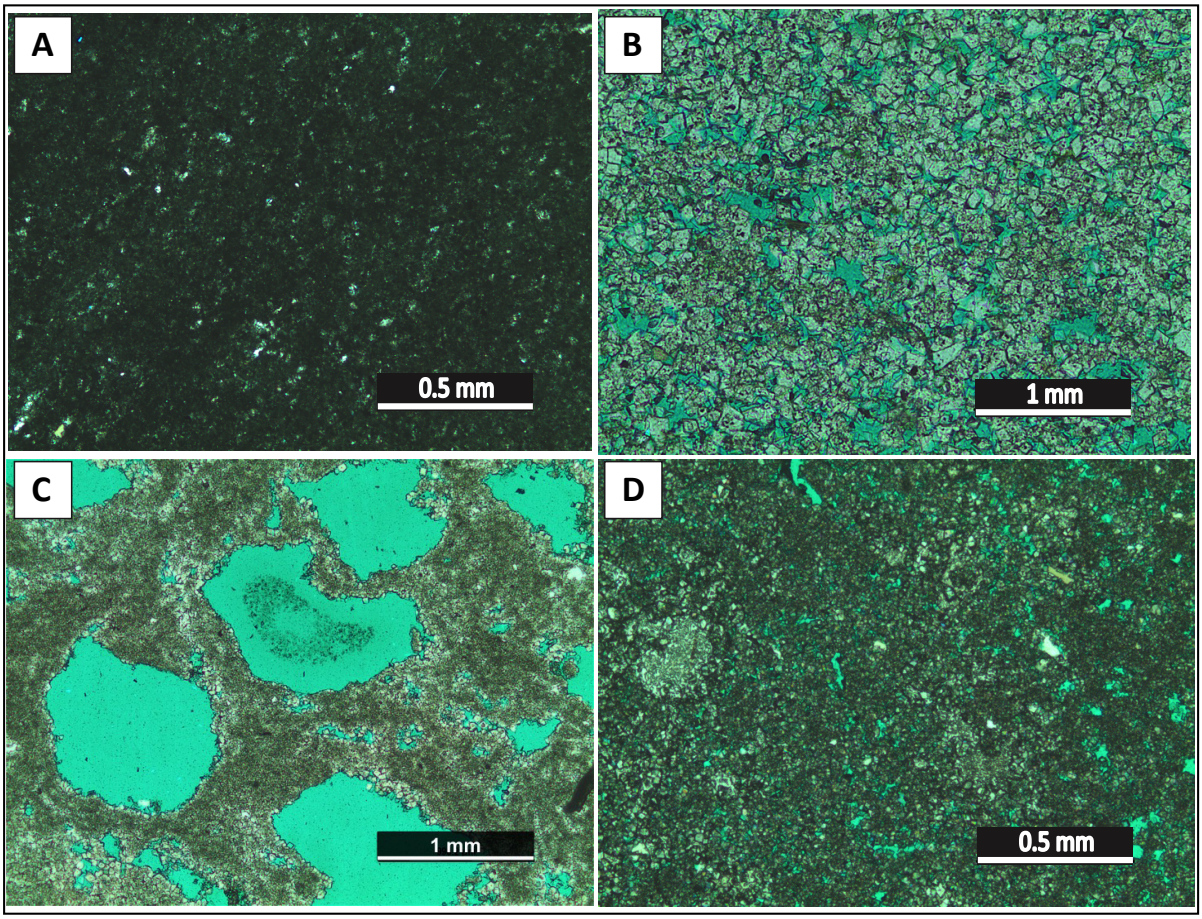

Figure 5.15. Micrograph of the different facies and their porosity distribution, pictures taken in plane light where the clear green areas are epoxy. (A) Tight porosity within undolomitized mudstone (F4) (B) Patchy intercrystalline meso- to macropores in the dolomitized mudstone (F4). (C) Huge subround moldic pores located within the dolomitized wackestone at 127.57 m depth. (D) Dolomitized intercrystalline wackestone with patchy meso and macropores.

Foraminiferic wackestone/packstone (F6): A few thin sections only represent the foraminiferic wackestone/packstone; however, the few specimens are showing that the

packstone appears as tight in areas unaffected by dolomitization. The dolomitized areas show a muddy look, where some patchy intercrystalline micropores occur together with patchy moldic meso- to macropores (Figure 5.16D).

Palaeoaplysina/*phylloid boundstone (F7)*: The *Palaeoaplysina/*phylloid boundstone (F7) is almost dominantly tight (Figure 5.16A) in areas unaffected by dolomitization except from some scarce patchy interparticle micro – macroporosity. Where the boundstone is partly dolomitized the porosity also appear as tight. In the dolomitized boundstone the porosity is dominated by patchy intercrystalline micro- to macroporosity (Figure 5.16B), however this porosity is often mixed with moldic macroporosity. Only occasionally patchy moldic macroporosity occur as dominant in the dolomitized boundstone.

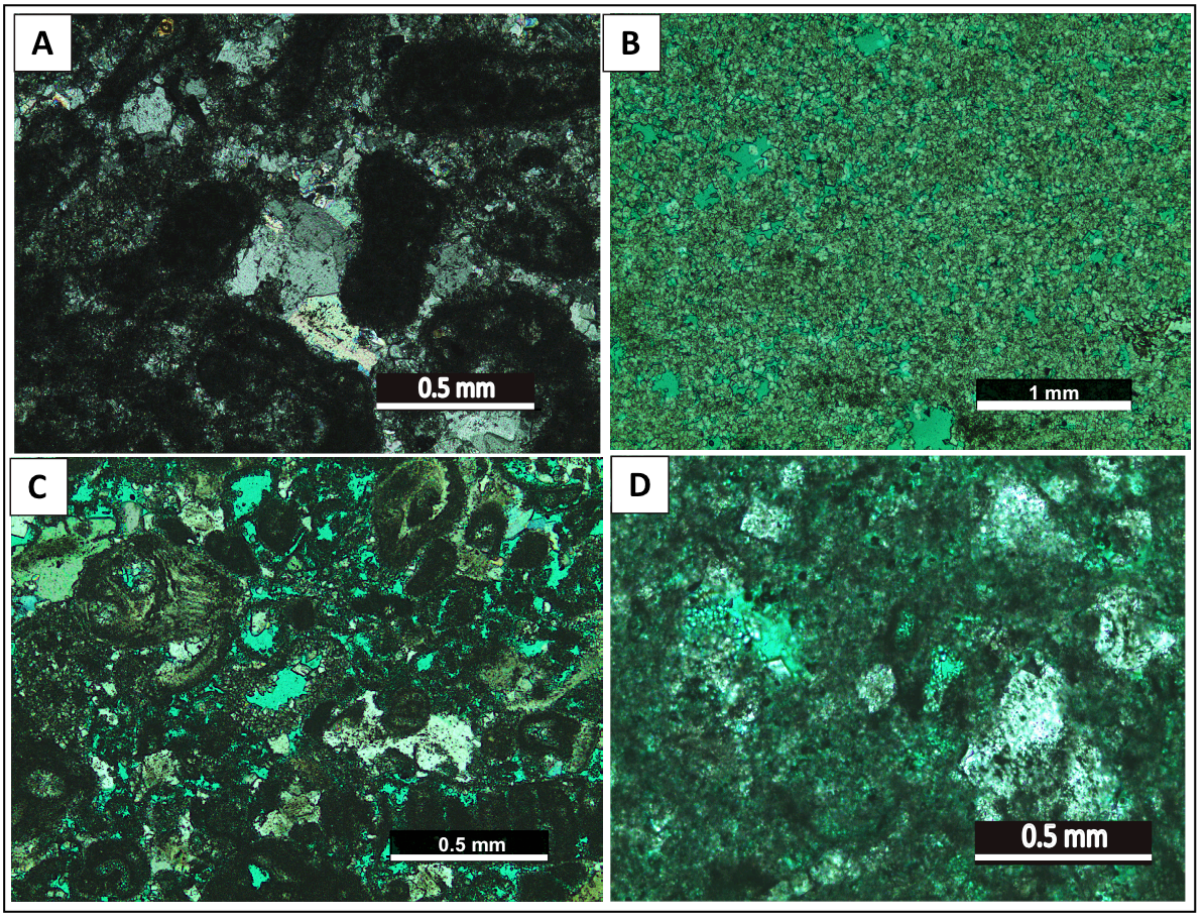

Figure 5.16 Micrograph of the different facies and their porosity distribution, pictures taken in plane light where the clear green areas are epoxy. (A) Tight undolomitized *Palaeoaplysina*/phylloid algae boundstone (F7) (B) Totally dolomitized *Palaeoaplysina/* phylloid boundstone with patchy micro – macro intercrystalline porosity (C) Grainstone (F9) with moldic macropores and patchy interparticle macropores. (D) Dolomitized foraminiferic wackestone/packstone with patchy intercrystalline meso- and macroporosity. Note the muddy look.

Bindstone (F8): The bindstone has an interparticle patchy mesoporosity in the areas where dolomitic limestone and calcite are prevailing. Also, where chert occurs within this facies the same porosity trend can be observed. Where the facies is completely dolomitized the porosity is intercrystalline patchy macropores.

Grainstone (F9): The study of the grainstone porosity was limited due to the lack of thin sections, however in the one specimen representing this facies the porosity is classified as moldic macropores and patchy interparticle macropores (Figure 5.16C).

Anhydrite (F10): The porosity within the anhydrite facies (F10) was classified as tight as no porosity was observed.

5.3.1 The overall picture

In Figure 5.17 a summary of the porosity distribution including the most dominating porosity classes of the core is presented, in addition, porosity values of the core presented in Appendix 1, panels 1-3 in Ehrenberg et al. (2000) are added for comparison. The result shows that the most dominating classes are intercrystalline and tight porosity. Interparticle porosity has an intermediary distribution, whereas moldic microporosity occurs much sparser. It is clear that the intercrystalline porosity is dominating in section 4, 7 and partly 8. The intercrystalline class is present within intervals affected by dolomitization. Generally the intercrystalline porosity has registered porosity values in the *Palaeoaplysina*/phylloid algae boundstone and the mudstone. The porosity values within the boundstone are maximum 17% and are mainly lying in a range between 6 and 15%, whereas the mudstone has a more widespread distribution of the porosity value, ranging between 7 - 31 %. The tight porosity is most common in the undolomitized intervals, as seen in sections 2, 7 and 8, though some registrations occur in intervals affected by dolomite. The tight porosity is most common among *Palaeoaplysina*/phylloid algae boundstone and the mudstone. No porosity values are registered for this class. The interparticle porosity is most common in section 7 and 8 and then within partly dolomitized mudstone and wackestone. A few porosity values of approximately 17 and 22% are coinciding with the mudstone where interparticle porosity prevails. However the value of 22% lies in close relation to registrations of moldic porosity so it is difficult to determine which of the two porosity classes that gives the value. The moldic porosity is

almost exclusively located in mudstone that is partly or totally dolomitized, as seen in section 3, 5, and 8 (Figure 5.17). The scarce registration of microporosity on the other hand is reserved undolomitized mudstone in section 8, here no porosity values are registered.

Generally, none of the porosity classes has a continuous distribution throughout the core, though, within almost all classes and within individual intervals, several registrations of the same porosity class are coincidence in clusters within a range from a few meters up to 20 m, though within a varying density. The intercrystalline porosity appears to be most densely packed followed by the classification of tight porosity. The other porosity types are observed to show less densely occurrence. In the lower part of the core some overlap along the depth among the tight, interparticle and intercrystalline classes occur but no apparent fixed trends are observed among these classes in this area of the core as the registrations seems to have a random scattered distribution. The lack of fixed trend also goes with the upper part of the core, however, also here an overlapping trend among the porosity classes are observed with depth concurrent as a more widespread distribution of different porosity types.

In overall Figure 4.17 shows that the measured porosity of the carbonate sediments mostly lies within a value range of 5 to approximately 25 %, only including three exceptions that have porosity values over 30%. The overall trend is showing an increased porosity above the anhydrite layer that ends at 79 m depth.

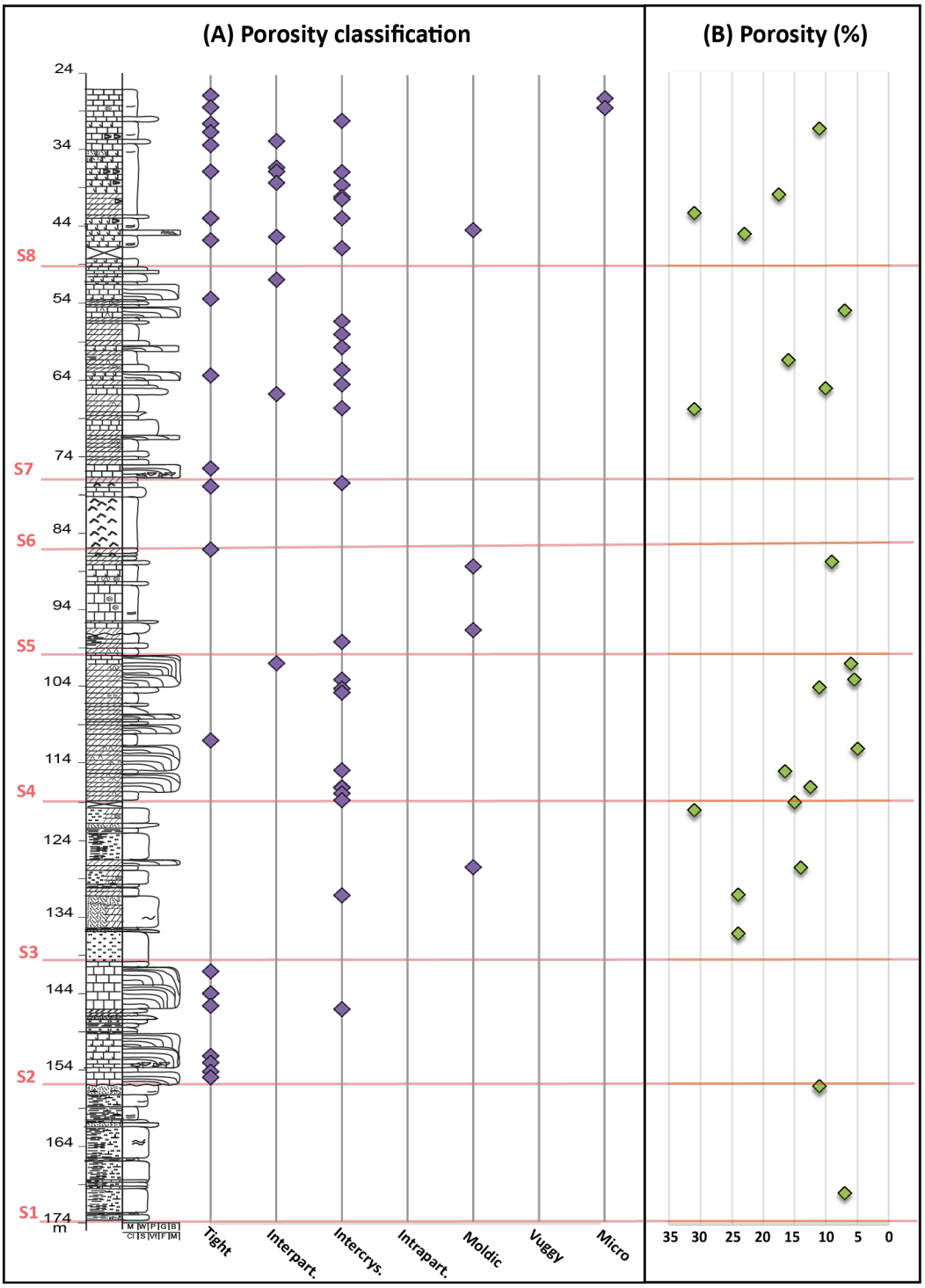

Figure 5.17. (A) A summary of the different porosity classes registered and their distribution throughout the core. Interpart. = interparticle, intercryst. = intercrysalline whereas intrapart.. = intraparticle. (B) The porosity values taken of the core by Ehrenberg et al. (2000). In addition the defined sections are added and marked with red lines The transition from section 1 to section 2 marks the boundary between the Falk and Ørn Formation.

6 Results

6.1 Classification of stylolites and dissolution seams

The different classifications of the pressure solution seams that are registered in the core have been plotted versus depth and lithology, and the facies to see if some trends could be observed. The calcite/dolomite ratio proportions of the weight percent calcite and dolomite expressed as CCD where added after Appendix 1, panels 1-3 in Ehrenberg et al. (2000). As the log is based on interpretation done in this study and the CCD is taken from another author, it must be stated that the lithology in the log and the CCD does not coincide at every point. Furthermore, to simplify the description, the eight defined sections are used as a base.

6.1.1 The number of pressure solution seams per meter

The total length of the core was divided into intervals of 1 m length, starting at 24.0 m. At each interval the number of dissolution seams and stylolites were registered and plotted against the mid point of each respective interval. Obviously, the chosen intervals do in general not coincide with the individual lithological layers, such that a given interval may include several carbonate facies within a meters range. Hence, Figure 6.1 is only meant to be an illustrative overview of the density distribution of the dissolution seams and the stylolites. The result shows that the total number of dissolution seams is both higher and more widespread than the stylolites through the core however; the two defined types of seams are mostly favoring the same intervals of facies, including *Palaeoaplysina*/phylloid algae boundstone (F7) and the mudstone (F4) in addition, some seams are also located in the wackestone. The stylolites are mainly concentrated within the *Palaeoaplysina*/phylloid algae boundstone in section 2, 4 and 7 whereas in section 8 they occur in the mudstone. The dissolution seams on the other hand, occurs frequently in the *Palaeoaplysina*/phylloid algae boundstone, mudstones and wackestone in section 2, 3, 4, 5, 7 and 8. Commonly for both the seams are devoid of the anhydrite layer in section 6 (Figure 6.1). Notable is section 2,

constituting the only section in the core where the stylolites are more frequent than the dissolution seams.

Among the observations, the dissolution seams are dominant in the intervals where the dolomite content usually is approximately 30% or more, in contrast the stylolites are prevailing where the rocks contain 100% calcite (Figure 6.1C). This is especially clear in the intervals in lower part of section 2 where the boundstones are represented with a varying degree of dolomitization. Here, the number of stylolites is more than twice as much as the dissolution seams where 100% calcite occur, but once dolomite is presented, the relationship is reversed and dissolution seams are the dominating seam. This trend is even clearer in the dolomite-dominated intervals in section 4. Here an overweight of dissolution seams is observed simultaneous as several areas are lacking stylolites, though once calcite is present as seen in the top of the boundstone the amount of stylolites is much higher. However, in spite of a greater number of dissolution seams in the dolomite rich intervals, a tendency of decreasing amount of seams occur as the degree of dolomite increase, as seen in section 7. It is notable that in section 5, which is lying below the anhydrite layer, includes a scarce number of dissolution seams, whereas stylolites are lacking.

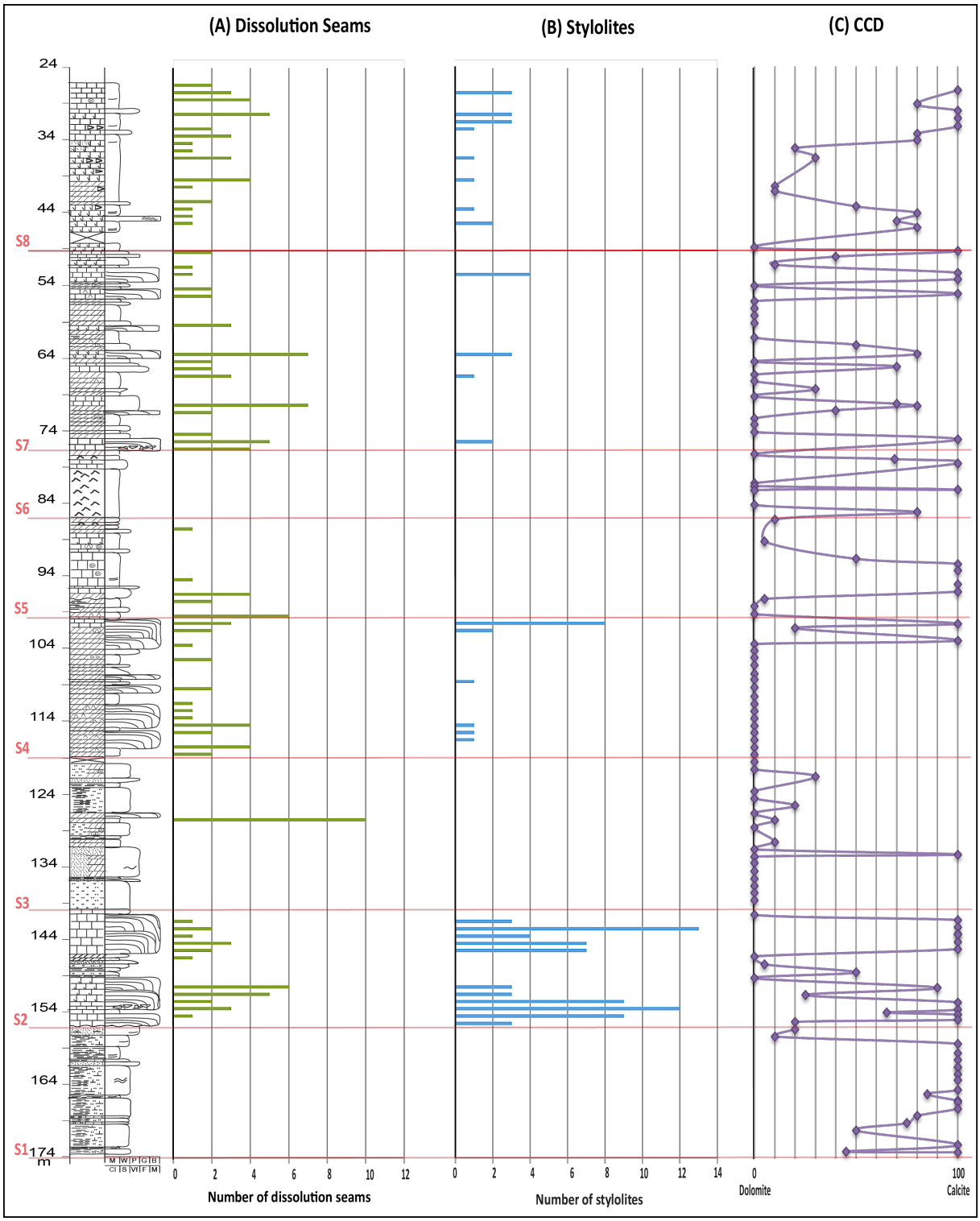

Figure 6.1. (A) The number of dissolution seams per meter, versus depth and lithology in the core. (B) The number of stylolites per meter versus depth and lithology in the core. (C) CCD is the relative proportions of weight percent calcite and dolomite based on the bulk XRD analysis which is presented in Appendix 1,panels 1-3 in Ehrenberg et al. (2000). In addition the 8 defined sections are added where the transition from section 1 to section 2 marks the boundary between the Falk and Ørn Formation.

6.1.2 High and low amplitudes

The individual dissolution seam and stylolite in the core were categorized with either low or high amplitude after the classification system presented in Figure 4.2A. This result is presented in Figure 6.2; in addition this figure would present a more detailed distribution of the seams than Figure 6.1. Figure 6.2A, B shows that there is a dominance of low amplitudes of both types of pressure solution seams, however the dissolution seams of low amplitude are most frequent throughout the core. The dissolution seams of low amplitude are commonly seen in those facies comprising high amount of mud (mudstone and wackestone), and in the boundstone. In contrast, the extension of the stylolites with low amplitude is minor and mostly located within the *Palaeoaplysina*/phylloid algae boundstone, except in section 8. Commonly for the two defined pressure solution seams characterized with low amplitude is a higher occurrence where some dolomite is presented (>10%, Figure 6.2D). The high amplitude dissolution seams are only located within section 2 and 4, whereas the high amplitude stylolites occur scattered throughout the core (section 2, 3, 4, 7 and 8). The *Palaeoaplysina*/phylloid algae boundstone facies is rich in both types of the high amplitude seams, though the dissolution seams occur mostly where 100% dolomite occurs, whereas the stylolites are generally located within the calcite-dominated boundstones. Only within section 8, stylolites characterized with high amplitude are located within the muddy facies, though also here 100% calcite is present. With the exception of the dissolution seams of high amplitude, the other categorized seams are more strongly accumulated within the build-ups in section 2. The occurrence of columnar style of stylolites is plotted in Figure 6.2C. Here the results shows that stylolites characterized by low amplitude has a columnar style where the amount of dolomite is 10% or more, whereas the combination of columnar style and high amplitude stylolites is present in relation with 100% calcite.

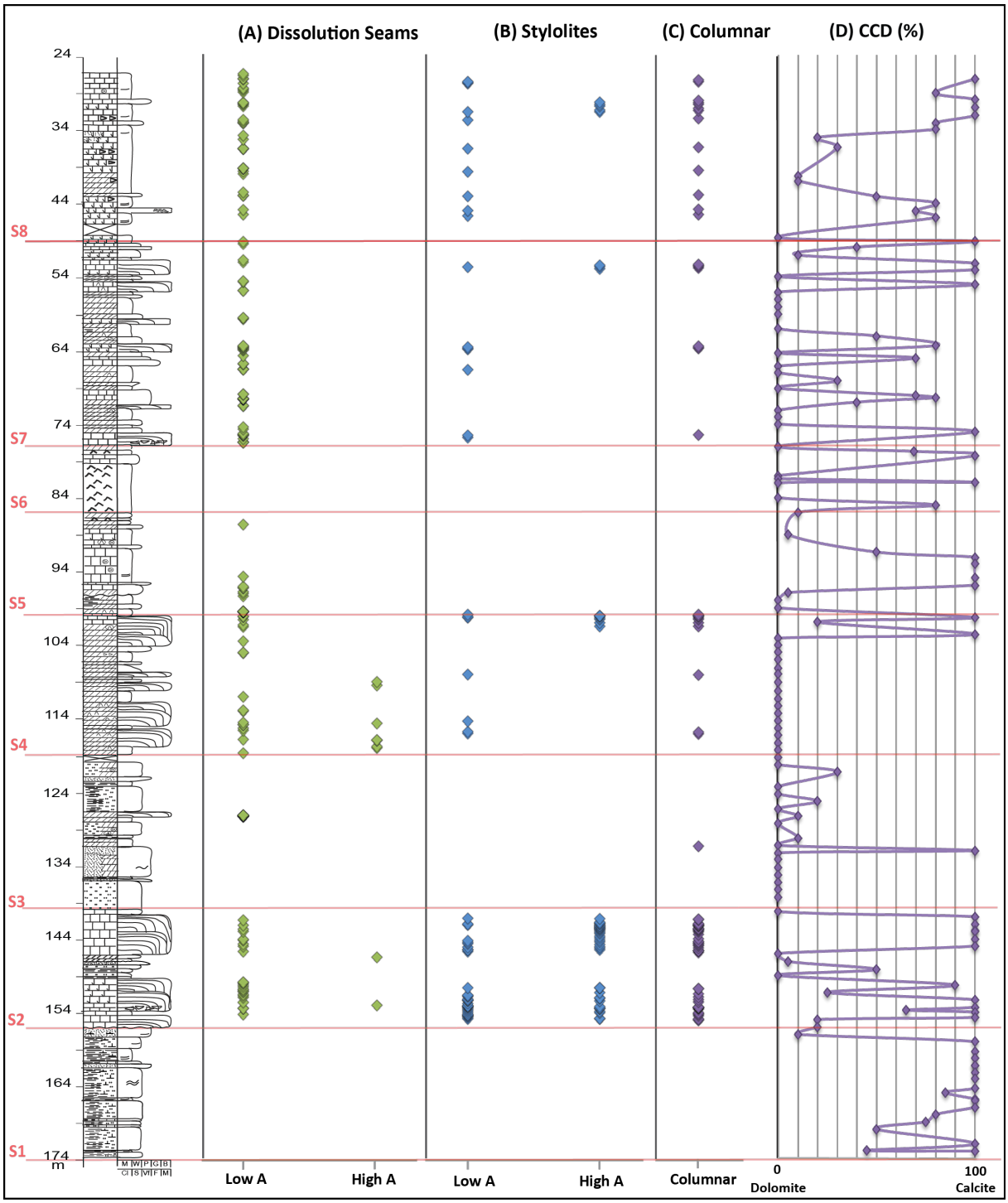

Figure 6.2. Figure showing the type of styles of stylolites and their distribution through the core. (A) Represents the occurrence of low and high amplitudes in the dissolutions seams. (B) Represent the distribution of high and low amplitudes of stylolites. Low A = Low amplitude, High A = high amplitude. (C) Shows where the columnar styles of the stylolites occur within the core. (D) CCD as introduced above, taken from Appendix 1,panels 1-3 in Ehrenberg et al. (2000). In addition the 8 defined sections are added, where the transition from section 1 to section 2 marks the boundary between the Falk and Ørn Formation.

6.1.3 Nodule-bounding

Several of the pressure solution seams in the core are classified as nodule-bounding after the classification presented in Figure 4.2B, and the two defined seams individual nodule-bounding distribution is presented within Figure 6.3. The figure shows that only five nodule-bounding stylolites are registered, whereas nodule-bounding dissolution seams are present in broadly speaking throughout the whole core with the exceptions of section 1, 3 and 6. Generally, the nodule-bounding dissolutions seams occur in clusters or in couples, though single ones occur occasionally (Figure 6.3). All of the nodule-bounding dissolution seams are favored within facies with more than 10 % fossil content including wackestone – boundstone (Figure 4.1), though a higher amount and most of the clusters occur within the *Palaeoaplysina*/phylloid algae boundstone facies (F7). The few registered nodule-bounding stylolites are concentrated within the boundstones in sections 2 and 4, whereas in sections 7 and 8 they are restricted to the mudstone facies (F4). Every nodule-bounding stylolite appears in the dolomite dominated units, with the exception of one in the upper boundstone in section 2. The same trend can be seen among the dissolution seams as well, where only a few of the registrations in sections 2, 7 and 8 occur in 100% calcite dominated areas, beyond this, the seams occur mostly in dolomite dominated intervals.

6.1.4 Stylolites - Mean amplitude value, depth and lithological relationship

The mean amplitude value was calculated for each stylolite in the core as explained in Figure 4.2D and the results are presented in Figure 6.4. Figure 6.4A shows that the registered data is concentrated to certain depths in the core, which furthermore can be seen in coherence with lithology and facies. In section 2, 4 and 7 the data is clustered at the depths coinciding with the *Palaeoaplysina*/phylloid algae boundstone (F7) (green areas in Figure 6.4A). In contrast, within section 8, the data is more scattered over a greater depth interval, limited to the mud-supported facies. Generally the maximum mean amplitude value is less than 9 mm high.

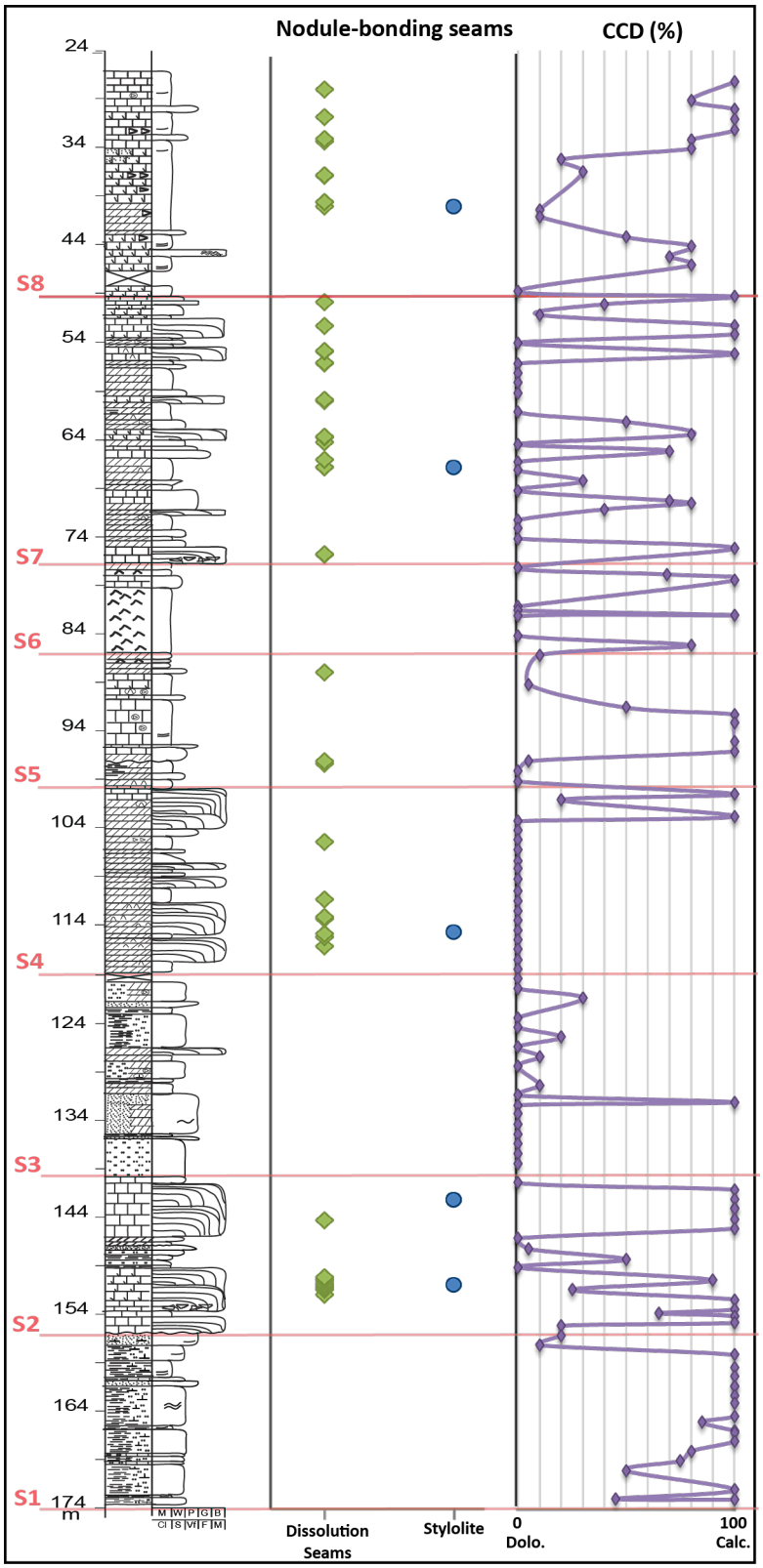

Figure 6.3. The distribution of the nodule-bonding seams in the core where the green rhombs represents the dissolution seams and the blue circles symbolizes the stylolites. In addition the CCD after Appendix 1, panels 1-3 in Ehrenberg et al. (2000) is added, and the 8 defined sections in the core. The transition from section 1 to section 2 marks the boundary between the Falk and Ørn Formation.

It is interesting that it is both more stylolites and higher registered mean amplitude values within calcite dominated *Palaeoaplysina*/phylloid algae boundstone (F7) than in dolomite-dominated *Palaeoaplysina*/phylloid algae boundstone, where only a few stylolites with lower mean amplitude values have been recorded. This is distinct in the calcite-dominated boundstone within section 2, at 144 m depth, where a high number of stylolites simultaneously with larger amplitudes values are seen, in contrast to the dolomitized boundstones in section 4, between 118 and 102 m depth where a low amount and low values occur. This pattern is also seen in the boundstone in the upper part of section 4 (100 m depth) where several stylolites with higher mean amplitude value occurs as the calcite amount is increasing (Figure 6.4).

Based on the observations above, it is evident that the *Palaeoaplysina*/phylloid algae boundstone (F7) is a facies that is distinguished from the rest by both higher amounts of stylolites and higher mean amplitude values. Therefore a closer look at this facies has been done. Based on Figure 6.4A, the two lower build-ups in section 2 can be distinguished from the rest by abundant amounts of registered values, compared to the other build-ups where the number of registered stylolites are so limited that usually no trend can be seen. Figure 6.5 shows an enlarged scale of the two lower build-ups in section 2 accompanied with their mean amplitude values and calcite/dolomite ratio (CCD) after Ehrenberg et al. (2000). The two build-ups show the same internal distributional pattern of mean amplitude values: The lower 3 m in the lowermost build-up and the lower 2 m in the upper one show trends with mean amplitude values equal to or lower than approximately 7 mm. These 2 m are followed by a 1-1.5 m thick interval with distinct increase in amplitude values reaching almost 11 mm in the lower build-up and 13 mm in the upper one, and then decreasing in the upper 2 m of both build-ups. However, only the lower build-up shows a correlation with calcite content. In the upper build-up this correlation is not so evident as the values decrease in spite of calcite compaction.

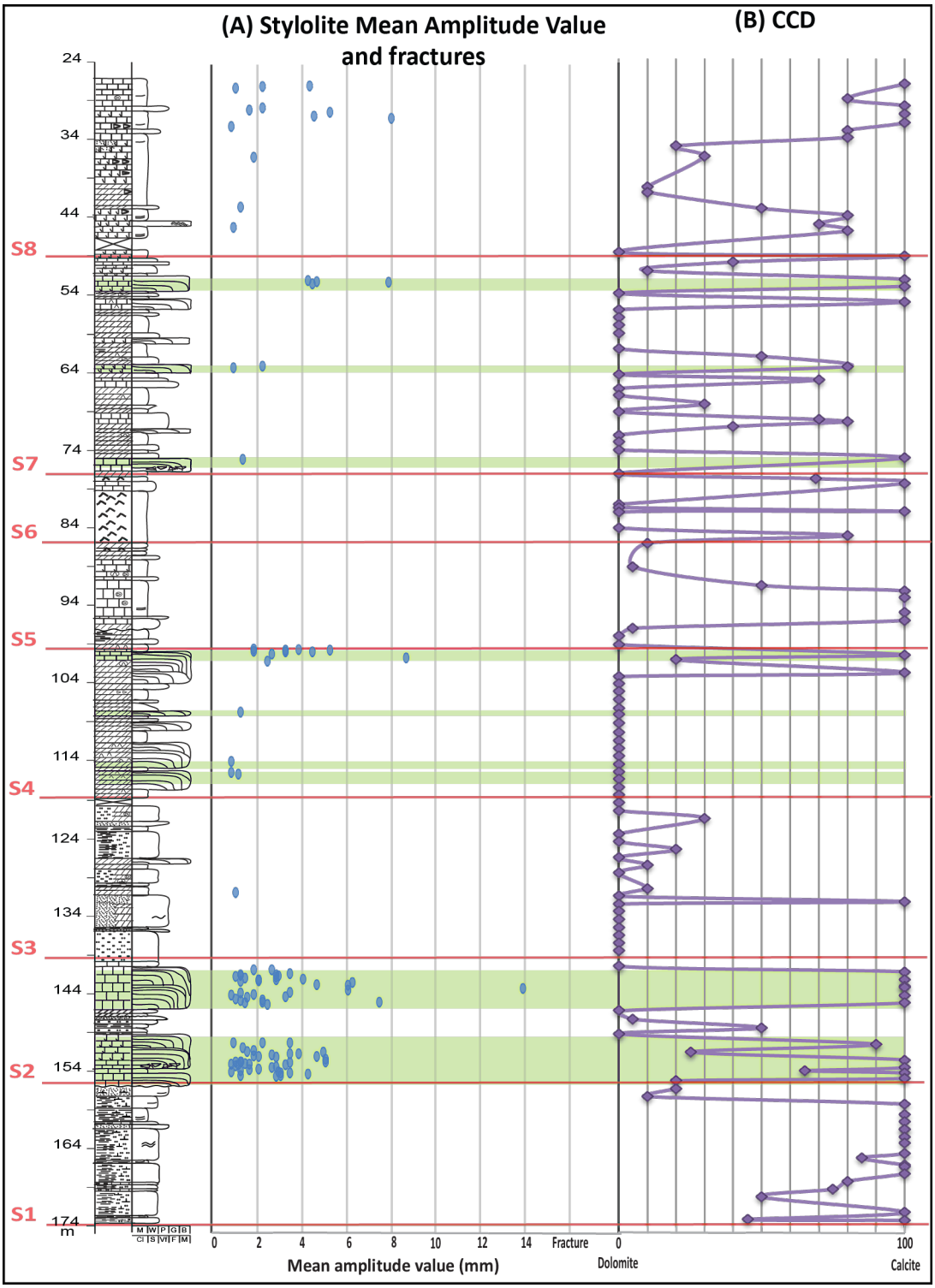

Figure 6.4(A) The mean amplitude value for the individual registered stylolite is plotted (blue circles) versus the depth and the accompanied lithology and thereby facies. Since the mean amplitude values only are registered for the stylolites (chapter 4.2.2), this figure only comprises these seams. The green areas are indicating the zones of clusters occurring within the *Palaeoaplysina*/phylloid algae boundstone (F7). (B) The CCD of the core taken from Appendix 1, panels 1-3 in Ehrenberg et al. (2000) for comparison. In addition the 8 defined sections are added, the transition from section 1 to section 2 marks the boundary between the Falk and Ørn Formation.

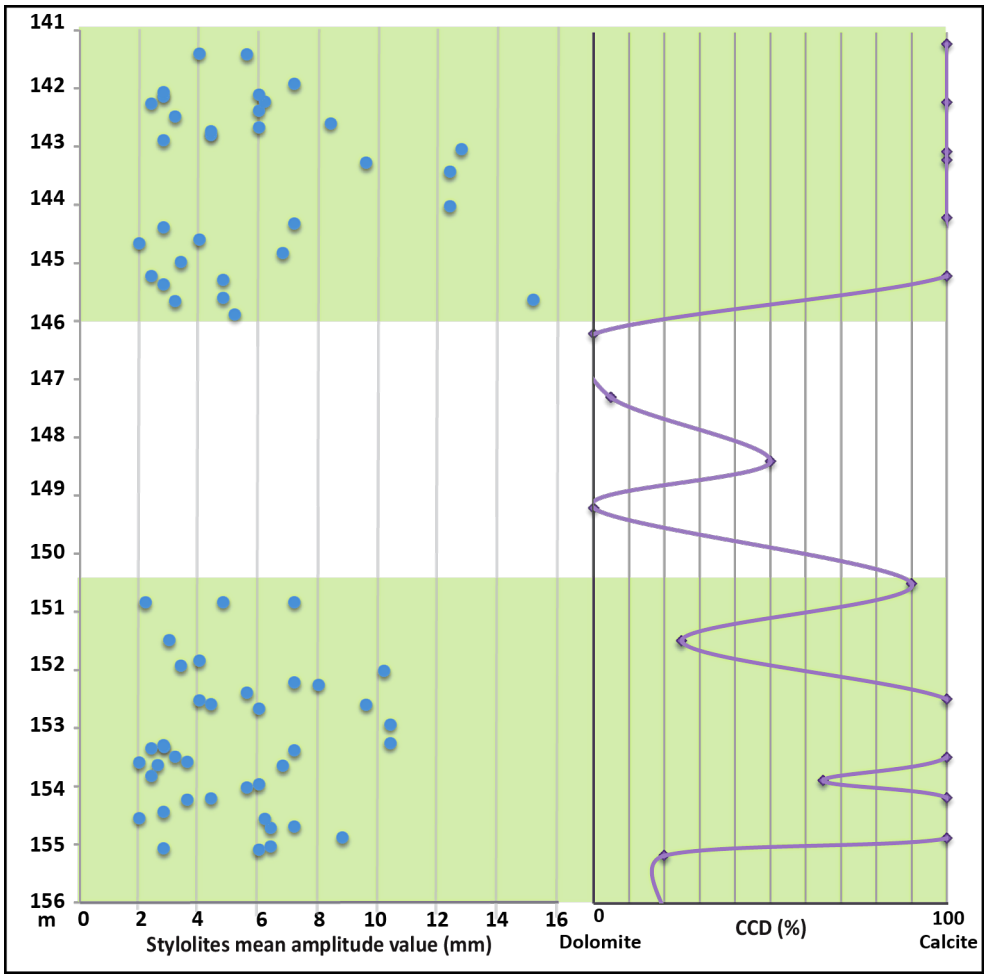

Figure 6.5. The two lower boundstones in section 2 blown up including the CCD after Appendix 1, panels 1-3 in Ehrenberg et al. (2000). The green areas are marking the interval of individual build-ups.

6.1.5 Stylolites - Style of amplitude

The individual stylolites morphology are after Figure 4.2C and the results are shown in Figure 6.6. From the figure it is difficult to see any trend among the different style as neither lithology nor the calcite/dolomite relationship could be related to the different styles at the same time as the different styles are overlapping in depth.

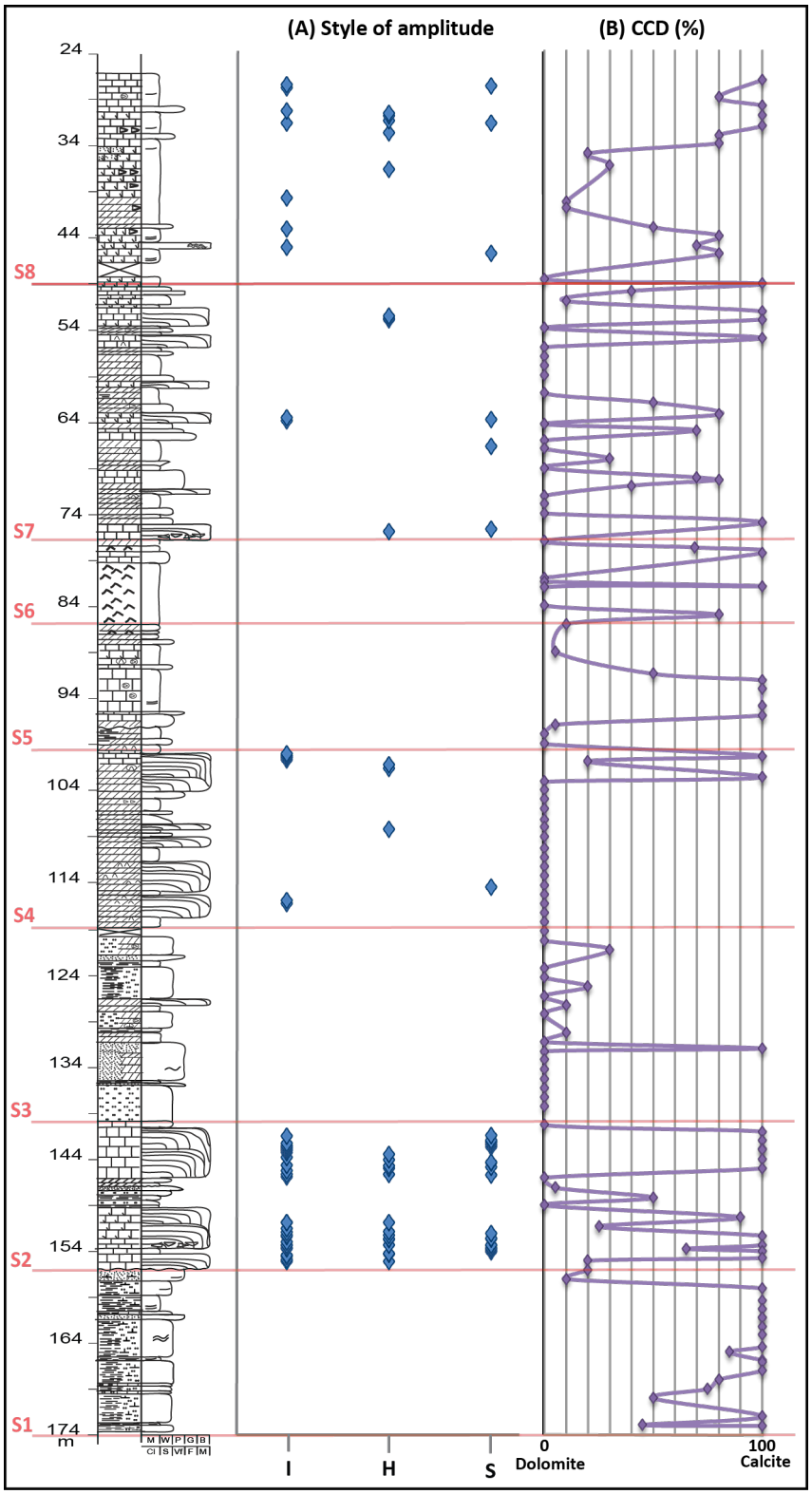

Figure 6.6. The style of the stylolites and their distributions with depth. I = irregular, H = hummocky, S= smooth, see figure 2.5 for closer description. In addition the CCD after Appendix 1, panes 1-3 in Ehrenberg et al. (2000) are added. The red lines marks the 8 defined sections, section 2 marks the transition between the Falk and Ørn Formation.

6.1.6 Swarms

The distribution of the swarms (Figure 4.2B) in the core is clearly more widespread among the dissolution seams than among stylolites (Figure 6.7). The swarms of both types of seams are generally concentrated within the *Palaeoaplysina/*phylloid algae boundstone and mudstone, though some swarms of dissolution seams are present in the wackestone. No preference of calcite or dolomite amount is seen among the swarms of the dissolutions seams, however the stylolites swarms favors calcite dominated facies. It is notable that most of the swarms including both the seams are occurring in clusters rather than as single swarms.

6.1.7 Pressure solution seams, lithology and porosity

When combining the porosity classification and porosity vales presented in Figure 5.17 with the distribution of the pressure solution seams in Figure 6.1, several correlations can be seen as the data are coinciding at the same depth (Figure 6.8). Where the frequency of registered seams is high e.g. section 2, 7 and 8, the porosity is characterized as tight and the calcite content is 80% or more. Where the porosity is classified as intercrystalline and a higher dolomite content occur in sections 4, 7 and 8, the number of seams are low i.e. number of dissolution seams are three or less and stylolites maximum one. The interparticle porosity is occurring in the intervals lacking stylolites and the number of dissolution seams is usually two or less, porosity values are not registered here. In the intervals where the number of dissolution seams could be up to 10, moldic porosity occurs, whereas stylolites are missing. Microporosity is appearing where a few stylolites and dissolution seams are present.

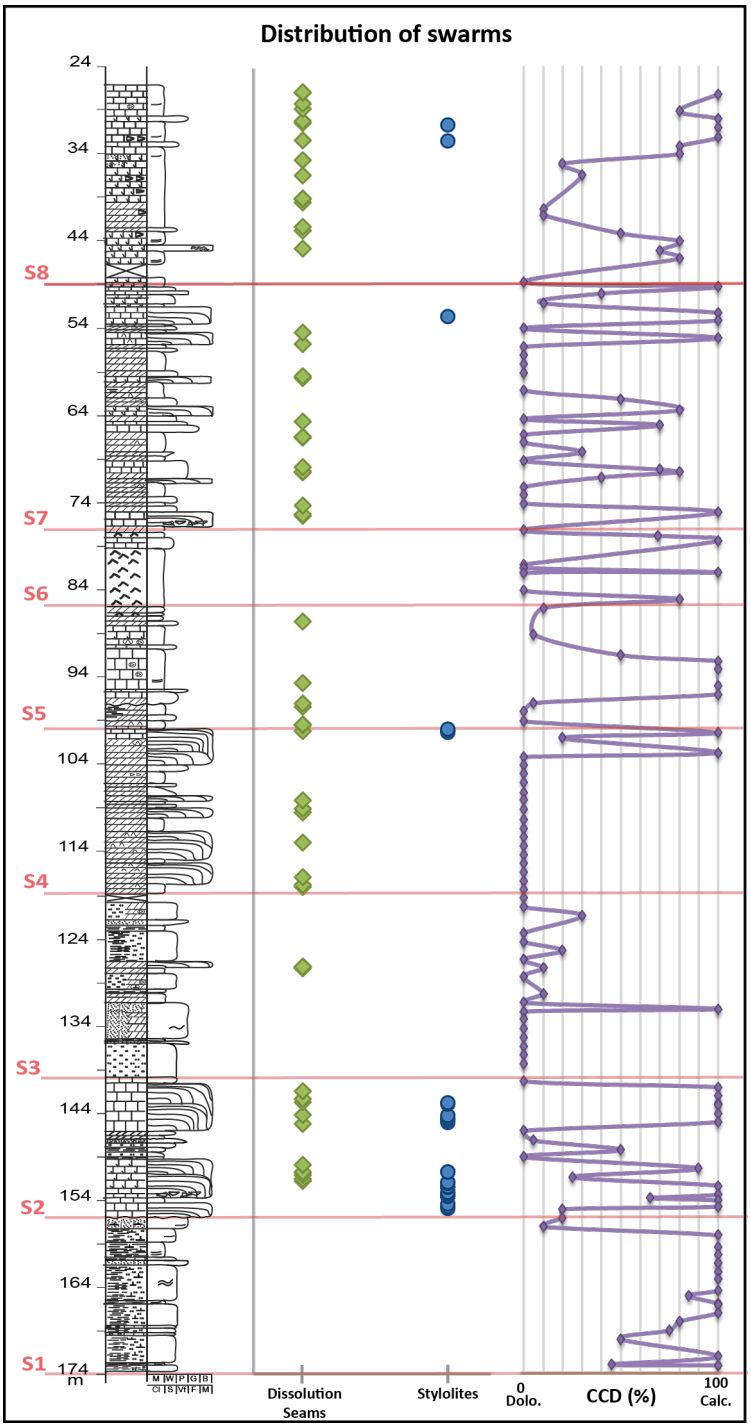

Figure 6.7. Shows how the swarms of dissolution seams (green rhombs) and swarms of stylolites (blue circles) occur throughout the core. The CCD values from Appendix 1, panels 1-3 in Ehrenberg et al. (2000) is also included and the 8 defined sections, section 2 marks the transition between the Falk and Ørn Formation.

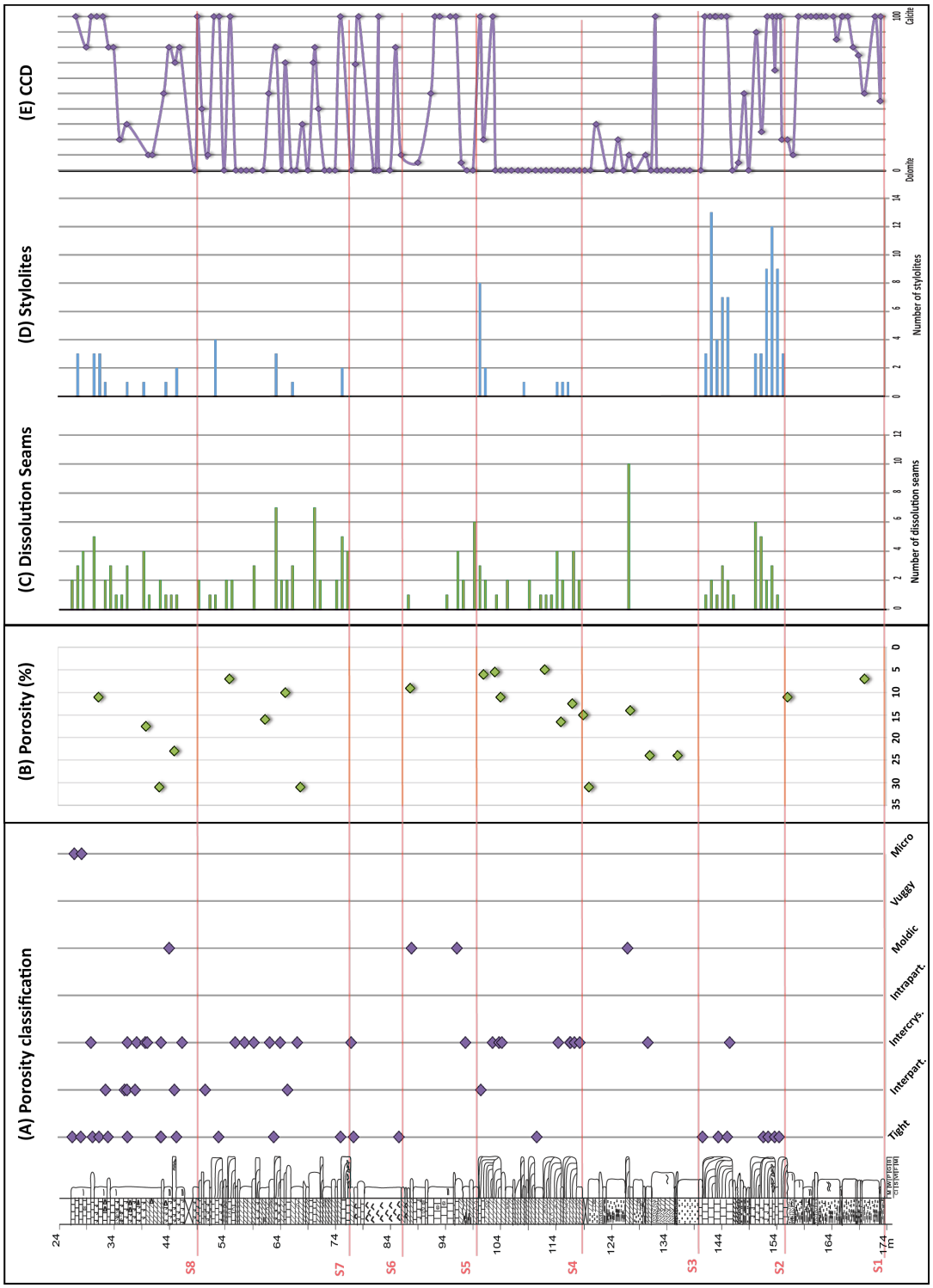

Figure 6.8. Includes Figure 5.17 representing the porosity distribution and porosity values in the core and Figure 6.1.1.16.1 with the distribution of the pressure solution seams and calcite/dolomite relationship.

6.1.8 Summary

Based on these classifications of the dissolution seams and stylolites, several trends can be observed and are briefly summarized below:

- Carbonate sections 2, 4, 7 and 8 includes several dissolution seams and stylolites than the other sections.
- The dissolution seams are presented with a higher number than the stylolites in the core, though the two seams are mostly favoring the same facies. This includes mudstone (F4) and *Palaeoaplysina*/phylloid algae boundstone (F7) whereas the seams are absent in the anhydrite facies (F10). By closer look the stylolites are mostly located in the boundstones whereas the dissolution seams are dominant in the mud-including facies, e.g. mudstone and wackestone.
- The presence of dolomitization is indicated to influence the occurrence and style of both the dissolution seams and stylolites.
- Based on the relationship between the seams distribution and the porosity characterization, sections 2, 4, 7 and 8 could also be distinguished from the other sections by good correlations between the number registered seams and the porosity classification.

6.2 Petrography of the carbonate sections

Based on the observations above it is clear that section 2, 4, 7 and 8 can be distinguished from the other sections by including carbonate facies, seams and porosity classification. In order to obtain an understanding of these observations, petrographic studies of the favored *Palaeoaplysina*/phylloid algae boundstone and mud-supported facies (mudstone and wackestone) with emphasis on cement, dolomite and if possible, a relation to the seams within these four sections have been done. The study of cement and dolomite has been correlated with Ehrenberg et al. (1998b) and therefore the same terminology have been used as presented in Table 4.

6.2.1 Section 2

Boundstone: Within the lowermost *Palaeoaplysina*/ phylloid algae boundstone in section 2, the canals of the *Palaeoaplysina* plates are filled with dark micrite cements (Figure 6.9A, arrow 3). Around the canals microspar occur (Figure 6.9A, arrow 1). Microspar could also be seen in the internal molds together with coarse spar (Figure 6.9A, arrow 2). In the upper *Palaeoaplysina*/ phylloid algae boundstone, a somehow higher amount of micrite occurs than the lowermost boundstone (Figure 6.9B). In association with a present seam some coarser spar can bee seen, beyond that the microspar and the coarse spar show the mostly the same trend as the boundstone below.

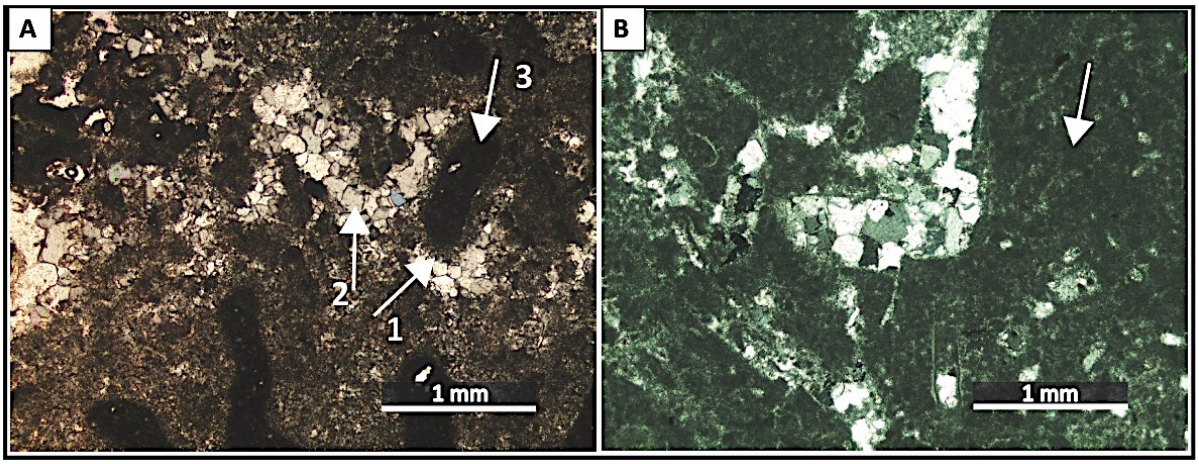

Figure 6.9. Micrograph showing the cement distribution composition of section 2. (A) Shows the lower *Palaeoaplysina*/phylloid boundstone algae, where arrow (1) marks the microspar around the canals, microspar around the channels (marked with arrow 3) whereas arrow 2 marks the blocky calcite spar. (B) Show the composition of the upper *Palaeoaplysina*/phylloid boundstone algae, here the cement appear as tight matrix comprising micrite and microsparite structure (marked with arrow).

6.2.2 Section 4

Mudstone: The lower dolomitized mudstone in section 4 comprises coarse dolomite crystals with slightly rounded crystal shapes together with alternating pores as seen in the texture above the seam in Figure 6.12E. In association with seams microcrystalline and fine rhombic dolomite is seen, here closer packing occurs and only some scarce pores are present. In some cases the seams are crosscutting the coarse dolomite crystals at one side of the seam, whereas the fine rhombic and microcrystalline are located underneath following the seams occurrence (Figure 6.12). Upwards in this mudstone a closely packed microdolomite occur where some crystal boundary of anhedral shapes could be seen, some anhedral bigger molds are intermixed. In the interbuild-up mudstone at 111 m depth a microdolomite much denser packed structure occurs (Figure 6.10A), and occasionally micropores can be seen.

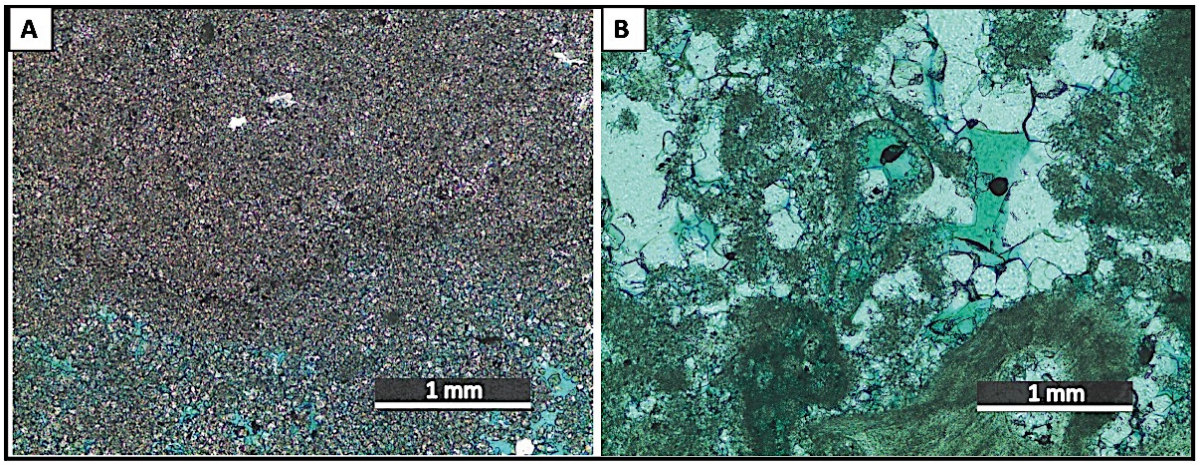

Figure 6.10. Micrograph of (A) Microdolomite texture present within the mudstone in section 4. (B) Coarse spar and some microspar in the boundstone in section 4.

Boundstone: In the lower dolomitized *Palaeoaplysina*/phylloid algae boundstone within this section, a microdolomite is dominating, only intermixed with some scarce fine rhombic dolomite. Accompanied with the dolomite, some molds can be seen, where the fine dolomite rhombs usually are surrounding the molds, whereas the microdolomite occurs away from the mold. In the dolomitized upper *Palaeoaplysina*/phylloid boundstone algae, microdolomite is intermixed with fine rhombic and some molds. Where the boundstone are calcite dominated, fine spar can be seen around canals, and internal in the mold some microspar, though mostly coarse spar (Figure 6.10B). Some porosity is also present.

6.2.3 Section 7

Mudstone: In the dolomitized mud-dominated facies at 72-71 m depth in this section, fine rhombic dolomite with clear boundaries. In the dolomitized mudstone at 67.55 m depth, rhombic dolomite crystals are scattered packed and intermixed with alternating amounts of pores (Figure 6.11). Upward in section 7, the dolomite in the mudstone facies becomes more densely packed and the microcrystalline dolomite is dominating, also the intermixed pores are decreasing. In the upper mudstones of this section, rhombe dolomite is prevailing and the amounts of pores are slightly higher than underneath.

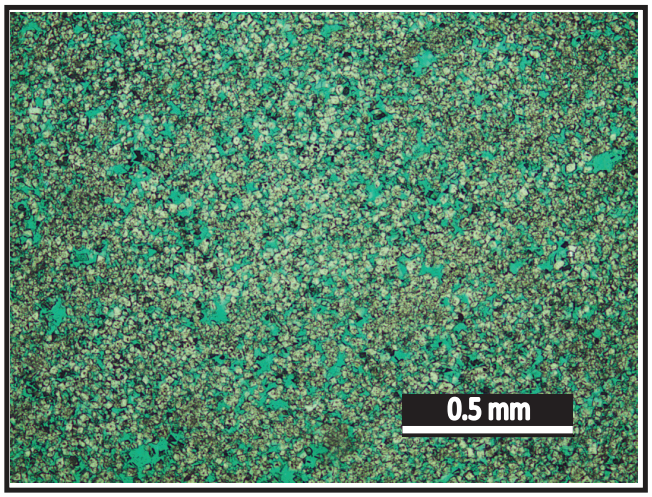

Figure 6.11. Scattered packet dolomitzed mudstone with rhombic dolomite crystals intermicxed with alternating amounts of pores in section 7.

Boundstone: The lowermost calcite dominated *Palaeoaplysina*/phylloid boundstone algae in section 7 has the same cement characteristic as the boundstones in section 2 (Figure 6.9). The partly dolomitized boundstone at app 60 m depth comprises fine rhombic dolomite intermixed with microspar and some coarse spar.

6.2.4 Section 8

Mudstone: The partly dolomitized mudstone in lowermost part of section 8 is thigh with a muddy occurrence intermixed with coarse spar and fine spar. Upwards a tight composition comprising a mixture of mud and micrite interbedded with microdolomite occur. Whereas at 39.90 m depth big molds are seen which are followed by a denser packing of fine rhombic dolomite with alternating porosity up to the undolomitized mudstone. The undolomitized mudstone comprises a tight composition including fine and coarse spar within and between the present fossils and mud, some scarce porosity could be seen. From 28 m depth the fine spar decreases upwards, and the composition gradually becomes tighter and homogeneous due to high mud content.

6.3 The pressure solution seams effect on the host rock

By studying the core and the available thin sections, several features were observed as occurring in correlation with the present pressure solution seams. Some features are observed within both of the scales whereas others were only seen in either one of them. Below a detailed description of the different features are presented. The term area would be used in this context and are defined as interval or band with an extension of a few cm, otherwise another range is specified. In several occasions rhombe formed crystals have been observed, these are interpreted to be dolomite based on the clear shape.

6.3.1 Cement

Core: In several occasions, the seams can be seen in close relation to an area with a different appearance than the host rock. This area is interpreted to be cement. The cemented areas are usually located below the seams and limited by the seam and its occurrence, and generally extend a few cm below the seam (Figure 6.12A). There are several ways to separate the cemented area from the host rock including different texture, different apparent grain density or different color (Figure 6.12A, B). In some cases, two separate seams that usually have a few cm spacing are enclosing the cement, and then the cement is just concentrated between the seams. Also here the cement can be separated from the host rock as described above (Figure 6.12B). This latter feature seems to be more common in relation with the dissolution seams.

Thin section: A close relation between seams and cement is also interpreted being observed in thin sections. Here the cement often can be separated from the host rock with texture including clear rhombohedra shaped dolomite crystals. The cement can often be seen with different color and a denser packed texture than the host rock, and the crystals are either coarser or more fine-grained than the host rock, though mostly with a homogeneous crystals size. Likewise as seen in core scale, the cement is following the seams occurrence, and can extend from 100 μm and up to a few cm and outside the thin section. The relation between the seams and the cement can usually be seen in two ways, 1) the cement extends out from the seam on both sides (Figure 6.12F) or the cement is limited to on side of the seam (Figure 6.12C, D, E). When the cement extends out from the seam on both sides, the host rock is observed in a porous dolomitized mudstone (F4), whereas when it is limited to one side, two

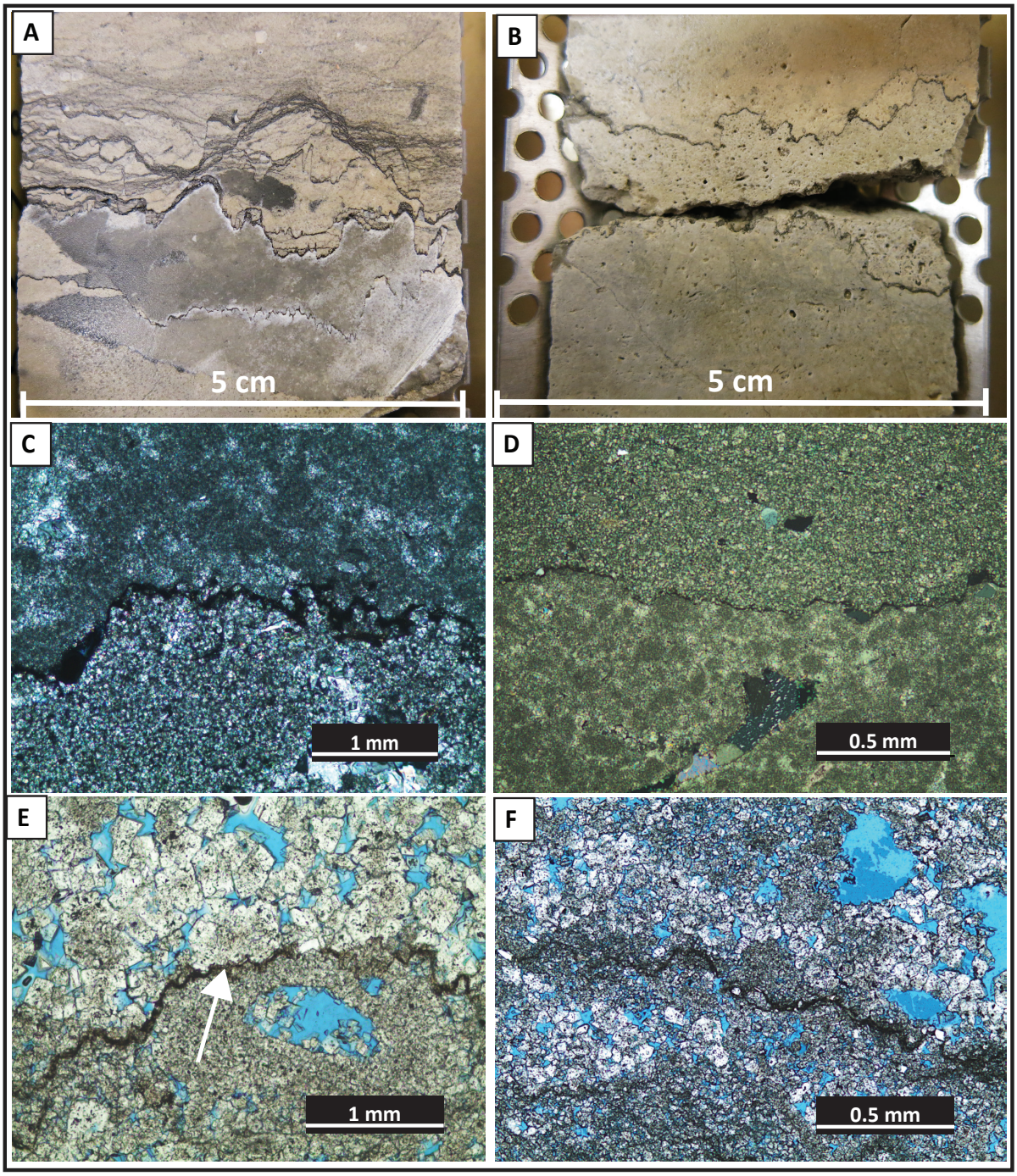

Figure 6.12. (A) Picture taken form the core where a pressure solution seam terminates an area (at the top) with a different color and texture than the host rock. (B) Picture taken from the core showing two pressure solution seams enclosing an altered area with apparent different density ratio than the host rock. (C) Micrographs taken in cross-polarized light, showing a clear boundary made by the stylolite, separating the fine-grained texture in the partly dolomitized boundstone in section 2 at the top from the coarse grained cement with dolomite rhombohedra crystals underneath. Note how the cement is selectively bounded by the stylolite. (D) Micrographs taken in cross-polarized light. Also showing the clear boundary between the host rock texture and the dolomite cement textures as in picture C, though here the dolomite cement is on top and host rock below the seam. (E) A clear boundary of the seam separating coarse dolomite crystals at the upper side in the dolomitized mudstone in section 4 from finer dolomite cement below the seam. Note how the seam is crosscutting the coarse dolomite crystals (marked with and arrow) (F) Fine-grained darker dolomite cement that extends out from the seam on both sides of the seam.

different host rocks occur, this includes the partly dolomitized mudstone in section 2 and the lower dolomitized mudstone in section 4. The texture of the partly dolomitized mudstone is appearing tightly packed with microcrystalline texture where the crystals mostly are impossible to distinguish from each other and only occasionally contours of fossils can be seen (Figure 6.12A, B, D), whereas the texture of dolomite mudstone is seen large dolomite crystals intermixed with porosity (Figure 6.12C). Mostly the dolomite areas and the host rock are separated and selectively following the stylolite boundaries, though in some rare situations mixing between the dolomite and the host rock occur across the seam. Commonly the dolomite area appears beneath the stylolites and host rock texture at the top.

6.3.2 The pressure solution seams relation to grains and fossils

Core: The pressure solution seams are observed to behave differently in correlation with grains and fossils in the core. Occasionally the stylolites can be seen as penetrating the different fragments, mostly fossils. This is seen as the stylolite is crosscutting the fossils, and often, just parts of the fossils are remaining, commonly at the upper side of the stylolites, and missing on the other side. This penetrating feature seems to be common when fossils as corals (Figure 6.13C) or foraminifera (Figure 6.13A) are present. Also seen when fossils and stylolites are present together is that grains /fossils are occurring at the peak of the teeth of the stylolite as shown in Figure 6.13B. Here the stylolite amplitude has developed around the grains instead of penetrating it, and if parts of the fossils are missing in these cases, it is the outer parts where the stylolite is occurring. The types of fossils are mostly not recognizable due to the small size and often seen just as a round white fragment. However, when the fossil can be determined it is proven to be cross-sections of crinoid stalks. Both of these described features are only observed within the undolomitized *Palaeoaplysina*/phylloid algae boundstone in the lower part of the core in section 2.

Thin section: The cross cutting of fossils are observed only in a few situations in the thin sections with appearances as described above. However, in thin sections, the stylolites are observed to develop around rhombohedra dolomite crystals. These dolomite crystals are just localized within the undolomitized mudstone (F4); though this feature is only present within a sparse number of thin sections therefore it is difficult to prove that this is a general trend. The presence of grains/fossils in the stylolites peak is also observed in thin section. Also here the

origin is impossible to determine as only white round fragments with no internal structure are remaining.

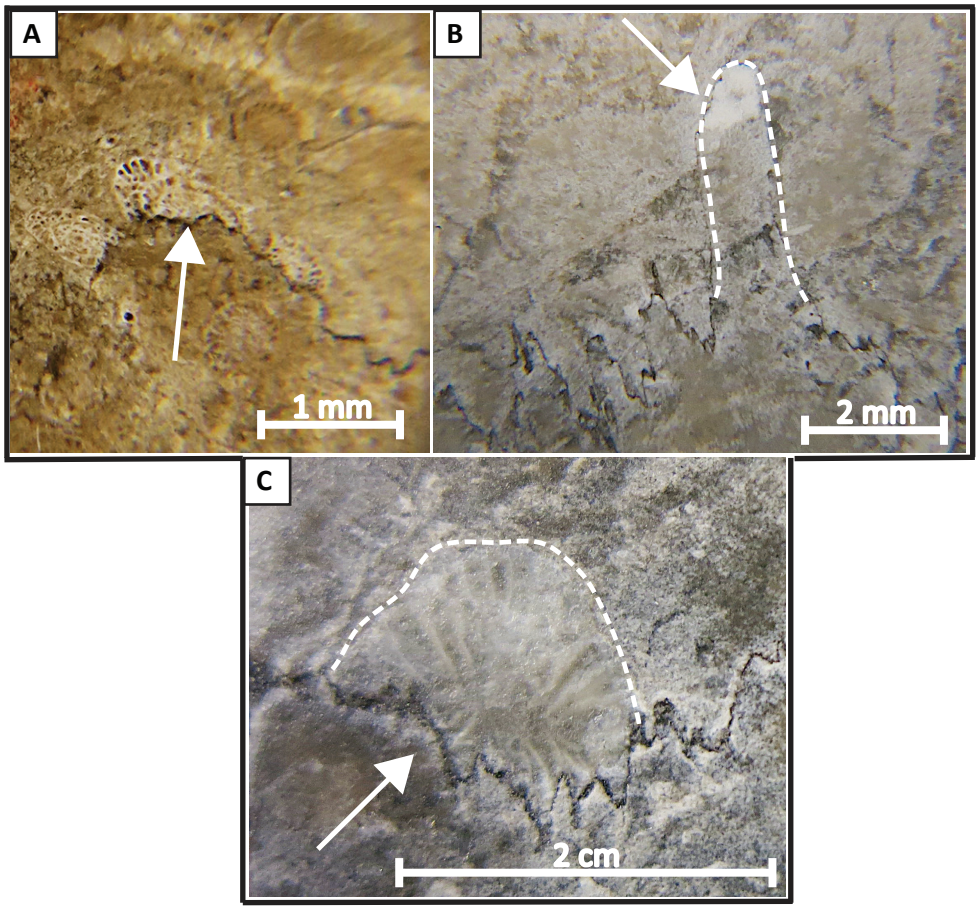

Figure 6.13. (A) A formaminifera that is crosscut by a stylolite (marked with the arrows), where the part of the foraminifera lying below the stylolite is missing. (B) The stylolite amplitude has developed around the cross section of a crinoid stalk (marked with arrow). To highlight the occurrence of the stylolite it have been marked with dashed white line (C) The stylolite crosscutting a coral, the corals occurrence have been marked with dashed white line whereas the stylolite is marked with the arrow.

6.3.3 Pressure solution seams and enclosed crystals

Thin section: The pressure solution seams are some times having a thicker appearance, with several of the seams enclosing individual crystals (Figure 6.14). The crystals present within the individual seams have heterogeneous size that varies from approximately 50 μm up to around 100 μm. The crystals lying within the seams have a similar morphology including color and shape with the crystals that occur at a distance from the seam that represent the host rock. Therefore, based on close relation between the host rock morphology and the enclosed

crystals the same origin is indicated. The enclosed crystals are usually lying close to parallel with the seam one next to another as seen in the dark seam in Figure 6.14, whereas crystals occurring in spherical clusters are more unusual. The number of crystals along a stylolite varies. The enclosing crystals seem to be common for dolomitized mudstone.

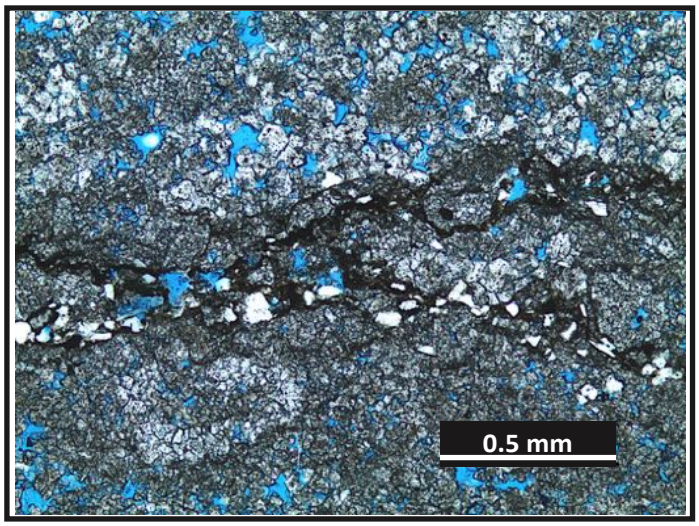

Figure 6.14. Micrograph taken in plane light showing thicker swarms that encloses dolomite crystals. Blue areas are epoxy.

6.3.4 Sets of seams

Core: In the core several of the pressure solution seams occur together in sets. These can be seen as parallel, either touching or non-touching, or they could occur as unparalleled sets with an anastomosing appearance that includes one or several connection points (Figure 6.15A). The overall appearance of these sets can be approximately horizontal or partly to very wavy. Often the style among the individual seams within parallel sets is similar, though clear individual dissimilarities among the seams are also common. Commonly, cement occurs in association with the parallel sets, similar to the cementation described. Different color, different texture and a different density to the host rock recognize the cement. In situations where cement can be seen in between sets of seams, the two outer seams of the sets are terminating the cement. Most of these sets are characterized with low amplitude. These sets of seams are observed to be most common in the undolomitized and partly dolomitized mud rich facies.

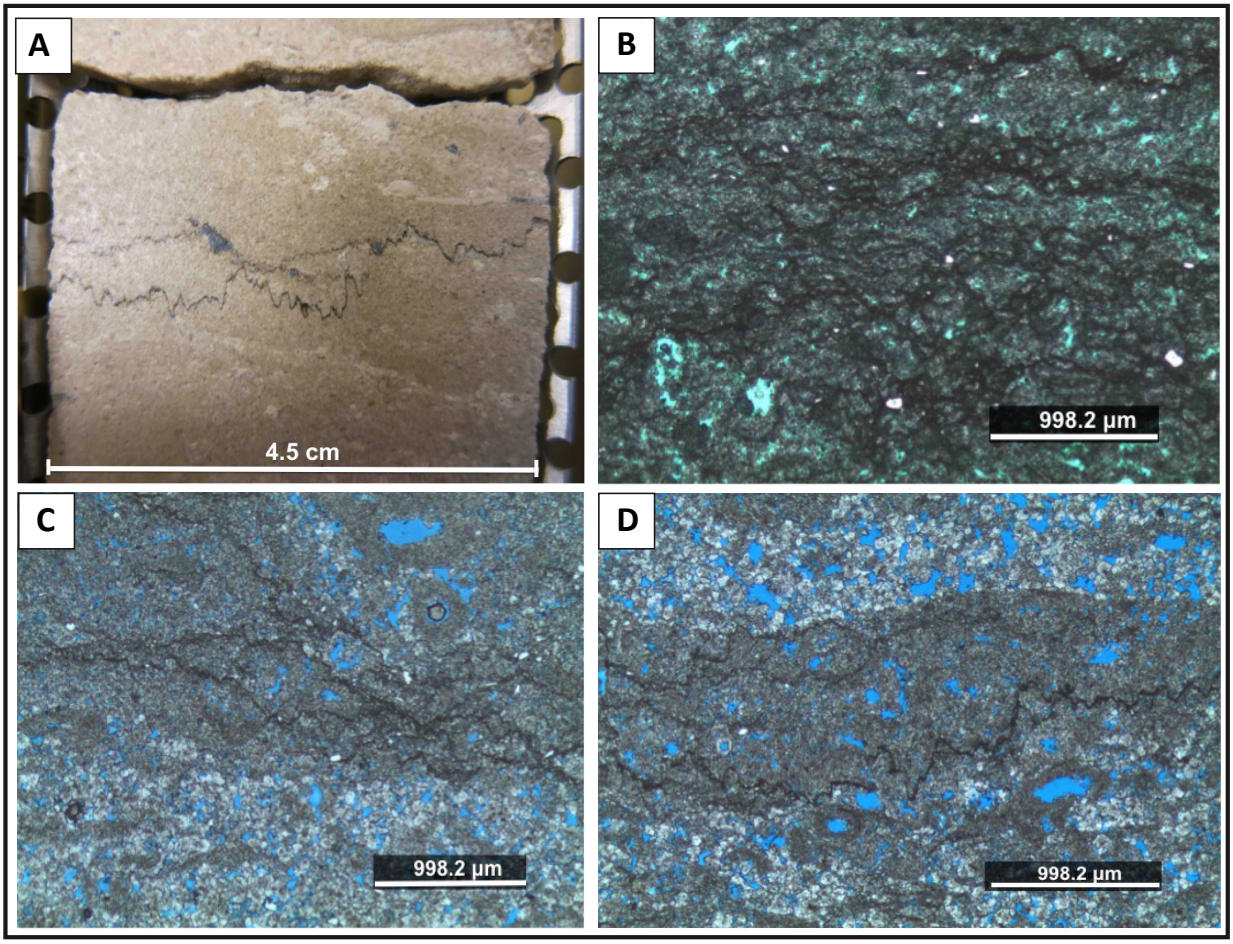

Figure 6.15. (A) Two stylolites where one of them terminates into the other in a connection point in the core. (B) Micrograph showing irregular anastomosing set of closely packed stylolites. Green areas are epoxy. Note the muddy look of the interseam areas (C) Micrograph showing simplified sets of dissolution seam/stylolites. Note the darker areas with cement where the seams occur. Blue areas are epoxy (D) Micrograph of dark cemented bands where the seams occur, whereas whiter coarser grained areas occur outside the cemented area. Blue areas are epoxy. Note in both picture B and C that a lower porosity occurs where the cement associated with the seam occur.

Thin section: Several of the pressure solution seams occur closely together in sets often seen as swarms in the thin section. All of the seams seen in the thin section appear darker than the matrix. Many of the seams are connected, making irregular anastomosing sets (Figure 6.15B). Some sets have a more complicated structure than others, whit a large number of seams interacting with each other at several connection points (Figure 6.15B, C). In these situations, the texture near the stylolites and individual seams, which is interpreted to be cement, is darker and very fine-grained, often with a cloudy appearance, and where the boundary of individual pressure solution seams appears blurry. Especially when these swarms occur in the mudstone (F4), the interseam areas within these sets show brown color and muddy texture. Also a common feature for these complex sets is the enclosing of crystals (as described

above), and where this occur, the seams are thicker than those without grains. In the less complex sets of pressure solution seams, only one or two interactions between individual seams are seen, and with an overall almost wavy, irregular structure. These sets are darker, with a finer and more densely packed cement between the seams (Figure 6.15D). In some thin sections a layered structure is seen, here bands of relatively fine-grained dark cement with dolomite crystals occur where sets of seams are present, these are further separated by some μm thick bands with whiter relatively coarser dolomite bands (Figure 6.15D). A common feature for all the sets seems to be a decrease in the porosity in the cemented areas lying inbetween individual seems compared to areas outside of the sets (Figure 6.15).

7 Discussion

7.1 Depositional Model

When combining the 10 different facies (section 4.1) and their vertical arrangement (section 4.2) in the core, a reconstruction of different facies zones in the depositional system can be arranged. These observations show typical characteristics of deposition on a carbonate ramp where low- to moderate energy levels prevailed. A carbonate ramp is defined as a gently slope (<1° slope) in a carbonate depositional system with gradual facies change from shallow water to deeper water and basinal sediments (Tucker et al., 1990, Burchette and Wright, 1992). This interpretation is in agreement with the other studies of the Finnmark Platform, which are based on wider data sets (Bugge et al., 1995, Ehrenberg et al., 1998a, Ehrenberg et al., 2000). The best way to present this interpretation is by placing the 8 defined core sections into a proximal to distal cross-section of the carbonate ramp system which includes a back-ramp comprising supratidal, intratidal environments and some parts of the shallow subtidal areas, the shallow ramp including shallow subtidal, and the deep ramp comprising deeper subtidal, and at last the basin, as shown in Figure 7.1 (Burchette and Wright, 1992, Pratt, 2010).

The sections are formed by multiple episodes of fluctuation in the sea level that can be seen mainly as shallowing-upwards cycles with a varying thickness. Since the environment is interpreted to be a shallow ramp, only a small change in the sea level would have major impact on the depositional conditions and accompanied sediments. According to Boggs (2011) sequences of third-order category have a duration of 1-10 million years and can be caused by ice growth and melting. Sequences of lower order (fourth- and fifth-order) have a shorter duration caused by alternations in the sea level. Fourth- order sequences could range from 0.2-0.5 million years, whereas fifth-order last from 0.01-0.2 million years (Boggs, 2011). Due to the rather limited data in this study it is difficult to determine the exact sequence order of the cycles. However, Ehrenberg et al. (1998a) has suggested either third-order sequences or lower order sequences with parts of third-order sequences for the same area.

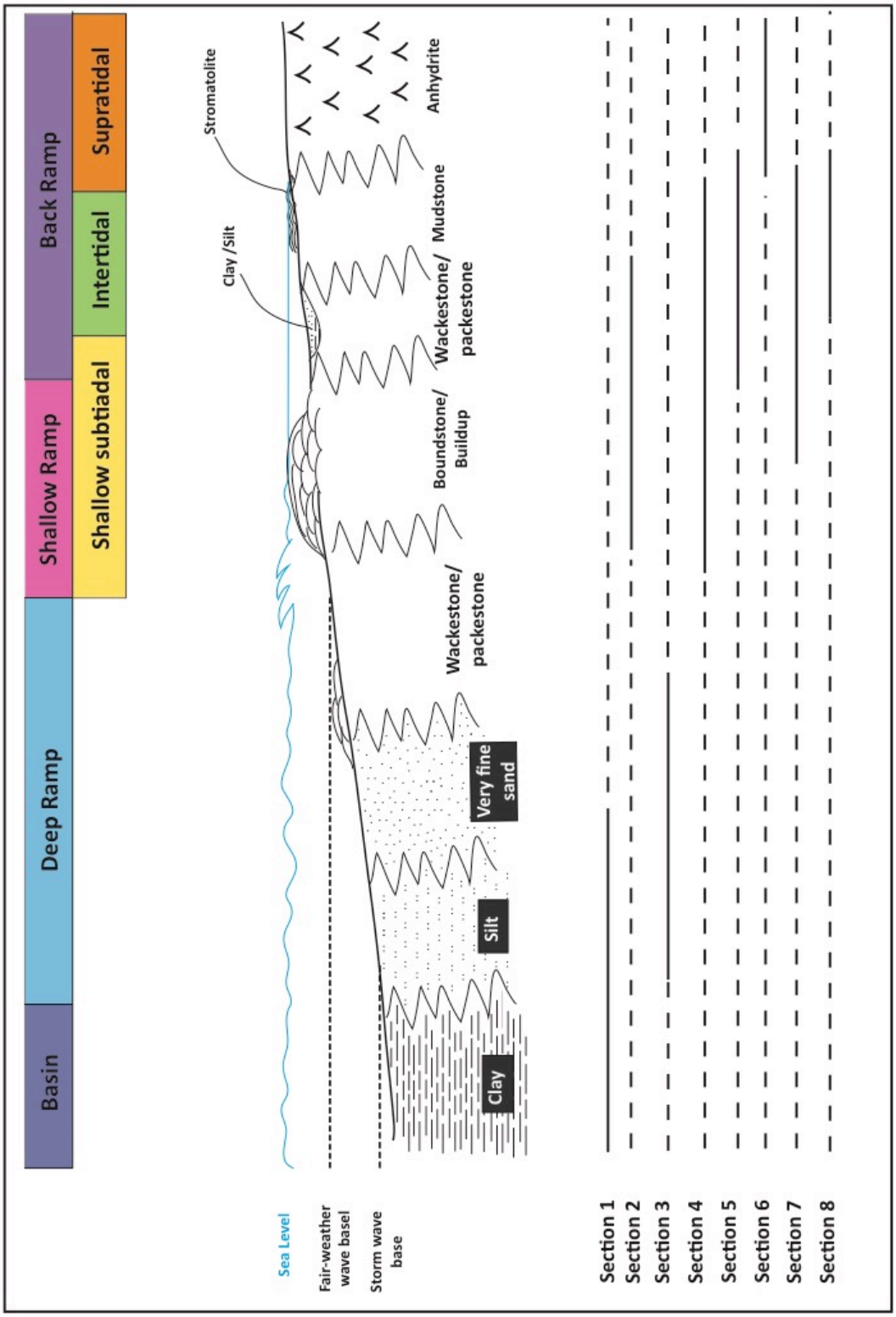

Figure 7.1. Cross section of the interpreted carbonate ramp model representing the depositional model of the core. The location the 8 different core sections are also presented.

In the following a brief review of the depositional environment for the interpreted sections and accompanied facies are presented.

Section 1

Section 1 and the Falk Formation represent the most distal areas of the carbonate platform (Figure 7.1) and is equivalent to the deep ramp or close to basin setting defined by Tucker et al. (1990). Facies 1, 2 and 3, which are dominant here, reflects an environment where siliciclastic sedimentation was favored, at the same time as the high content of carbonate cement and fossils indicate presence of carbonate production. Fair-weather conditions have allowed fine-grained sediments to settle and bioturbation to occur. The fossil fragments in the siltstone were sporadic transported to the deep ramp areas during periods of higher energy levels. The small differences in the particle sizes within section 1 can be explained by the distance to the sediment source and slightly different energy levels, where clay represent the deepest deposits within the core. Siliciclastic delta lobes building in the height, reaching conditions of carbonate production similar as assert in Ehrenberg et al. (2000), though in a smaller scale could explain the silt-rich wackestone. A storm event is most likely the reason for the erosional surface at 161.15 m depth, which scoured and eroded the lobe by transporting and depositing coarser grains. The upper up-coarsening unit suggests the formation of a larger delta lobe.

Section 2

The transition from section 1 to section 2 marks a change in the depositional conditions where reduction of siliciclastic sediment supply allowed carbonate sediments to form. The fossil fauna reflects a warmer climate at the same time as a rising sea level must have taken place giving accommodation space to the growing build-ups. The abundant production of *Palaeoaplysina*/phylloid algae boundstone indicates rapid growth rates occurring in a shallow subtidal setting, as shown in Figure 7.1 where a lagoon was formed. From this section the *Palaeoaplysina*/phylloid algae boundstone became the prominent facies. Based on the high degree of cementation, good water circulation is indicated, most likely at the windward margins of the reef. The brecciation of the lower boundstone in the lower carbonate unit could be a result of storm-events based on the limited extension. The alteration between the types of sediments deposited reflects changing access of siliciclastic supply, within a lagoon.

Section 3

The change of sediment type within this section compared with section 2 is suggested to be a result of the frequent sea level alternation characterizing the Upper Paleozoic. During highstand the deposition of carbonates was favored due to drowning of available material to erode and the build-ups could form as in section 2. However, during lowstand the siliciclastic sediments would dominate the depositions because of available material to erode as seen in section 3. The presence of facies 1 – 3 a calm environment and therefore indicates a similar depositional environment as in section 1 though, based on the higher abundance of facies 2 and 3 at the beginning of the section, a slightly higher energy level occurred. Therefore deposition in the upper areas of the deep ramp setting, still below fair-weather wave base has occurred in the lower part of this section (Figure 7.1). The higher abundance of facies 1 and 2 higher up in the section, reflects deposition at the transition between the deep ramp and basin as a result of increased sea level.

Section 4

Section 4 is characterized by repeated carbonates with up-shallowing trend. A gradual sea level rise gave accommodation space for build-ups to form. Again, the build-ups formed a lagoon with protected areas and the deposition of mudstone, thin beds of wackestone and occasionally packstone occurred. According to Ehrenberg et al. (1998a) and Ehrenberg et al. (2000) the sediments in section 4 were deposited in shallow variable hypersaline environment based on the reduced biogenic diversity, dolomitization and precipitation of anhydrite. Furthermore, as Ehrenberg et al. (1998b) asserted, this may be due to shallow lagoons where evaporatization could take place during minor lowstands. Based on the thickness of the mudstones in the section, they could very likely be interbuild-up sediments as described in the facies interpretation of the *Palaeoaplysina*/phylloid algae boundstone. Another explanation could be that the mudstone, wackstone and packstone result from accumulation in the back reef area in the lagoon. The abundance of dolomitized boundstone and muddy sediments in this section indicates a location at the shallow subtidal to intertidal environment (Figure 7.1).

Section 5

Section 5 represented by the muddy facies 4, 5, 6 and laminated structures reflecting calmer conditions than section 4 that allowed accumulation of muddy sediments to occur, therefore lagoonal intertidal environment is interpreted. Dolomite and anhydrite formed in marginal

areas with hypersaline conditions. In deeper waters a better water circulation is suggested where normal salinities occurred. Here, more sensitive organism as trilobite and corals could develop, also seen by the bioturbation (Scholle and Ulmer-Scholle, 2003, Hanken et al., 2010). The intermixed clay and silt could have been deposited by wind or storm. The erosional unconformity in the lower part of the section is interpreted as abrupt increase in the sea level at the lagoon margin forming conditions of wackestone over mudstone. The occurrence of stromatolites in the upper part of the section still indicates a placement in the intertidal environment, though closer to the supratidal areas with low wave action and shallow depths.

Section 6

Section 6 represents supratidal environment, which is the most proximal areas of the carbonate ramp (Figure 7.1). High temperature and dry conditions were dominating and favored formation of highly saline brines making gypsum. As the dry conditions continued, dehydration of gypsum occurred and anhydrite were formed. The presence of chickenwire anhydrite indicates that of the original muddy sediments are displaced by the intrasediment growth of anhydrite (Boggs, 2011). The gradual transition from chickenwire anhydrite to structureless anhydrite indicates alternating relationship between available brines and the host sediments upwards in the section. The interbedded siltstone implies a short term increase of clastic input. The interlayered mudstone and wackestone were deposited during increased sea level.

Section 7

An increase the in sea level drowned the previous supratidal evaporitic environment and stabilized the salinity. The area was changed back to shallow subtidal conditions and the development of *Palaeoaplysina*/phylloid boundstone resumed. Likewise as in section 4, the boundstones formed a lagoon and gave rise to the mud-dominated facies 4, 5, 6 and 7. The brecciaton within the first build-up in the section suggest a storm event. The varying degree of dolomitization can be explained as in section 4. The abundance of preserved foraminifera with low species diversity, mainly limited to fusulinida indicates well-oxygenated conditions simultaneously as the energy level must have favored preservation of foraminfera. Also, the presence of grainstone with high amounts of foraminifera, crinoids and peloids indicates a sand shoal accumulated by a tidal current (Flügel, 2010).

Section 8

Based on the dominating muddy sediments and higher occurrence of stromatolites with a varying dolomitization in this section, the deposition is interpreted to have occurred at the upper part of the intertidal area (Figure 7.1), where the wave action was minor. At the beginning of the deposition of the section, the conditions were favoring some degree of dolomitization. However, at the end the water circulation was mainly good favoring high production of corals in distinct intervals. The closer position to the land also made winnowed fine-grained siliclastic sediments intermix with the carbonate depositions periodically.

7.2 The seams distribution

From the results of the classification of the dissolution seams and stylolites, it is clear that the two seams distribution can be correlated with facies. It also correlates with the dolomite-calcite proportions shown in Ehrenberg et al. (2000). As an attempt to understand these results, some explanations are discussed in the following subchapters.

7.2.1 The seams distribution related to carbonate lithology

From the results it is shown that the *Palaeoaplysina*/phylloid algae boundstone and the mud-rich facies (mudstone and wackestone) include several pressure solution seams where calcite dominate, whereas the anhydrite facies is totally lacking seams. Based on the seams distribution between these facies it is suggested that depositional environment and the primary composition of the carbonate rock is important for determining the type of seams that would form. Settlement of clay particles at relatively quiet conditions in a lagoon is suggested favorable for later development of dissolution seams. Also, the fine-grained size of mud-rich facies favors the high amount of dissolution seams in these facies, rather than formation of stylolites. The limited amount of grains of the mudstone facies with a uniform morphology, favors formation of dissolution seams. However, as mudstone and associated wackestones may also contain varying amount of fossils causing obstacles, seams could deviate from the horizontal development by offsets and promote stylolite development. This could explain the occurrence of both, the dissolution seams and stylolites within these facies, as documented in section 8. In conclusion, as the type and amount of seams show an alternating occurrence it is suggested to reflect a varying ratio between fossil and mud contents in the sediments.

In contrast to the muddy facies, the higher amounts of stylolites in the *Palaeoaplysina*/phylloid algae boundstone reflects a more heterogeneous composition. This may be explained by the boundstones structure that includes different fossils with a varying composition and thereby obstacles favoring stylolites. Also, the depositional environment seems to be essential here. The higher energy level of the water at the shallow ramp would prevent a high accumulation and settlement of clay, which would favor stylolites. At the same time, these boundstones are observed being interbedded and intermixed with varying amounts of carbonate mud (chapter 5.1.9). This means alternating intervals that include higher clay content favoring dissolution seams which explains the coinciding presence of both types of seams in the boundstone.

In general, all of the carbonate facies recognized in the core are interpreted to include a distinct content of carbonate mud. Therefore, when considering the theories of the dissolution seams occurrence presented above, the more widespread abundance of dissolution seams compared to stylolites in the carbonate units can be explained.

As opposite to the *Palaeoaplysina*/phylloid algae boundstone and the mudstone above, the lack of pressure solution seams in the anhydrite facies in section 6 indicates that this facies has high resistance towards chemical compaction. An explanation for this may be the interpreted homogeneous composition for the facies, especially in the structureless anhydrite (F10A) (chapter 5.1.12). As both the impurities and the clay that is required for pressure solution seams to form is lacking it would explain and support the absence of seams in this layer. The presence of clay in the chickenwire/mosaic anhydrite would in theory promote the seams formation. However, as the amount is considered to be very small, it is suggested that the thickness and homogeneousness of the anhydrite layer is inhibiting chemical compaction. Based on the distribution of the seams, the anhydrite layer has also prevented compaction of the underlying carbonate layers where seams are lacking (section 5, Figure 6.2).

7.2.2 Seams and calcite cementation

By now it is clear that the formation of seams were facilitated in the boundstone and the muddy facies. Another observation is that seams and especially stylolites are also more

frequent in the boundstones, which are dominated by calcite. Good examples of this are the boundstones in section 2 and upper part of section 4 (Figure 6.4) which also show extensive cementation by calcite. The cementation is interpreted to be of two generations, including microspar and coarse cement. When comparing these cement types with the ones interpreted by Ehrenberg et al. (1998b), the microspar is suggested to correspond with early calcite cementation formed in the phreatic environment. The coarse calcite cement on the other hand, is as late calcite cementation. Based on these observations, it suggested that early diagenesis and cementation has lithified the boundstone and thereby made a stable framework where the applied stress would be spread out (Scoffin, 1987, Railsback, 1993a, Hanken et al., 2010). The fact that the early cement commonly occurs in the boundstones is suggested to reflect both the facies composition and the depositional environment. Buxton and Sibley (1981) assert that mud-free sediments are more susceptible of lithification, and even though the boundstone facies here has been interpreted to include significant amounts of mud, this could explain cementation within the fossil-rich intervals. Microspar cement is often seen associated with the canals within the *Palaeoaplysina*. This could be explained by the small channels size which could trap fine sediments that could produced cement, filling the canals (Marshall, 1983). The boundstones depositional environment is also favoring cementation, as deposition in the shallow ramp area makes the sediments exposed to high water circulations and low sedimentation, which would favor cementation (Flügel, 2010). Furthermore, when chemical compaction takes place in highly cemented rocks, Flügel (2010) claimed that pressure solution would develop along wide surfaces forming seams or as Wanless (1979) asserted, chemical compaction would take place in "limestone units having structural resistance to stress". The degree of early cementation is observed to vary in the present boundstones and may be related to the number of seams. As mentioned in the theory (3.2.2), during pressure solution, the $CaCO_3$-saturated pore fluid is precipitated as cement in nearby areas, which in this case could explain the coarse calcite spar. However, as this process requires free pores, Hanken et al. (2010) asserted that the stylolites would evolve as long as pore space is available, and when cemented, the stylolites growth will stop.

For comparison and in contrast to the frequent stylolite number in the boundstone, Buxton and Sibley (1981) argues that mud act as an cement-inhibiting factor. Based on this the low amount of cement seen in the mudstones in the core is explained. Also, the depositional environment in the lagoon would favor low cementation due to calmer water, higher sedimentation rates and deposition of fine-grained sediments (Flügel, 2010). Despite this,

stylolites in association with coarse calcite spar are present in the mudstone facies (section 8, Figure 6.4), though the amount is reflecting the limiting conditions including restricted early cementation, available fossils and pore space. When considering the formation of dissolution seams, their formation is indicated to be less dependent of early calcite cementation as these also occurs in uncemented areas as well.

7.2.3 Seams and dolomite

The dolomitized facies in the core, generally includes microdolomite and fine rhombic dolomite, indicating an early diagenetic origin (Ehrenberg et al., 1998b). Only within the lowermost part of section 4, coarse dolomite suggests a late development according to Ehrenberg et al. (1998b). However, as some of the seams crosscut the coarse crystals, the dolomite is interpreted to predate the dissolution seam (Figure 6.12E). A close spatial relation between dolomite and seams is seen in Figure 6.12 in partly dolomitized mudstones. This may be explained by the dolomites lower solubility to chemical compaction than calcite, and that the solution and precipitation around the seam would be rich in clay minerals which furthermore could release some Mg-ion (Hanken et al., 2010). Generally dissolution seams appear to be more common than stylolites in the dolomitized facies in section 4 (Figure 6.2). It is suggested in the literature that when a stable framework of dolomite crystals is established, a generally high resistance to chemical compaction occurs which is favorable for dissolution seams (Choquette and James, 1987, Hanken et al., 2010), and mostly just allowing dissolution seams to form, and only occasionally stylolites. Similar interpretations have been made by Railsback (1993b) for Paleozoic carbonates from the mid-Eastern United States.

From the previous discussion, the formation of stylolites is favored in areas including heterogeneities, while dissolution seams occur in more homogeneous areas. Texturally the dolomite-dominated areas in the core have varying compositions e.g. different crystal size, porosity, and possible remnants of original composition and that some are more homogeneous than others. Fine-grained dolomite crystals Figure 6.11 generated a uniform morphology and resistance, favoring the development of dissolution seams. In contrast, the more heterogeneous intervals (upper part of the seam in Figure 6.12E) of alternating dolomite crystal sizes and porosity are showing minor or the lack of dissolution seams. Certainly,

heterogeneous compositions would favor stylolites, though in a dolomite rock, the presence of dolomite would generally dominate over the heterogeneities and thereby unfavor these seams.

7.2.4 Style of dissolution seams

In this chapter and the following chapter the results of the morphology classifications of dissolution seams and stylolites would be discussed. To avoid confusion in these two chapters, it must be stated that when the amplitude is mentioned as low or high, it is referred to the characterization of the amplitude (Figure 4.2A) if not stated otherwise.

Based on the wide distribution of dissolution seams in the core, it is indicated that the presence of clay is common in most facies, although the amount is varying and most frequent in the mudstone. From the results of the characterization of these seams it is indicated that the seams style relies on the content of clay, and if fossils are present, these would also affect. When a high mud content in combination with fossils occur, the nodule-bounding dissolution seams would form, as seen in section 2, 4 and 7 (Figure 6.3). In contrast, if only a high clay content occurs, as in the mudstone facies, different sets including anastomosing and swarms (Figure 6.15) are usually present, whereas where the clay content is lower single seams are developed, characterized by either low or high amplitude (Figure 6.2A).

When considering the widespread distribution of low amplitude dissolution seams in the core, it is suggested that the development of these seams could form under most circumstances also in presence of dolomite. This indicates that these low amplitude seams forms most easily. In contrast the high amplitudes are limited to the *Palaeoaplysina*/phylloid algae boundstone, indicating to rely on more heterogeneous composition for developing. When dissolution seams has managed to form in dolomite host rocks, the texture is considered as important for the amplitudes characterization of low or high. Texture including microdolomite and/or fine rhombic crystals with limited pores, is indicated to favor low amplitudes due to the limited vertical deviation. In contrast, high amplitude is suggested to form when the texture is more scattered packed or have larger dolomite crystals. Here the seams have had a wider freedom of movement, and in order to form, they had to develop around the large crystals resulting in high amplitudes. As the coarse texture is limited in the core, it could explain the few dissolution seams with high amplitude. Scoffin (1987) asserted, that greater thickness of

insoluble material constituting the seam is associated with smaller amplitude height. Based on this and the widespread distribution of the dissolution seams with low amplitude, the core is considered to have a high clay content. The combination of the dolomite limitations and high clay content is suggested to explain the enclosed dolomite crystals (Figure 6.14), where seams had to enclose the crystals instead of develop around. Likewise with the nodule-bounding seams, only here the mud content was smaller.

7.2.5 Style of stylolite

Dolomites relation to stylolites style and mean amplitude value

From the results it is indicated that the limitations of dolomite and clay content that control the dissolution seams behavior and style are also controlling the stylolites. When the texture includes microdolomite and/or fine rhombic crystals with limited pores, stylolites do not develop. However, when the stylolites manage to form in a dolomite host rock, it is within a dolomite texture that is scattered packed or has larger dolomite crystals. Here, the result would be small amplitude values, where the amplitude is characterized as low and often columnar (boundstones in section 4, Figure 6.2 and 6.4) and nodule-bounding seams.

Calcite cementations relation to stylolites style and mean amplitude value

In contrast to the limitations caused by dolomite, both stylolite frequency and amplitude values are higher, in addition as the characterized high amplitudes are more widespread in calcite-dominated intervals. When comparing the stylolites mean amplitude values in calcite dominated boundstones with the ones in the calcite dominated mud-supported rocks (mudstone and wackestone), a minor difference occur, and both includes stylolites with amplitudes characterized as high. This suggests that the mean amplitude size and characterization of low or high, relies on the presence of features that acts as obstacles rather than the amount, this includes fossils constituting the primary composition of the rock. The sizes and resistance of the obstacles would reflect the necessary offsets the stylolites needed to take in order to form, and thereby controlling the mean amplitude value. In the core, stylolites are seen crosscutting and dissolving mainly corals (Figure 6.13B) and foraminifera (Figure 6.13A) implying that these fossils have low resistance and do not influence on the stylolites amplitude. In contrast crinoid stalks and dolomite rhombohedra crystals suggest the opposite, as stylolites are forced to develop around these features during their formation and

thereby promoting higher amplitudes both in values. The high resistance among crinoids could be explained by epitaxial cementation that normally develops among these fossils, whereas the dolomite high resistance to chemical compaction have already been discussed (James and Choquette, 1984, Hanken et al., 2010). These and other actual obstacles could include numerous variations e.g. in composition, porosity, early cementation, dolomite etc., and resulting in variable mean amplitude sizes, as seen in the upper boundstone of section 2. When considering the mean amplitude values of the stylolites in the core, they seem to be limited to approximately 9 mm, independently of depth, suggesting a threshold of maximum size in the core.

As mentioned earlier Scoffin (1987) asserted that the complexity of the stylolites morphology relies on the amount of clay. Based on this the stylolites of smooth style would represents high mud content and the irregular style lower mud content. As the irregular and hummocky style correlates with the same depth as the swarms that are interpreted to represent high clay content, support the styles relation to mud content.

7.3 The seams effect on the host rock

From the petrography results, the influence of chemical compaction on the host rock and thereby porosity is shown to be significant. Correlations between cementation and seams (Figure 6.12 and 6.13), suggests that the dissolved ions have migrated away from the seam into areas of less pressure where cement was deposited (Choquette and James, 1987, Scoffin, 1987, Moore and Wade, 2013). A somehow larger distance of the cementation occurs near the sets of seams (Figure 6.15B,C, D). However, as seen in the results (Figure 6.12B and 6.15D), cementation is often limited to the two outer seams or just outside. This indicates that these two seams act as permeability barriers.

In several occasions the alteration of the host rock or dissolution of fossils often are located to one side of the seam (Figure 6.12A, B, C, D and Figure 6.13A,B), this is suggested to reflect extensive calcite cementation (Figure 6.12C, D), early dolomitization near the seam (Figure 6.12E), or presence of fossils (Figure 6.13A,B), acting as barriers for ion migrations. Also, often the seam is suggested to act as a seal, limiting any ion transportation across it (Figure 6.12A, C, D and Figure 6.13B), this is seen among both single and sets of seams. It is

suggested that presence of higher contents of insoluble material has increased the strength and formed a tighter structure at the seam and thereby favoring sealing.

7.4 Porosity distribution

It is clear that all of the carbonate sediments in the core have been exposed to different degree of diagenesis. The porosity results (chapter 5.3) show that intercrystalline and tight porosity are the most common porosity types in the core, whereas interparticle porosity has intermediate distribution while the moldic and microporosity do occur, but are considered as insignificant as they only are registered with three and two values which makes it difficult to evaluate their occurrence. Therefore it has been chosen to exclude the moldic and microporosity from the discussion. It is suggested that the diagenetic factors of early calcite cementation, dolomitization, and chemical compaction controls the pressure solution seams distribution, but also are essential for the porosity distribution. In addition, the primary composition of the rock has major impact by determining how susceptible the rock is to diagenesis and thereby influence how the final porosity would develop.

7.4.1 Intercrystalline porosity

The most dominating porosity class in the core is the intercrystalline, which occurs in the intervals where partial or total dolomitization has taken place. This porosity type occurs in all of the carbonate facies and carbonate dominated intervals in the core when excluding the anhydrite facies (Figure 5.17). A higher frequency of this porosity class occurs in section 4, 7 and 8. All of these sections are interpreted to been deposited in shallow subtidal or intertidal environments (chapter 7.1). This suggests a relation between porosity type and depositional environment. As discussed above, a small degree of dolomitization occur in relation to the seams in mudstones. Since this dolomitization mostly occurs in relation to fine-grained mudstones that often show lack of porosity in depth, the formation of intercrystalline porosity in a limited zone could have a significant effect on reservoir quality.

When considering the available porosity values after Ehrenberg et al. (2000), the mudstone facies has a wide distribution ranging from 7-31%, where the highest values are located in sections 7 and 8 e.g. the mudstone in subtidal areas. The boundstone facies has a maximum of

17%, though usually between 6-15%. Both of these two facies includes a patchy pore distribution, which according to Lønøy (2006) would have a high permeability. Therefore based on the pore distribution and porosity values it is indicated that both of these facies have optimal reservoir porosity (Moore and Wade, 2013). The porosity values in the dolomitized boundstone and mudstone are distinctly higher than in the undolomitized intervals of the same facies. However, presence of the seams could contribute to lowering of the porosity in a dolomitized host rock as the areas near seams have a lower porosity due do cementation.

7.4.2 Tight porosity

The tight porosity class is common in the *Palaeoaplysina*/phylloid algae boundstone, mudstone and anhydrite. In the boundstone and the mudstone it is dominating when calcite cemented and partly dolomitized, and in addition it occurs where the mudstone is dolomitized. From the previous discussion (chapter 7.2.2) it is shown that boundstones are commonly exposed to early calcite cementation, resulting in a tight rock as seen in the lower boundstone in section 7 (Figure 5.17). This is seen in tight undolomitized mudstone as well. However, early calcite cementation also favors stylolites. The formation of stylolites is porosity destructive as the produced ions may oversaturate the pore fluid and precipitate cement in nearby pores (Hanken et al., 2010). This suggests a negative correlation between porosity and the number of stylolites. This correlates also well with the porosity profiles and stylolite frequency presented in Ehrenberg et al. (1998b), where a high number of stylolites are correlated with low porosity and where the main cause is interpreted to be coarse calcite spar. It is difficult to predict the same trend among the mudstone facies, as these could be tight due to other factors such as mechanical compaction or early cementation. Both mudstone and boundstone are appearing tight when only partly dolomitized, due to extensive calcite cementation. In a few occasions dolomitic mudstone appears tight due to closely packed dolomite crystals. Another significant process that could explain the tight composition in the undolomitized mudstone is mechanical compaction. Compaction is known to be very porosity destructive during the first meters of burial (Choquette and James, 1987, Flügel, 2010). When considering the anhydrite, it is suggested that this is tight due to the original compositions low porosity and its exposure to mechanical compaction.

7.4.3 Interparticle porosity

Interparticle porosity classification is dominantly occurring among the undolomitized or partly dolomitized mud-dominated facies (mudstone and wackestone) (Figure 5.17). Due to early cementation mechanical compaction is prevented (Scoffin, 1987). At the same time, the limited extension of cement is suggested and therefore interparticle porosity was favored. Also, due to the lack of seams the intervals interparticle porosity has favored a preservation of the remaining porosity after early cementation. The interparticle porosity is most common in section 7 and 8 when representing intertidal environment (Figure 7.1). Presence of interparticle porosity in partly dolomitized mudstone resulted in a significant higher porosity than in undolomitized boundstone and mudstone with the same porosity classes. This suggests that presence of dolomite has enhanced the porosity. However, it is difficult to estimate an overall trend as the data is limited, and much would rely on the degree of cementation and dolomitization.

8 Conclusion

This study concludes that Core 7030/03-U-01 comprises 10 facies where 7 of these include carbonate sediments and are located in the Ørn Formation. Based on the vertical arrangement of the interpreted facies, 8 facies sections have been defined and interpreted to represent different facies zones of a distal to proximal cross section of a shallow carbonate ramp environment.

From the grouping and classification of the dissolution seams and stylolites in the Ørn Formation it is concluded:

- The dissolution seams require a significant amount of clay in order to develop, though they form under several conditions and consequently are the most common type of seam in the core. The formation of stylolites require lesser amount of clay than the dissolution seams and in addition they rely on the presence of early calcite cementation in order to form. Therefore, the depositional environment and facies composition is controlling the type of seams that would form. The dissolution seams are favored by mud-rich facies (mudstone and wackestone) uniform morphology and deposition in calm environments in the lagoon. The stylolites are favored by the heterogeneous composition of the *Palaeoaplysina*/phylloid algae boundstone. The higher water energy level occurring during deposition of the *Palaeoaplysina*/phylloid algae boundstone at the shallow ramp prevents a high accumulation of clay; though favor early cementation that is necessary for stylolites to develop.
- Stylolites and dissolution seams are inhibited in host rocks comprising dolomite. However dissolution seams appear in homogenous fine-grained dolomite texture. Dolomite cement also appears in small amounts adjacent to the seams.
- With higher clay content, dissolution seams would form swarms, anastomosing sets and low style amplitudes; and if fossils are present also nodule-bounding seams would form. If the clay content is lower a high amplitude style would formed. The dolomite texture of the host rock is also important for the dissolution seam amplitude style, so when densely packed and fine-grained crystals of dolomite occur, it favors formation of a low amplitude style. With a coarser dolomite texture and/or more pores high amplitudes would form.

- Dolomite texture is also important for the style of the stylolite. Fine-grained densely packed crystals would inhibit formation of stylolites, while with coarse-grained dolomite crystals a style of low and columnar amplitude would form, and smaller mean amplitude values, as well as nodule-bounding stylolites. In calcite-dominated intervals the mean amplitude value relies on the size of the obstacle or fossils. Crinoid stalks and dolomite crystals favor higher amplitude values due to high resistance to chemical compaction whereas foraminifera and corals appear to not affect the value. High clay content favors complex stylolite styles.
- The petrography of the pressure solution seams shows that early cementation, early dolomitization or fossils and the seam itself act as barriers for the ion-migration associated with chemical compaction. Also, the seam itself could act as a barrier. During chemical compaction the ions usually migrate away from the seam and deposit as cement.

The main porosity classes in the core are intercrystalline, tight and interparticle porosity. These have shown to mainly be controlled by dolomitization, early carbonate cementation, chemical and mechanical compaction. The intercrystalline porosity is most common and has developed in relation to dolomitization of *Palaeoaplysina*/phylloid algae boundstone and mudstone and is indicated to have occurred already in the depositional environment in the shallow subtidal and intertidal environment. These lithologies have porosity values making good candidates for reservoirs, where the mudstone has the highest porosity values.

9 Further work

- Further work should be done by correlating the results from this study with comparable data from several locations, in order to investigate if the results in this study are a general trend.
- The heterogeneities in this study is limited to Dunham classification and visual comparison, therefore heterogeneities should be investigated at a smaller scale to obtain a better understanding of what the controlling factors are.
- The dolomite should be investigated on a more detailed scale to find out when it becomes a limitation for the development and occurrence of dissolution seams and stylolites.
- To obtain a better understanding how the clay are controlling the stylolites and dissolutions seams behavior, the quantitative clay content and the clay mineralogy should be investigated.
- Investigate the controlling factors of where the ions formed by chemical compaction would migrate and precipitate as cement.
- A further study of the dolomitization related to the pressure solution seams would give an better understanding of the amount and effect the developed intercrystalline porosity would have on the reservoirs conditions.

10 References

ADAMS, A. & MACKENZIE, I. R. 1998. *Carbonate Sediments and Rocks Under the Microscope: A Colour Atlas*, CRC Press.

AHR, W. M. 2011. *Geology of carbonate reservoirs: the identification, description and characterization of hydrocarbon reservoirs in carbonate rocks*, John Wiley & Sons.

ANDERSON, K. D. & BEAUCHAMP, B. 2014. Paleobiology and paleoecology of Palaeoaplysina and Eopalaeoaplysina new genus in Arctic Canada. *Journal of Paleontology,* 88**,** 1056-1071.

ARCHIE, G. E. 1952. Classification of carbonate reservoir rocks and petrophysical considerations. *AAPG Bulletin,* 36**,** 278-298.

BARNES, M., BARNES, W. & BUSTIN, R. 1984. Diagenesis 8. Chemistry and evolution of organic matter. *Geoscience Canada,* 11.

BOGGS, S. 2009. *Petrology of sedimentary rocks*, Cambridge University Press.

BOGGS, S. 2011. *Principles of sedimentology and stratigraphy,* Boston, Prentice Hall.

BOSENCE, D. W. & WILSON, C. L. 2003. Carbonate depostional systems. *In:* COE, A. L. (ed.) *The Sedimentary Record of Sea-Level Change.* The Open University, Cambridge.

BUGGE, T., MANGERUD, G., ELVEBAKK, G., MØRK, A. & NILSSON, I. 1995. The Upper Palaeozoic successton on the Finnmark Platform, Barents Sea. *Norsk Geologisk Tiddsskrift***,** 3-30.

BURCHETTE, T. & WRIGHT, V. 1992. Carbonate ramp depositional systems. *Sedimentary Geology,* 79**,** 3-57.

BUXTON, T. M. & SIBLEY, D. F. 1981. Pressure Solution Features in a Shallow Burled Limestone. *Journal of Sedimentary Research,* 51.

CHOQUETTE, P. W. & JAMES, N. P. 1987. Diagenesis# 12. Diagenesis in Limestones-3. The deep burial environment. *Geoscience Canada,* 14.

CHOQUETTE, P. W. & PRAY, L. C. 1970. Geologic nomenclature and classification of porosity in sedimentary carbonates. *AAPG bulletin,* 54**,** 207-250.

DENGO, C. A. & RØSSLAND, K. G. 1992. Extensional tectonic history of the western Barents Sea. *In:* LARSEN, R. M. (ed.) *Structural and tectonic modelling and its application to petroleum geology.* Amsterdam: Norwegian Petroleum Society (NPF).

DIMICHELE, W. A. & PHILLIPS, T. L. 2002. The ecology of Paleozoic ferns. *Review of Palaeobotany and Palynology,* 119**,** 143-159.

DORÉ, A. 1995. Barents Sea geology, petroleum resources and commercial potential. *Arctic***,** 207-221.

DUNHAM, R. J. 1962. Classification of carbonate rocks according to depositional textures.

EHRENBERG, S. N., NIELSEN, E., SVÅNÅ, T. & STEMMERIK, L. 1998a. Depositional evolution of the Finnmark carbonate platform, Barents Sea: results from wells 7128/6-1 and 7128/4-1. *Norsk Geologisk Tidsskrift,* 78**,** 185-224.

EHRENBERG, S. N., NIELSEN, E. B., SVANA, T. & STEMMERIK, L. 1998b. Diagenesis and reservoir quality of the Finnmark carbonate platform, Barents Sea: results from wells 7128/6-1 and 7128/4-1. *Norsk Geologisk Tidsskrift,* 78**,** 225-251.

EHRENBERG, S. N., PICKARD, N. A., SVÅNÅ, T. A., NILSSON, I. & DAVYDOV, V. I. 2000. Sequence stratigraphy of the inner Finnmark carbonate platform (Upper Carboniferous-Permian), Barents Sea-correlation between well 7128/6-1 and the shallow IKU cores. *Norsk Geologisk Tidsskrift,* 80**,** 129-161.

EMBRY, A. F. & KLOVAN, J. E. 1971. A Late Devonian reef tract on northeastern Banks Island, NWT. *Bulletin of Canadian Petroleum Geology,* 19**,** 730-781.

FALEIDE, J. I., GUDLAUGSSON, S. T. & JACQUART, G. 1984. Evolution of the western Barents Sea. *Marine and Petroleum Geology,* 1**,** 123-150.

FLÜGEL, E. 2010. *Microfacies of Carbonate Rocks: Analysis, Interpretation and Application,* Berlin, Heidelberg, Springer Berlin Heidelberg: Berlin, Heidelberg.

FOLK, R. L. & LAND, L. S. 1975. Mg/Ca ratio and salinity: two controls over crystallization of dolomite. *AAPG bulletin,* 59**,** 60-68.

GABRIELSEN, R. H., FAERSETH, R. B., JENSEN, L. N., KALHEIM, J. E. & RIIS, F. 1990. Structural Elements of the Norwegian Continental Shelf. Part 1. The Barents Sea Region. *Bulletin 6***,** 33.

GUDLAUGSSON, S. T., FALEIDE, J. I., JOHANSEN, S. E. & BREIVIK, A. J. 1998. Late Palaeozoic structural development of the South-western Barents Sea. *Marine and Petroleum Geology,* 15**,** 73-102.

HANKEN, N.-M., BJØRLYKKE, K. & NIELSEN, J. K. 2010. Carbonate sediments. *Petroleum Geoscience***,** 141-200.

HANKEN, N.-M. & NIELSEN, J. K. 2013. Upper Carboniferous–Lower Permian Palaeoaplysina build-ups on Svalbard: the influence of climate, salinity and sea-level. *Geological Society, London, Special Publications,* 376**,** 269-305.

JAMES, N. P. & CHOQUETTE, P. W. 1984. Diagenesis 9. Limestones—the meteoric diagenetic environment. *Carbonate Sedimentology and Petrology***,** 45-78.

JAMES, N. P. & WOOD, R. 2010. Reefs. *In:* DALRYMPLE, R. W. & JAMES, N. P. (eds.) *Facies Models 4* Canada: Geological Association of Canada.

KENDAL, A. C. 2010. Marine Evaporites. *In:* DALRYMPLE, R. W. & JAMES, N. P. (eds.) *Facies Models 4.* Canada: Geological Association of Canada.

KOEHN, D., RENARD, F., TOUSSAINT, R. & PASSCHIER, C. W. 2007. Growth of stylolite teeth patterns depending on normal stress and finite compaction. *Earth and Planetary Science Letters,* 257**,** 582-595.

LARSSEN, G., ELVEBAKK, G., HENRIKSEN, L. B., KRISTENSEN, S., NILSSON, I., SAMUELSBERG, T., SVÅNÅ, T., STEMMERIK, L. & WORSLEY, D. 2002. Upper Palaeozoic lithostratigraphy of the Southern Norwegian Barents Sea. *Norwegian Petroleum Directorate Bulletin,* 9**,** 76.

LOGAN, B. W. & SEMENIUK, V. 1976. *Dynamic metamorphism: processes and products in Devonian carbonate rocks, Canning Basin, Western Australia*, Geological Society of Australia.

LUCIA, F. J. 1995. Rock-fabric/petrophysical classification of carbonate pore space for reservoir characterization. *AAPG bulletin,* 79**,** 1275-1300.

LUCIA, F. J. 2007. *Carbonate reservoir characterization: an integrated approach*, Springer Science & Business Media.

LØNØY, A. 2006. Making sense of carbonate pore systems. *AAPG bulletin,* 90**,** 1381-1405.

MARSHALL, J. F. 1983. Submarine cementation in a high-energy platform reef: One Tree Reef, southern Great Barrier Reef. *Journal of Sedimentary Research,* 53.

MOORE, C. H. 1989. *Carbonate diagenesis and porosity*, Elsevier.

MOORE, C. H. & WADE, W. J. 2013. *Carbonate Reservoirs: Porosity and diagenesis in a sequence stratigraphic framework*, Elsevier.

NICHOLS, G. 2009. *Sedimentology and stratigraphy*, John Wiley & Sons.

PARK, W. C. & SCHOT, E. H. 1968. Stylolites: their nature and origin. *Journal of Sedimentary Research,* 38.

PRATT, B. R. 2010. Peritidal Carbonates. *In:* DALRYMPLE, R. W. & JAMES, N. P. (eds.) *Facies Models 4.* Canada: Geological Association of Canada.

RAILSBACK, L. B. 1993a. Contrasting styles of chemical compaction in the Upper Pennsylvanian Dennis Limestone in the Mid-Continent region, USA. *Journal of Sedimentary Research,* 63.

RAILSBACK, L. B. 1993b. Lithologic controls on morphology of pressure-dissolution surfaces (stylolites and dissolution seams) in Paleozoic carbonate rocks from the mideastern United States. *Journal of Sedimentary Research,* 63.

RAMBERG, I. B., BRYHNI, I. & NØTTVEDT, A. 2007. *Landet blir til: Norges geologi,* Trondheim, Norsk geologisk forening.

READING, H. G. 1978. *Sedimentary environments and facies,* Oxford, Blackwell Scientific Publications.

SAMUELSBERG, T., ELVEBAKK, G. & STEMMERIK, L. 2003. Late Palaeozoic evolution of the Finnmark Platform southern Norwegian Barents Sea. *Norw. J. Geol.,* 83**,** 351-362.

SCHOLLE, P. A. & ULMER-SCHOLLE, D. S. 2003. *A Color Guide to the Petrography of Carbonate Rocks: Grains, Textures, Porosity, Diagenesis, AAPG Memoir 77*, AAPG.

SCOFFIN, T. P. 1987. *An introduction to carbonate sediments and rocks,* Glasgow, Blackie.

SHINN, E. A. & ROBBIN, D. M. 1983. Mechanical and chemical compaction in fine-grained shallow-water limestones. *Journal of Sedimentary Research,* 53.

SIEDLECKA, A. 1975. Late Precambrian stratigraphy and structure of the north-eastern margin of the Fennoscandian Shield (East Finnmark-Timan Region). *Geological Survey of Norway Bulletin* 316**,** 313-348.

SKAUG, M., DONS, C. E., LAURITZEN, Ø. & WORSLEY, D. 1982. Lower Permian palaeoaplysinid bioherms and associated sediments from central Spitsbergen. *Polar Research,* 1982**,** 57-76.

SMELROR, M., BASOV, V. A. & NORGES GEOLOGISKE, U. 2009. *Atlas : geological history of the Barents Sea,* Trondheim, Geological Survey of Norway.

STEEL, R. J. & WORSLEY, D. 1984. Svalbard's post-Caledonian strata—an atlas of sedimentational patterns and palaeogeographic evolution. *Petroleum geology of the North European margin.* Springer.

STEMMERIK, L. 1997. Permian (Artinskian Kazanian) Cool-Water Carbonates in North Greenland, Svalbard and the Western Barents Sea.

STEMMERIK, L. 2000. Late Palaeozoic evolution of the North Atlantic margin of Pangea. *Palaeogeography, Palaeoclimatology, Palaeoecology,* 161**,** 95-126.

STEMMERIK, L., VIGRAN, J. O. & PIASECKI, S. 1991. Dating of late Paleozoic rifting events in the North Atlantic: New biostratigraphic data from the uppermost Devonian and Carboniferous of East Greenland. *Geology,* 19**,** 218-221.

STEMMERIK, L. & WORSLEY, D. 1989. Late Palaeozoic sequence correlations, North Greenland, Svalbard and the Barents Shelf. *Correlation in hydrocarbon exploration.* Springer.

STEMMERIK, L. & WORSLEY, D. 2005. 30 years on - Arctic Upper Palaeozoic stratigraphy, depositional evolution and hydrocarbon prospectivity. *Norsk Geologisk Tidsskrift,* 85**,** 151-168.

STEPHENS, D. G., EASON, J. E. & PEDLOW, G. W. 1973. Dissolution of shell material with no disruption of primary sedimentary structures. *Journal of Sedimentary Research,* 43.

TAYLOR, E. L., TAYLOR, T. N. & KRINGS, M. 2009. *Paleobotany: the biology and evolution of fossil plants*, Academic Press.

TUCKER, M. E., WRIGHT, V. P. & DICKSON, J. A. D. 1990. Carbonate sedimentology. Chichester: Wiley.

WALDERHAUG, O. & BJØRKUM, P. 1998. Calcite cement in shallow marine sandstones: growth mechanisms and geometry. *Carbonate Cementation in Sandstones: Distribution Patterns and Geochemical Evolution*, 179-192.

WANLESS, H. R. 1979. Limestone response to stress: pressure solution and dolomitization. *Journal of Sedimentary Research,* 49.

WENTWORTH, C. K. 1922. A scale of grade and class terms for clastic sediments. *The Journal of Geology*, 377-392.

WILSON, J. L. 1975. *Carbonate Facies in Geologic History,* New York, Springer Verlag.

WORSLEY, D. 2008. The post‐Caledonian development of Svalbard and the western Barents Sea. *Polar Research,* 27, 298-317.